INFORMATION TO USERS

This manuscript has been reproduced from the microfilm master. UMI films the text directly from the original or copy submitted. Thus, some thesis and dissertation copies are in typewriter face, while others may be from any type of computer printer.

The quality of this reproduction is dependent upon the quality of the copy submitted. Broken or indistinct print, colored or poor quality illustrations and photographs, print bleedthrough, substandard margins, and improper alignment can adversely affect reproduction.

In the unlikely event that the author did not send UMI a complete manuscript and there are missing pages, these will be noted. Also, if unauthorized copyright material had to be removed, a note will indicate the deletion.

Oversize materials (e.g., maps, drawings, charts) are reproduced by sectioning the original, beginning at the upper left-hand corner and continuing from left to right in equal sections with small overlaps.

Photographs included in the original manuscript have been reproduced xerographically in this copy. Higher quality 6" x 9" black and white photographic prints are available for any photographs or illustrations appearing in this copy for an additional charge. Contact UMI directly to order.

Bell & Howell Information and Learning
300 North Zeeb Road, Ann Arbor, MI 48106-1346 USA
800-521-0600

UMI®

Université d'Ottawa · University of Ottawa

IMMUNOAFFINITY SELECTION WITH MASS SPECTROMETRY FOR THE CHARACTERIZATION OF EXPRESSED SINGLE CHAIN ANTIBODIES AND THE *C-MYC* PEPTIDE FROM COMPLEX MATRICES

TAMMY LERICHE

Thesis submitted to the
School of Graduate Studies and Research
University of Ottawa
In partial fulfillment of the requirements for the
M. Sc. degree in the
Ottawa-Carleton Chemistry Institute

Abstract

The purification of a desired protein or peptide from complex matrices such as tissue culture media is often problematic due to the presence of cellular contaminants. Immunological methods, however, allow for the selective removal and preconcentration of target analytes. The primary objective of this project was the development of affinity selection techniques that can be used with mass spectral detection for the direct identification of trace level target antigens from complex matrices.

Mouse monoclonal antibody IgG1 specific for the human *c-myc* epitope—EQKLISEEDLN—was covalently immobilized on recombinant protein G beads using chemical crosslinking. This immunomatrix was then used to selectively enrich both the wild-type and mutant single chain (scFv) antibodies (containing the *c-myc* epitope) from the periplasmic extract of *Escherichia coli* (*E. coli*). To identify the point mutation within the scFv mutant, a tryptic digest was performed followed by LC-MS of the tryptic peptides. This novel approach was applied to a number of scFv proteins containing single point mutations. In particular, mass spectrometry was used to confirm the site of mutation L46N on one specific mutant using LC-MS/MS. Immunoaffinity enrichment was also used to select the *c-myc* peptide from a spiked sample of human serum at a concentration of 20 ng/ml. LC-MS/MS was performed to confirm the identity of the selected peptide.

Interestingly, unexpected proteins were selected in both immunopurification procedures. Peptide sequencing by LC-MS/MS together with database searching was used to identify the extraneous *E. coli* proteins selected. Identification of the selected

human serum proteins was achieved using polyacrylamide gel electrophoresis (SDS-PAGE) followed by tryptic digestion of the identified bands and database searching using the tryptic peptide masses. It was discovered that human IgG1 antibody fragments were being selected from the serum due to binding to underivatized sites on the protein G beads. Selection of the *E. coli* proteins and human serum albumin is proposed to be due to the cross-reactivity of the anti-*c-myc* IgG antibody. Despite the presence of these proteins, affinity selection and detection of the target analyte was achieved by immunoaffinity purification and mass spectrometry.

Acknowledgements

I wish to express my gratitude to Dr. Pierre Thibault for his guidance, support, and advice throughout the course of this research project. As with any scientific endeavor, this project was filled with many interesting "surprises" and intricacies, and Dr. Thibault's ideas and extensive knowledge were invaluable to its completion.

I was very fortunate to be able to carry out the research for this Master's dissertation at the National Research Council. There, I was able to use state-of-the-art instrumentation and work with many outstanding scientists. The experience and knowledge that I gained from my time there are inestimable. I would like to thank my co-supervisor Dr. René Roy for enabling me to have this opportunity while attending the University of Ottawa.

Over the past two years I have worked with a number of remarkable people who have been incredibly supportive and encouraging throughout the progress of my studies. I wish to thank the members of Dr. Thibault's group for their kind words and humorous outlooks. Thank you John, José, Don, Jianjun, Ken, and Pat. I would also like to extend my gratitude to Rhoula Wehbi, Tomoko Hirama, and Dr. Roger Mackenzie for their insightful discussions and patience.

I wish to express my appreciation to my family for their love and encouragement. Thank you for understanding and listening even to the "science" stuff. Finally, thank you to all my wonderful friends who have ensured my sanity (I think) and kept me laughing. You all have given me many memories that I will savor and enjoy no matter where we are geographically.

Table of Contents

Abstract ii

Acknowledgements iv

Table of Contents v

List of Figures viii

List of Tables xiii

List of Abbreviations xiv

List of Amino Acids xvii

Chapter 1 Theory

1.1 Introduction 1
1.2 Antibodies 2
1.3 Immunoaffinity Extraction 5
1.4 Mass Spectrometry 6
1.4.1 Matrix Assisted Laser Desorption/Ionization Mass Spectrometry 7
1.4.2 Electrospray 10
1.4.3 Nanoelectrospray 13
1.4.4 Quadrupole Mass Analyzers 14
1.4.5 Tandem Mass Spectrometry 16
1.4.6 Quadrupole-Time-of-Flight Mass Analyzers 17
1.5 Protein Identification using MALDI-MS and/or ES-MS with Database Searching 18
1.5.1 Peptide Mapping 19
1.5.2 Peptide Sequencing using Tandem Mass Spectrometry 20
1.5.3 Database Searching 21
1.6 Capillary Zone Electrophoresis (CZE) 22
1.6.1 Sensitivity Enhancement for Capillary Electrophoresis 26
1.7 Surface Plasmon Resonance Optical Sensors 27
1.8 Summary 29

Chapter 2 Experimental Procedures

2.1 Chemicals and Materials 31
2.2 Antibody Purification 32
2.3 Antibody Coupling to Solid Phase 33
2.3.1 Amine Coupling with 1,1'-Carbonyldiimidazole Activated Beads 33
2.3.2 Solution Affinity Selection 34

2.3.3 Hydrazide Activated Gels and Oxidized Antibody Carbohydrate Moieties 34
2.3.4 Immobilization of the Antibody to Protein G through Chemical Crosslinking 35
2.4. Antibody Quantitation 36
2.4.1 Absorbance Spectrophotometry 36
2.4.2 Surface Plasmon Resonance Analyses 36
2.5 Affinity Selection Protocol 37
2.6 Periplasm Extraction of scFv 38
2.6.1 Immobilized Metal Affinity Chromatography 38
2.7 Affinity Selection of *c-Myc* Peptide from Sera 39
2.7.1 Fetal Bovine Serum 39
2.7.2 Human Serum 40
2.8 Gel Electrophoresis 41
2.9 Preparation of Gel Electrophoresis Samples 42
2.9.1 Regular SDS-PAGE 42
2.9.2 Mini SDS-PAGE 43
2.10 Protein Digestion 43
2.10.1 In-gel Protein Digestion 43
2.10.2 Solution Protein Digestion 44
2.10.3 Endoproteinase Glu-C Digestion 45
2.11 Desalting Peptides 45
2.12 MALDI-MS 46
2.13 Capillary Zone Electrophoresis (CZE-UV) 47
2.14 BCQ Capillary Coating 47
2.15 Immunoaffinity Chromatography 48
2.16 Concentration Study of *c-Myc* Selection from PBS using LC-MS 49
2.17 Nanoelectrospray Emitters 50
2.18 LC-ESMS 50
2.19 Database Searching 51

Chapter 3 Development of *c-Myc* Affinity Selection

3.1 *c-Myc* Epitope 53
3.2 Antibody Immobilization 55
3.3 *c-Myc* Peptide 56
3.4 Antibody Immobilization on Activated Beads 56
3.5 Antigen Capture in Solution 59
3.6 Immobilization through Antibody and Matrix Activation 64
3.7 Immobilization of Antibody to Protein G through Crosslinking 67
3.8 Development of Immunoaffinity Chromatography with On-Line Mass Spectral Detection 69

Chapter 4 Affinity Selection for the Enrichment of Single Chain Antibodies (scFvs)

4.1 Single Chain Antibodies 76
4.2 Identification of Mutation Sites in Human Blood Group A scFv Antibodies 77
4.3 Identification of Extraneous *E. coli* Proteins Co-Selected with the scFv Antibodies 85

Chapter 5 Affinity Selection of the *c-Myc* Peptide

5.1 Introduction 94
5.2 LC-ESMS of the Affinity-Selected *c-Myc* Peptide from a Non-Complex Matrix 94
5.3 Mass Spectral Analysis of the Synthetic *c-Myc* Peptide 98
5.4 Affinity Selection of the *c-Myc* Peptide from Fetal Bovine Serum 101
5.5 Affinity Selection of the *c-Myc* Peptide from Human Serum 102
5.6 Removal of the Extraneous Human Serum Components 104
5.7 Identification of Extraneous Serum Proteins 112
5.8 Removal of Human Serum Immunoglobulins 116

Chapter 6 Conclusion 125

References 129

Claims to Original Research 133

Thesis Related Presentations 134

List of Figures

1.1	Schematic diagram of immunoglobulin G	3
1.2	Schematic diagram of Matrix Assisted Laser Desorption/Ionization	8
1.3	Schematic diagram of a time-of-flight mass analyzer coupled with MALDI in linear mode	9
1.4	Schematic diagram of a time-of-flight mass analyzer coupled with MALDI in reflectron mode	9
1.5	Schematic diagram of electrospray ionization	13
1.6	Schematic diagram of a quadrupole mass analyzer	16
1.7	Schematic diagram of the quadrupole/orthogonal-acceleration time-of-flight mass spectrometer	18
1.8	Characteristic peptide fragment ions in tandem mass spectrometry	21
1.9	Schematic diagram of capillary electrophoresis instrumentation	23
1.10	Schematic diagram showing electroosmotic flow	25
1.11	Schematic diagram showing surface plasmon resonance optical detection	29
2.1	On-line immunoaffinity column arrangement	49
3.1	The sequence of the light and heavy variable domains of the anti-*c-myc* IgG1 mouse monoclonal antibody	55
3.2	Covalent immobilization of antibody on Reacti-Gel matrix	57
3.3	MALDI-MS of the 9E10 *c-myc* peptide (prior to desalting). A) Affinity-selected using the Reacti-Gel immunomatrix and B) not retained by the immunomatrix during the affinity selection	58
3.4	MALDI-MS of the 9E10 *c-myc* peptide (Figure 3.3) after desalting	58
3.5	MALDI-MS of A) the standard peptide mixture in PBS buffer and B) the desalted affinity-selected 9E10 *c-myc* peptide purified using the Centri•Spin-10 column	61
3.6	MALDI-MS of A) the standard peptide mixture in PBS buffer and B) the desalted affinity-selected *c-myc* peptide purified using Centri•Spin-20	61

3.7	MALDI-MS of A) the protein mixture in PBS buffer and B) the affinity-selected scFv after purification with the Centri•Spin-40 column	63
3.8	MALDI-MS of the standard *c-myc* peptide mixture after purification with the Centri•Spin-40 column	63
3.9	Antibody immobilization using a hydrazide-activated gel	64
3.10	MALDI-MS of the *c-myc* peptide affinity-selected using the CarboLink immunomatrix	66
3.11	MALDI-MS of the *c-myc* peptide in deionized water (25 μg/ml)	66
3.12	Immobilization of antibody to protein G through the crosslinker dimethyl pimelimidate	69
3.13	Preconcentration CE-UV calibration curve for *c-myc* peptide	71
3.14	Preconcentration electropherogram of the *c-myc* peptide eluted from the immunoaffinity column after a 20 minute incubation of the sample with the column	71
3.15	Preconcentration electropherogram of the *c-myc* peptide eluted from the immunoaffinity column after a 60 minute incubation of the sample with the column	71
3.16	Preconcentration electropherogram showing the first 10 μl of elution buffer removed from the immunoaffinity column after a 25 minute incubation with the elution buffer	72
3.17	Preconcentration electropherogram showing the second 10 μl of elution buffer removed from the immunoaffinity column after a 25 minute incubation with the elution buffer	72
3.18	Preconcentration electropherogram showing the amount of applied *c-myc* peptide not retained by the immunoaffinity column	72
3.19	Electrospray mass spectrum of on-line *c-myc* immunoaffinity selection from PBS buffer	75
3.20	Electrospray mass spectrum of 1 μg/ml *c-myc* peptide in 0.1 M formic acid	75
4.1	Sequence of the human blood group A scFv antibody	77

4.2	MALDI-MS showing scFv mutant #1 A) in shock buffer periplasmic extract of *E. coli* and B) affinity-selected	78
4.3	MALDI-MS of the scFv wild-type tryptic digest	81
4.4	MALDI-MS of the mutant #1 tryptic digest	81
4.5	LC-MS reconstructed ion chromatograms of A) scFv wild-type and B) mutant tryptic digests	83
4.6	LC-MS/MS sequencing of the scFv wild-type 46-53 tryptic peptide	86
4.7	LC-MS/MS sequencing of the scFv mutant 46-53 tryptic peptide	86
4.8	MALDI-MS of affinity-selected scFv mutant #1	91
4.9	Sequence of the human *c-myc* (amino acids 408-439) synthetic peptide immunogen selected by the anti-*c-myc* IgG antibody and the homologous mouse and chicken *myc* sequences	91
4.10	The *c-myc* epitope of the MYC-X-5/1 monoclonal antibody and the cross-reactive epitope on the sigma factor of *E. coli*	91
5.1	Calibration curve for *c-myc* (in DIW) using LC-ESMS (triple quadrupole)	95
5.2	Affinity selection calibration curve by LC-ESMS (triple quadrupole)	95
5.3	Affinity selection calibration curve using LC-ESMS (Q-TOF)	95
5.4	Affinity selection calibration curve using CE-UV (preconcentration)	95
5.5	LC-MS showing the amount of *c-myc* selected vs. amount applied to the immunomatrix	98
5.6	Electrospray mass spectrum of *c-myc* affinity selection from PBS buffer	99
5.7	Electrospray mass spectrum of *c-myc* peptides in DIW	99
5.8	MS/MS sequencing of m/z 574 *c-myc* peptide	99
5.9	MS/MS sequencing of m/z 623 *c-myc* peptide	99
5.10	MALDI-MS of the *c-myc* peptide A) affinity-selected and B) 300 μg/ml in DIW	101
5.11	MALDI-MS of the affinity-selected *c-myc* peptide from fetal bovine serum A) pH 7.9 and B) pH 7	102

5.12	LC-MS reconstructed ion chromatogram showing affinity selection of the *c-myc* peptide from human serum (100 ng/ml)	103
5.13	LC-MS/MS identifying the 20.66 min peak (m/z 687.8) shown in Figure 5.12 as that of the *c-myc* peptide	103
5.14	Electropherograms showing A) non-retained peptide and protein, B) first, C) second, and D) third deionized water washes for affinity selection from a 10 μg/ml spiked serum solution	105
5.15	Electropherogram showing the serum proteins selected along with the *c-myc* peptide from a 10 μg/ml spiked human serum solution	105
5.16	Electropherograms showing the formic acid washes of the immunomatrix during regeneration	107
5.17	Affinity selection of the *c-myc* peptide from a 1 μg/ml PBS buffer solution using a regenerated immunomatrix	107
5.18	Affinity selection eluent of control human serum (CE-UV preconcentration)	107
5.19	Affinity selection eluent from a 1 μg/ml *c-myc* spiked serum solution using the three wash buffer system	109
5.20	A) MALDI-MS of the *c-myc* peptide affinity-selected and B) electropherogram of the serum proteins present with affinity selection from a 1 μg/ml human serum solution after ten β-alanine washes	109
5.21	Electropherograms showing the serum proteins removed from the immunomatrix after the A) sixth and B) seventh β-alanine rinses	109
5.22	A) MALDI-MS of the *c-myc* peptide affinity-selected and B) electropherogram of the serum proteins present with affinity selection from a 1 μg/ml human serum solution after five washes of the immunomatrix with 0.5% Tween	109
5.23	A) MALDI-MS and B) electropherogram of the *c-myc* peptide affinity-selected from human serum that had been precipitated with acetonitrile before spiking (1 μg/ml) with the peptide	111
5.24	MALDI-MS of the *c-myc* peptide affinity-selected from human serum after protein precipitation of the 1 μg/ml spiked serum solution	111

5.25	Regular SDS-PAGE of proteins selected by protein G and the anti-*c-myc* IgG immunomatrix	114
5.26	Removal of human serum proteins from a 10 μg/ml *c-myc* spiked serum solution using a 10 kDa NMWL filter unit. A) Electropherogram and B) MALDI-MS of the *c-myc* affinity-selected from the purified serum	118
5.27	Electropherogram of the affinity-selected *c-myc* peptide from a 10 μg/ml spiked serum that had been purified using a 100 kDa NMWL filter unit prior to selection (preconcentration CE-UV method)	118
5.28	MALDI-MS of the *c-myc* peptide affinity-selected from a 0.1 μg/ml spiked serum solution where the serum was passed through a 100 kDa NMWL filter unit prior to being spiked with the peptide	118
5.29	Mini SDS-PAGE of human serum purified through a 100 kDa filtration unit and of affinity-selected proteins from a 0.1 μg/ml *c-myc* spiked serum solution (serum passed through a 100 kDa filter prior to spiking)	121
5.30	MALDI-MS of the *c-myc* peptide affinity-selected from a 20 ng/ml spiked human serum solution (peptide was added after purification of the serum using a 100 kDa NMWL filter unit)	124
5.31	Electropherogram showing the human serum proteins selected by 200 μl of protein G resin	124
5.32	Electropherogram showing the human serum proteins selected by the immunomatrix after purification by the protein G resin	124
5.33	Electropherogram showing the human serum proteins selected by 100 μl of protein G resin	124

List of Tables

4.1	Calculated and observed masses (MALDI-MS) for human blood group A scFv wild-type and mutant proteins	78
4.2	Tryptic peptides of the scFv wild-type protein as observed by MALDI-MS	80
4.3	Tryptic peptides of the scFv mutant #1 antibody as observed by MALDI-MS	80
4.4	Tryptic peptides observed by LC-MS (Q-TOF) of scFv wild-type protein	84
4.5	Tryptic peptides observed by LC-MS (Q-TOF) of affinity-purified scFv mutant protein #1	84
4.6	The sequence tags obtained by LC-MS/MS of the scFv mutant tryptic digest and the corresponding proteins identified from database searches with the sequence tags and respective tryptic peptide masses	87
4.7	*E. coli* proteins identified by database searching to be present in the selection of the scFv mutant #1 from the *E. coli* periplasmic extract	88
5.1	Amounts of the *c-myc* peptide applied and selected by the anti-*c-myc* immunomatrix as determined by LC-ESMS	97
5.2	Identification (by in-gel digestion and peptide mass database searching) of serum proteins selected after incubation with the protein G resin	112
5.3	Identification (by in-gel digestion and peptide mass database searching) of serum proteins selected after incubation with the anti-*c-myc* immunomatrix	113
5.4	Identification (by in-gel digestion and peptide mass database searching) of proteins selected after incubation of the 0.1 μg/ml spiked human serum (serum was passed through a 100 kDa filtration unit prior to spiking) with the anti-*c-myc* immunomatrix	119
5.5	Identification (by in-gel digestion and peptide mass database searching) of serum proteins from 100 kDa filtered human serum	119

List of Abbreviations

Ab	Antibody
Ac	Alternating current
Ag	Antigen
API	Atmospheric pressure ionization
BCQ	[(Acryloylamino)propyl]trimethylammonium chloride
BSA	Bovine serum albumin
CCD	Charge-coupled device
CDR	Complementarity determining region
C_H	Heavy chain constant region
α-CHCA	α-Cyano-4-hydroxycinnamic acid
CHO	Carbohydrate chain
CID	Collision-induced dissociation
C_L	Light chain constant region
Cps	Counts per second
CZE	Capillary zone electrophoresis
Da	Dalton
Dc	Direct current
2,5-DHB	2,5-Dihydroxybenzoic acid
DIW	Deionized water
DMP	Dimethyl pimelimidate
DTT	DL-Dithiothreitol
E. coli	*Escherichia coli*

EDTA	Ethylenediaminetetraacetic acid
EOF	Electroosmotic flow
ES	Electrospray
eV	electron volt
FA	Formic acid
Fab	Fragment having the antigen-binding site
Fc	Fragment that crystallizes
HPLC	High performance liquid chromatography
IAC	Immunoaffinity chromatography
Ig	Immunoglobulin
IMAC	Immobilized metal affinity chromatography
LC	Liquid chromatography
MALDI	Matrix assisted laser desorption/ionization
MCP	Microchannel plate
MH^+	Singly protonated molecular ion
MS	Mass spectrometry
MS/MS	Mass spectrometry/mass spectrometry
M/z	Mass-to-charge ratio
NanoES	Nanoelectrospray
NMWL	Nominal molecular weight limit
PAGE	Polyacrylamide gel electrophoresis
PBS	Phosphate buffered saline
q	Collision cell
Q	Quadrupole mass filter

Q-TOF	Quadrupole-time-of-flight
Rf	Radio frequency
RU	Resonance or response units
scFv	Single chain antibody
SDS	Sodium dodecyl sulfate
SIM	Selected ion monitoring
Sinapinic acid	3,5-dimethoxy-4-hydroxycinnamic acid
SPR	Surface plasmon resonance
TEMED	N,N,N′,N′-Tetramethylethylenediamine
TFA	Trifluoroacetic acid
TOF	Time-of-flight
V	Volt
V_H	Heavy chain variable region
V_L	Light chain variable region

List of Amino Acids

Amino Acid		Side Chain Structure	Monoisotopic Mass
Alanine	Ala, A	—CH_3	71.03711
Arginine	Arg, R	—CH_2-$(CH_2)_2$-NH-C(=NH)-NH_2	156.10111
Asparagine	Asn, N	—CH_2-$CONH_2$	114.04293
Aspartic Acid	Asp, D	—CH_2-COOH	115.02694
Cysteine	Cys, C	—CH_2-SH	103.00919
Glutamic Acid	Glu, E	—CH_2-CH_2-COOH	129.04259
Glutamine	Gln, Q	—CH_2-CH_2-$CONH_2$	128.05858
Glycine	Gly, G	—H	57.02146
Histidine	His, H	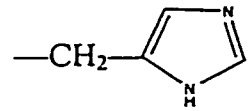	137.05891
Isoleucine	Ile, I	—CH(CH_3)-CH_2-CH_3	113.08406
Leucine	Leu, L	—$CH_2CH(CH_3)_2$	113.08406
Lysine	Lys, K	—CH_2-$(CH_2)_3$-NH_2	128.09496
Methionine	Met, M	—CH_2-CH_2-S-CH_3	131.04049
Phenylalanine	Phe, F	—CH_2-Ph	147.06841
Proline	Pro, P	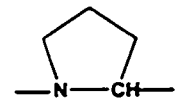	97.05276
Serine	Ser, S	—CH_2-OH	87.03203
Threonine	Thr, T	—CH(OH)-CH_3	101.04768

Tryptophan	Trp, W	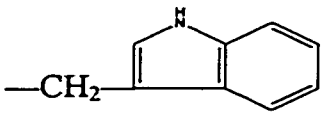	186.07931
Tyrosine	Tyr, Y	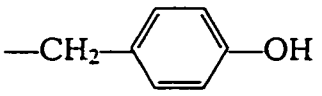	163.06333
Valine	Val, V	—$CH(CH_3)_2$	99.06841

Chapter 1 Theory

1.1 Introduction

The purification of both expressed and native proteins from complex matrices, such as tissue culture media, is often difficult due to the presence of numerous other cellular components and, in the case of expression systems, artifacts of the recombinant protein.[1] The traditional solid-phase and liquid-liquid extraction methods used for protein isolation were generally non-specific, labour-intensive, and often involved extensive sample loss.[2] Immunoaffinity extraction, however, provides a powerful means of selectively removing and preconcentrating target analytes.[1,3]

Immunoaffinity chromatography (IAC) is a separation method that uses antibodies as a part of the stationary phase. The use of this chromatographic method was first reported in 1951 by Campbell and coworkers who used an immobilized antigen to purify antibodies.[4] Today, the high selectivity and availability of antibodies specific to a wide range of molecules has resulted in IAC being used for the isolation and analysis of a number of different analytes such as antibodies, hormones, peptides, and enzymes from a variety of different biological matrices including blood, plasma, and urine.[5,6,7] Immunoaffinity selection has several advantages: 1) due to the high specificity of antibodies, this method can be highly selective; 2) large amounts of sample can be concentrated and purified thereby allowing for detection at levels that may not have been feasible with the original solution; 3) this method can be coupled with numerous chromatographic or detection techniques such as HPLC or mass spectrometry; and 4) the amount of solvent used to remove the target analyte from the matrix sample is minimized.[2]

Since the introduction of 'soft' desorption and ionization techniques, mass spectrometry has become an important tool for the characterization of biomolecules. It is only natural then that mass spectrometry and immunoaffinity extraction should be paired together. The selective preconcentration of the molecule of interest from biological fluids together with mass spectrometry provides a very powerful method for the rapid and sensitive characterization of specific proteins. This methodology was used in this study for the extraction and characterization of biological molecules having an antigen epitope in extracts from *Eschericia coli* (*E. coli*) and human and fetal bovine sera.

1.2 Antibodies

An antibody is a glycoprotein produced by the body in response to foreign molecules. They are mainly produced by plasma cells and travel throughout the blood and lymph where they bind to foreign molecules and are then subsequently removed through phagocytosis by macrophages. Any molecule that can bind to an antibody is known as an antigen. It is estimated that a body can produce between 10^6 and 10^8 types of antibodies with each type being able to bind to a different antigen.[8]

The basic structure of an antibody consists of four polypeptide chains—two identical heavy and two identical light chains—forming a Y-shaped structure (Figure 1.1). The entire unit is held together by disulfide bridges and non-covalent interactions. There are five classes of antibodies—IgG, IgM, IgA, IgE, and IgD—depending on the number of Y-shaped units and the type of heavy chain they contain. A specific immunoglobulin G (having the γ heavy chain) was used for all the

immunoaffinity selections performed in this work, and for the purpose of simplicity the following discussion will pertain to the IgG antibody.

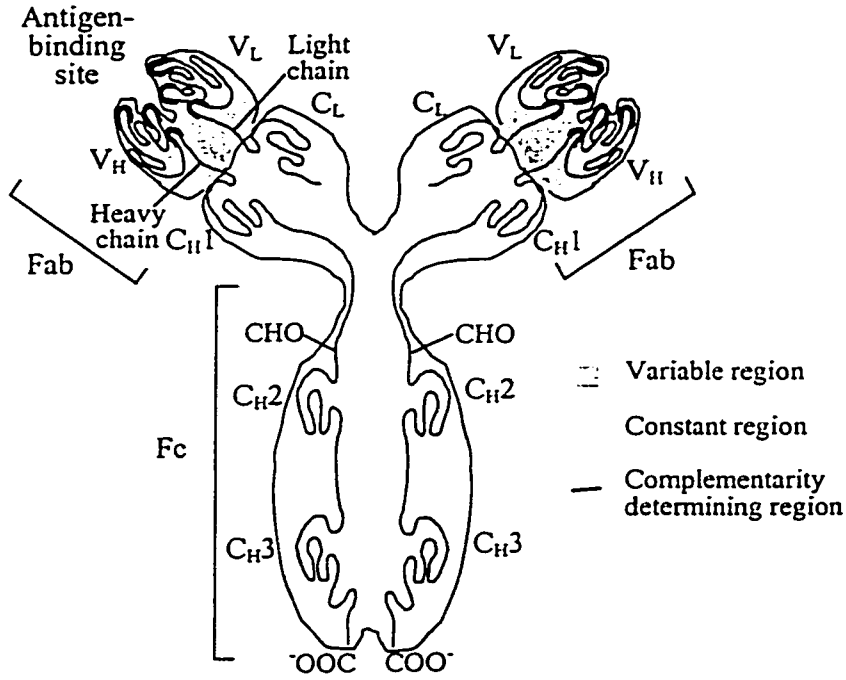

Figure 1.1 A schematic diagram of the immunoglobulin G where V and C indicate the variable and constant regions of the light (L) and heavy (H) chains and CHO represents carbohydrate chains.[9]

Light chains are approximately 220 amino acids long with a molecular mass of 25 kDa. Heavy chains, on the other hand, are approximately 440 amino acids in length and have a molecular mass of 55 kDa. Each chain can be divided into regions of approximately 110 amino acids. For both polypeptide chains, the first amino-terminal region has been found to be heterogeneous in amino acid composition and is known as the variable region. The remaining portions of the respective chains have been shown to be highly conserved and are referred to as the constant regions. The heavy chain constant regions form the Fc (named for the fragment that crystallizes)

domain of the antibody unit. It is here that a number of carbohydrate moieties are found covalently attached to the heavy chains. There are only two types of light chain constant regions, one for κ and one for λ light chains. The type present varies with each antibody type.

The variable regions of one heavy chain and one light chain combine to form an antigen-binding site. Interestingly, the heterogeneity within the variable region does not occur randomly but is concentrated in three short regions on each chain for a total of six hypervariable regions or complementarity determining regions (CDRs) in the antigen-binding site (see Figures 1.1, 3.1, and 4.1). These CDRs consist of the contact residues for the binding of the antigen to the antibody. It is the variability in the amino acid composition of these regions that determines the specificity and binding affinity of the antibody to the antigen. Each IgG antibody has two equivalent sites available for antigen binding.

The region of an antigen that binds to the antibody is referred to as an epitope. The size of the epitope varies and is dependent on the size of the corresponding binding site. Epitopes can be formed by contiguous or noncontiguous amino acid sequences since they exist as surface structures on the antigen.[1,10] For example, a lysozyme-antibody complex showed that the epitope amino acids in contact with the CDRs of the antibody were from two distant stretches of the primary sequence (amino acids 18-27 and 116-129).[10] The interactions between the antibody and antigen are entirely noncovalent and reversible, with the complex being in equilibrium with the nonbound antigens. The equilibrium is that of a reversible bimolecular interaction:

$$Ab + Ag \rightleftarrows Ab\text{-}Ag$$

$$K_A = \frac{[Ab-Ag]}{[Ag][Ab]} \qquad [1]$$

where K_a is the affinity constant, [Ag] is the molar concentration of free antigen, [Ab] is the molar concentration of free antibody, and [Ab-Ag] is the molar concentration of the antibody/antigen complex.[8] The affinity constant for the antibody/antigen interaction is dependent on temperature, pH, and solvent. Interestingly, small changes in the epitope structure resulting in a loss of interaction(s) between the antibody and antigen can severely decrease the affinity of the antibody for the antigen. In addition to amino acids, epitopes composed of carbohydrates, lipids, and nucleic acids have also been identified.[10]

1.3 Immunoaffinity Extraction

Affinity selection generally begins with the covalent immobilization of an antibody onto a solid phase. Once the immunomatrix has been prepared, a sample containing the target analyte is introduced, and the immobilized antibody selectively removes the target analyte(s) from the solution. After rinsing to remove the unbound matrix components, the selected analyte(s) is eluted from the antibody resin. Elution can be achieved by using a competing agent that has a higher affinity for the binding site than that of the bound ligand.[8] Although this method does not alter the activity of the antibody or bound antigen, it has limited use since it is only effective for low affinity antibodies.

The most effective way that antigens can usually be eluted from antibodies is to alter the column conditions such that the antibody-antigen complex is no longer stable.[2,10,11] Acidic buffers (e.g., formic acid or glycine pH 1-3), denaturing agents (e.g., urea) as well as high ionic strength buffers are all commonly used for antigen elution. The choice of elution buffer depends on how quickly the antigen must be released and whether or not the biological activity of the antigen must be preserved. Since mass spectrometry was used for the analysis of the eluted components in this study, denaturation of the antigen during elution was not a concern, rather elution conditions compatible with the operation of the mass spectrometer were selected (volatile and acidic buffers).

1.4 Mass Spectrometry

Mass spectrometry (MS) involves the separation and detection of charged molecules in the gas phase according to their mass-to-charge ratios (m/z). For many years, this versatile analytical tool has been invaluable to numerous fields for the quantitative and qualitative analysis of small molecules. Mass spectral analysis of biomolecules such as proteins has been feasible recently with the advent of "soft" ionization techniques enabling ionization with minimal structural changes. In 1988 two very different techniques—matrix-assisted laser desorption/ionization (MALDI)[12] and electrospray (ES)[13,14]—were introduced for the soft desorption and ionization of proteins. Both techniques are now indispensable methods in biomolecule research offering rapid, simple, and accurate mass measurements for a wide range of compounds including proteins and polymers. Mass spectrometry has

also become a valuable tool for the characterization of the primary structure of proteins and their modifications. Both of these methods will be described in further detail below.

1.4.1 Matrix-Assisted Laser Desorption/Ionization Mass Spectrometry

MALDI ionizes molecules with molecular masses ranging between 100 and 500,000 Da for analysis by mass spectrometry. This instrument provides high sensitivity, high sample throughput, and facile operation.[15,16,17,18] The MALDI ionization technique is shown in Figure 1.2. Initially, the analyte is cocrystallized onto a polished metal surface with a small organic molecule absorbing ultraviolet light (e.g., 2,5-dihydroxybenzoic acid or sinapinic acid). An intense pulsed UV laser beam is then used to desorb and ionize the cocrystallized sample/matrix. Energy from the laser beam is absorbed by the matrix causing the matrix molecules to rapidly expand and dissociate. This dissociation results in the desorption of neutral matrix and sample molecules from the crystal surface into the gas phase. Ionization then occurs by a variety of reactions involving proton and radical transfers between the excited matrix molecules and the analyte molecules to produce singly or multiply charged ions (singly charged ions are typically the most prominent ionic species). The mechanistic details by which the sample desorption and ionization occur are still under investigation. Once ions are formed in the gas phase, they are directed to the mass analyzer.

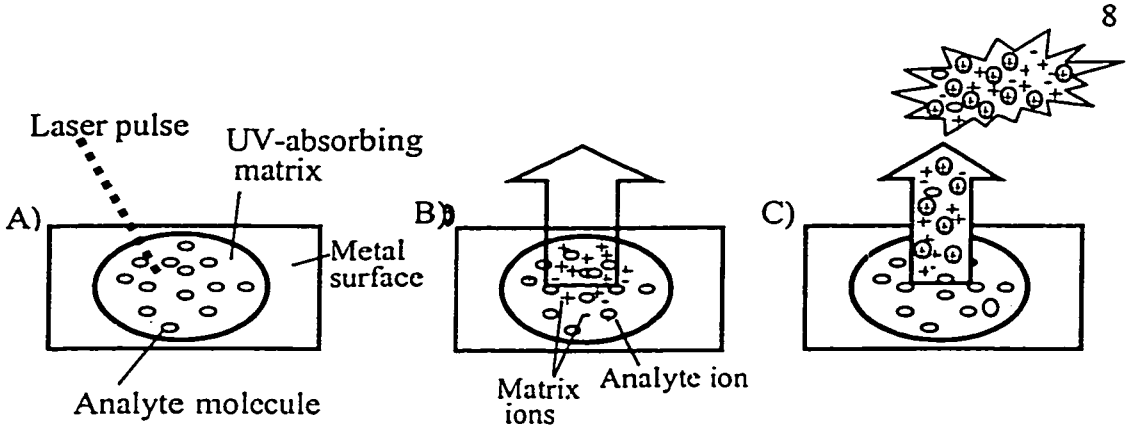

Figure 1.2 Schematic mechanism of MALDI. A) Matrix absorption of ultraviolet radiation resulting in B) the ionization and dissociation of the matrix and phase change into gaseous state. C) The matrix further expands into the gaseous state taking the analyte with it during which the transfer of charge from the matrix to the analyte is occurring.

Typically MALDI is used in conjunction with a time-of-flight (TOF) mass analyzer (Figure 1.3). These analyzers are relatively simple consisting of a long straight tube (1.3-4.2 m) with an ion source at one end and a detector at the other. A pulse of ions from the ion source is accelerated to a common kinetic energy in an electrostatic field and is then directed into the field-free flight tube. Lighter ions travel more quickly down the tube than the heavier ions and therefore hit the detector first. The masses of the ions can be determined from the respective flight times using the relationship:

$$m = \frac{2qVt_m^2}{l^2} \qquad [2]$$

where m is the ion mass, q is the charge on the ion, V is the acceleration potential, t_m is the travel time of the ion from the source to the detector, and l is the length of the flight tube.

Ions of a common mass generated by the MALDI source do not all have exactly the same kinetic energy.[17] A broad distribution of velocities is observed which results

in a corresponding variation in arrival time at the detector. The net result of this is a degradation in both resolution and mass accuracy. This situation can be improved by using an ion mirror to reflect the ions back towards a detector located near the ion source. Ions with a higher kinetic energy will penetrate the ion mirror further than those with lower kinetic energies thereby focusing the ions of a common mass at the detector. This mode of operation is referred to as "reflectron" (Figure 1.4). The mass resolution and mass accuracy is superior using the reflectron compared to the linear TOF mode. Above a mass-to-charge ratio of 10,000, large ions generally decay into smaller fragments during the increased flight time resulting in poorer resolution.

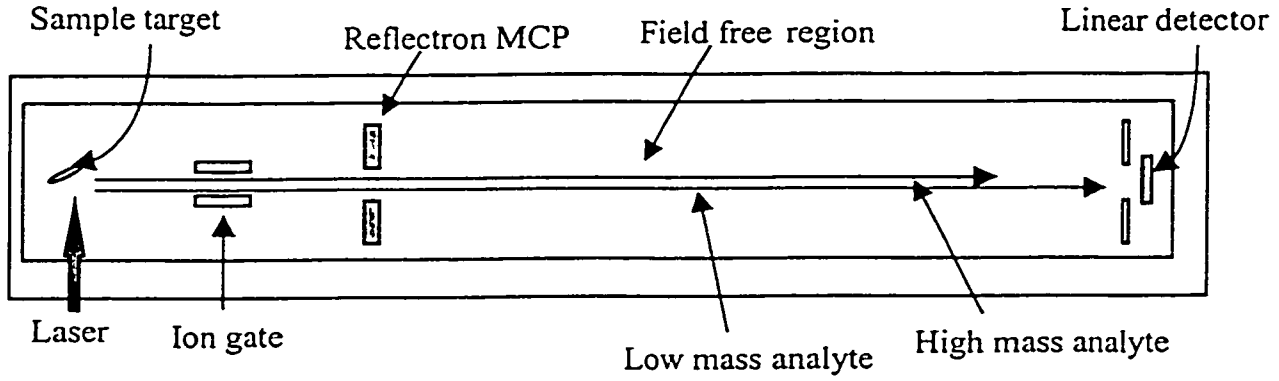

Figure 1.3 Time-of-flight mass analyzer coupled with MALDI in linear mode.

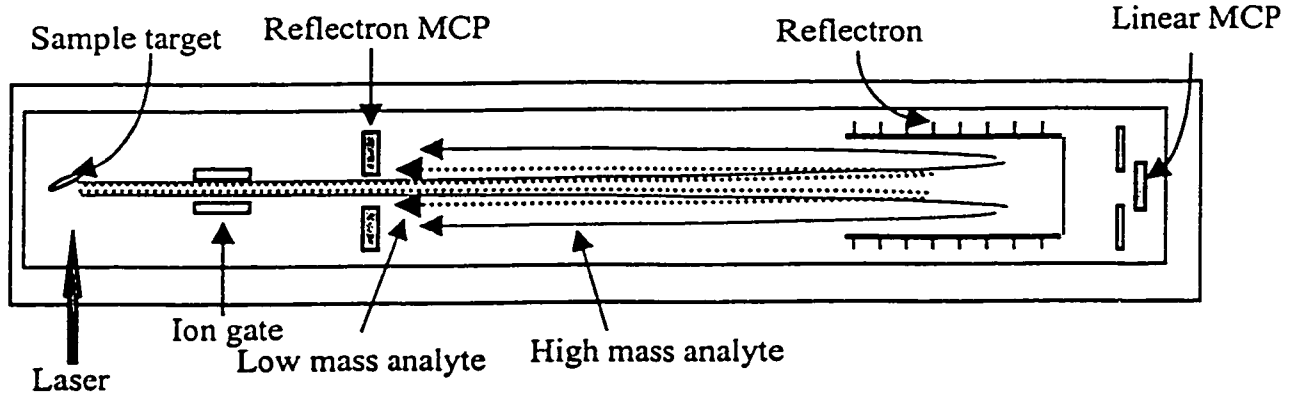

Figure 1.4 Time-of-flight mass analyzer coupled with MALDI in reflectron mode.

MALDI-MS has become a central tool in the routine analysis of biomolecules including proteins, peptides, carbohydrates, and oligonucleotides. This technique offers picomole to femtomole sensitivity with a mass accuracy of ± 0.01%.[15,16,17,18] For molecules with a molecular mass less than 10 kDa, a mass resolution of 15,000 can be achieved.[18] A decrease in resolution is observed with increasing molecular mass resulting in a resolution of less than 1000 for molecules with masses greater than 20 kDa. MALDI-MS also offers the advantage of rapid analysis of biological samples without the need for extensive purification. Buffers and salts (mM levels) can often be tolerated without a severe drop in sensitivity. In addition, MALDI-MS is able to analyze complex mixtures, producing spectra that are not complicated by multiply charged species or fragmentation. Unfortunately, MALDI-MS is not often effective for the analysis of species with a mass-to-charge ratio less than 700 due to interference from matrix molecules. Quantitation by MALDI-MS is often difficult due to the heterogeneity of the matrix/sample crystal and the resulting non-reproducibility of sample signals.

1.4.2 Electrospray

Electrospray (ES) involves the transfer and ionization of molecules from the liquid phase to the gas phase. This interface requires a constant delivery of liquid and is therefore ideal for coupling with separation techniques such as liquid chromatography or capillary electrophoresis. Both of these methods offer the advantage of cleaning up and concentrating the sample prior to its introduction to the mass spectrometer.

The sample solution flow rate in an electrospray interface is usually in the 1-10 μl/min range. The key feature of this process is the formation of multiply charged species depending on the number of sites available on the molecule for protonation.[19] Electrospray of proteins produces a series of peaks each spaced by the addition or subtraction of a proton to the native molecule. From these different m/z values the molecular mass of the protein can be determined simply by using the charge states of two proximal molecular ions in the charge series. This can be done automatically by the appropriate software with an accuracy of ± 0.01% (using a quadrupole mass analyzer—Section 1.4.4). When configured with ES, mass analyzers having a mass-to-charge range of ≤ 3000 can be used to analyze proteins having masses up to 200 kDa since multiple charging brings the m/z values within the range available with common mass analyzers. However, the observation of these multiple charge envelopes produces complex spectra that can often be difficult to deconvolute when two or more envelopes overlap.

Electrospray involves the transition of sample molecules from solution into an electrically charged aerosol (Figure 1.5).[20] A solution of analyte molecules is passed through a capillary that is held at a potential of several kV. Assuming a positive potential, positive species within the solution will build up at the liquid surface resulting in an instability of the liquid. A Taylor cone results since the positive ions are drawn downfield, but cannot escape the liquid surface. At a sufficiently high potential the Coulomb repulsion forces are large enough to overcome the surface tension at the liquid surface and small (< 1 μm) charged droplets are emitted from the Taylor cone into dry air or nitrogen at atmospheric pressure. The size of the droplets

is determined by the applied potential, the flow rate to the capillary, and the solvent properties.

Evaporation of the solvent from these droplets follows as they travel the pressure and potential gradient towards the mass analyzer, with collisional warming preventing freezing.[21] As the diameter of these droplets decreases, a point (Rayleigh limit) is reached at which the charge density is large enough to overcome the surface tension holding the droplet together, and fission (Coulomb explosion) occurs. Through repeated evaporation and fission it can be postulated that a solvent-free single ion results. A second mechanism for gas-phase ion production has been proposed in which ion emission is believed to occur from small, highly charged droplets.[22] After adequate evaporation of solvent the solute ions escape (evaporate) from the liquid phase into the gas phase.

Nebulization of the solution leaving the capillary may be assisted by a sheath flow of nebulizer gas (e.g., nitrogen). This technique is known as 'ionspray'.[23] The necessity of a nebulizer gas is determined by the flow rate and solvent used as well as the sign of the potential applied to the capillary tip (it is often necessary for negative ion analyses).

Compared to MALDI-MS, electrospray is very sensitive to the presence of salts.[24] Ionic buffers in the sample can disturb the spraying process and compete with the sample for charges. The presence of involatile species can hamper the desorption process by forming a solid core in the sprayed droplet thereby trapping analyte ions. The ability to couple liquid chromatography and capillary electrophoresis to the

electrospray interface, however, allows for the on-line desalting and concentration of samples.

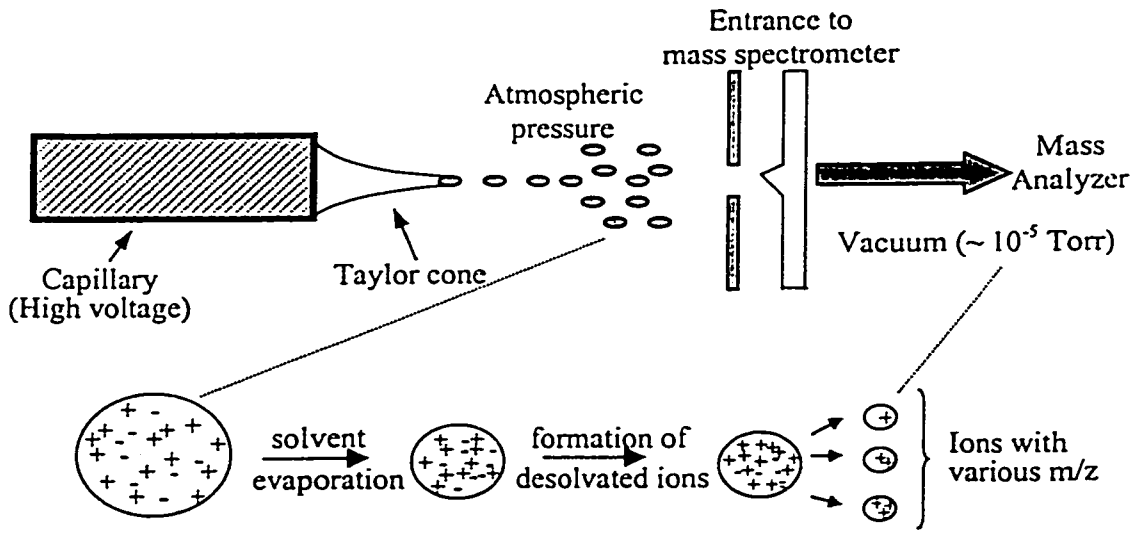

Figure 1.5 Schematic diagram of electrospray ionization.[20,21,22]

1.4.3 Nanoelectrospray

It has been shown that lowering the flow rates used with electrospray results in improved sample sensitivity.[25] To further lower the flow rates delivered to the mass spectrometer and further increase the sample sensitivity, a new electrospray ion source–nanoelectrospray (nanoES)–was developed by Mann and coworkers.[26] This interface involves the use of borosilicate capillaries tapered to a fine tip (~ 1-2 μm inner diameter) and coated with gold for electrical conductivity. The tapered capillaries used with nanoelectrospray act as sample reservoirs without the presence of solvent pumps or inlet valves to force the flow of the sample. With electrospray emitters of such small inner diameters, the flow rate is determined by the electrospray

process itself and operates at low nl/min flow rates (20-40 nl/min).[27] The low flow rate provides a long measurement lifetime at a steady signal level (1-2 μl of sample can last 30-120 min) with reduced sample consumption (0.2-2 μl of sample). A backing gas pressure can be used to aid the flow stability especially for samples having a high salt content (up to 0.1 M). The small inner diameter of the nanoES capillaries produces droplets with volumes 100-1000 times smaller (< 200 nm) than observed with conventional electrospray ion sources. As a result, the charge-to-volume ratios within the droplets are higher and desolvation occurs more rapidly leading to increased sensitivity (Mann and coworkers reported ~ 2 orders of magnitude greater ionization efficiency for nanoES than for the conventional ES ion source).[26] Because of the small inner diameters of these capillaries, however, capillary tip blockage is frequent and sample filtration is often necessary.

1.4.4 Quadrupole Mass Analyzers

The mass analyzer most commonly used with electrospray and nanoelectrospray ion sources is the quadrupole mass filter (Figure 1.6). These analyzers are generally more compact, less expensive, and more rugged than other analyzers (e.g., magnetic sector).[28] They also have low scan times (< 100 ms) which is important for real-time analysis of chromatographic peaks.

Mass separation is accomplished by creating an electric field in which ions of specific mass-to-charge ratios have stable trajectories through the field. This electric field is established using four cylindrical metal rods (quadrupoles) as the electrodes of the mass filter. A direct current (dc) voltage and an oscillating voltage (ac voltage at

radio frequencies (rf)) are placed on the rods with the adjacent rods having opposite polarity. Ions pass through the center of the electrodes in a circular motion along the length of the rods. The ion trajectories within the quadrupole field can be described mathematically by the Mathieu equation:

$$\frac{d^2u}{d\xi^2} + (a - 2q\cos 2\xi)u = 0 \qquad [3]$$

$$\xi = \frac{\omega t}{2} \qquad a = a_x = -a_y = \frac{8eU}{m\omega^2 r_o^2} \qquad q = q_x = -q_y = \frac{8eV}{m\omega^2 r_o^2}$$

where u is the ion trajectory in either the x or y axis, ω is the angular frequency $2\pi f$ (f is the rf frequency), t is time, U is the dc potential, m is mass, r_o is the half distance between the rods, and V is the rf voltage.

The solution for u indicates that the oscillations of the ions within the quadrupole field have either 1) a finite amplitude in the x and y axes resulting in the passage of the ions through the quadrupole field or 2) amplitudes increasing rapidly with time resulting in the ions impacting the quadrupoles. By increasing the magnitude of the dc and rf voltages while maintaining a constant dc-to-rf ratio, stable trajectories allow ions of varying mass-to-charge ratios to pass through the quadrupoles for detection. The mass resolution may be optimized by adjusting the dc-to-rf ratio. Resolution is dependent on the number rf cycles an ion spends in the field; however, with an increasing number of cycles, ion transmission and therefore sensitivity is sacrificed.

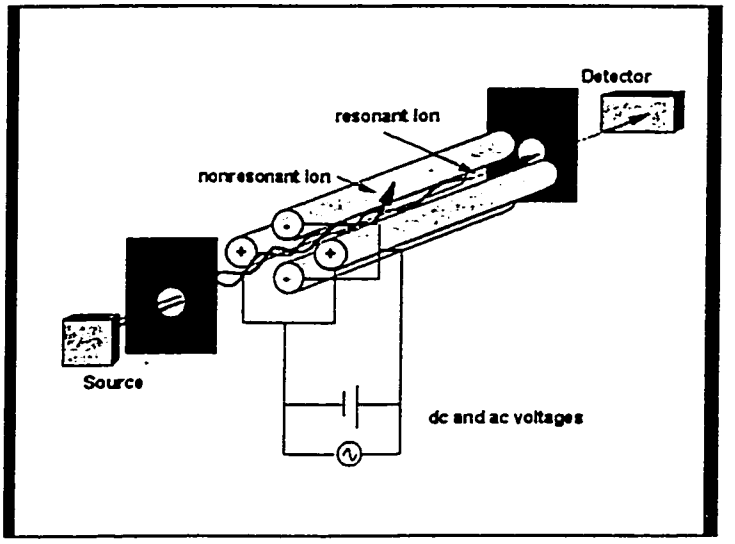

Figure 1.6 Schematic diagram of a quadrupole mass analyzer.[29]

1.4.5 Tandem Mass Spectrometry

Quadrupole mass filters are often coupled together. The most common configuration is the triple-quadrupole instrument in which three single quadrupole analyzers are placed in tandem. Often the second quadrupole mass filter (q) is operated with only a radio frequency potential. The lack of the dc voltage means that ions of all mass-to-charge ratios will have stable trajectories through the filter. This quadrupole can be enclosed in a cell allowing the pressure to be raised to a level where multiple, low-energy collisions between the ions (10-50 eV) and an inert gas such as argon can be performed. As a consequence of these collisions, the internal energy of the ion is increased, and structurally informative fragmentation of this ion may result (collision-induced dissociation). Tandem mass spectrometers are most commonly used in the product ion scanning mode in which the first quadrupole mass

filter (Q1) is set such that only ions of a specific mass-to-charge ratio pass through the reaction cell. The third quadrupole (Q2) is scanned to provide the mass spectrum of the fragment ions (this mass spectrum is referred to as a product ion spectrum). Other common modes of tandem mass spectrometry include precursor ion and constant neutral loss scanning, both of which were not used in this investigation.

1.4.6 Quadrupole-Time-of-Flight Mass Analyzers

The quadrupole and time-of-flight mass analyzers have also been coupled together to produce a hybrid tandem instrument.[30] The quadrupole time-of-flight mass spectrometer consists of a quadrupole mass filter followed by a hexapole collision cell and an orthogonal-acceleration time-of-flight tube in reflectron geometry for mass analysis (Figure 1.7). For conventional mass spectrometric analysis, the quadrupole filter is operated in rf-only mode with mass analysis being performed by the TOF analyzer. For tandem mass spectrometry, the quadrupole is operated as a mass filter in which only ions of a selected mass-to-charge ratio are transmitted into the collision cell. The resulting fragment ions are then focused through a hexapole filter operated in rf-only mode and pulsed at a frequency of typically 16 kHz into the time-of-flight tube operating in reflectron geometry for mass analysis. This instrument design alleviates the inherent sensitivity and resolution problems associated with the triple quadrupole arrangement. The use of the time-of-flight mass analyzer allows for the simultaneous detection of fragment ions (contrary to the quadrupole analyzer, which must be scanned over the mass range of interest) at good resolution over a broad mass range (3000 Da). Mass accuracies of ± 0.05 Da

with resolution > 5000 have been routinely reported.[30,31,32] As a result, the differentiation of isotopes as well as the determination of singly-, doubly-, and triply-charged species can be easily achieved. When interfaced with a nanoelectrospray ion source, low femtomole-attomole sample quantities have been analyzed successfully.[31,33] The good signal-to-noise ratios, high resolution, and sensitivity observed with this instrument makes it an ideal choice for the sequencing and identification of proteins from their proteolytic digests.

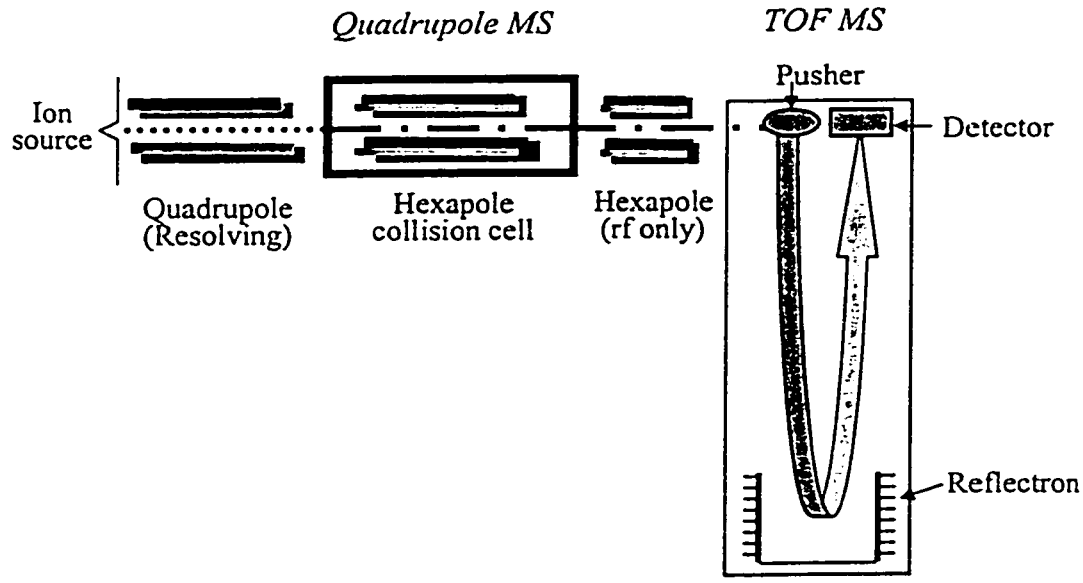

Figure 1.7 Schematic diagram of the quadrupole/orthogonal-acceleration time-of-flight mass spectrometer.

1.5 Protein Identification using MALDI-MS and/or ES-MS with Database Searching

The introduction of the soft ionization techniques of MALDI and ES coupled to various mass analyzers has revolutionized the analysis of biomolecules from complex biological mixtures. Mass spectrometry, in conjunction with database searching, is now routinely used for the characterization and identification of proteins and peptides

isolated from biological sources. Identification usually begins with the isolation of the protein or proteins of interest from complex mixtures using techniques such as gel electrophoresis or immunoaffinity extraction. The protein is then enzymatically digested (e.g., using trypsin) to produce a series of peptides that can be used in the identification of the protein.

1.5.1 Peptide Mapping

The high sensitivity (fmol) and ease of operation of MALDI-MS has made it an ideal tool for the relatively rapid identification and characterization of proteins by peptide mapping. Mass values obtained for the digestion products of an 'unknown' protein can be compared with lists of peptide masses expected from known protein sequences exposed to the same digestive enzyme. Search programs such as ProteinProspector and PeptideSearch are designed to perform searches of protein databases using the peptide mass data obtained by either MALDI-MS or ES-MS. Accurate protein identification has been obtained with only 7% of the total protein masses used in the database search.[34] Peptide mass mapping is dependent on the mass-to-charge ratios measured for the peptides obtained from the protein digestion. Unfortunately, in some situations only a small number of peptides are detected, thereby rendering mass mapping ineffective. This technique is also limited to a single protein per gel spot since analysis of the digestion of a protein mixture is difficult. Sequencing of the detected peptides can then be performed in order to obtain sequence information for database searching (Section 1.5.2).

1.5.2 Peptide Sequencing using Tandem Mass Spectrometry

Protein identification can also be accomplished by the use of sequence tags in database searching. The combination of liquid chromatography with tandem mass spectrometry results in a powerful tool for the separation, clean-up, and sequencing of complex peptide mixtures obtained from the enzymatic digestion of a protein.[34,35] This approach offers several advantages in comparison to the traditional sequencing method of Edman degradation. The speed, sensitivity, the ability to attain sequence information on peptide mixtures that are not completely resolved by liquid chromatography, and the ability to obtain sequence information for peptides with blocked N-termini makes this method highly favorable for the characterization of proteins and their post-translational modifications.

The multiple, low-energy collisions experienced between the peptide ions and the neutral gas in the reaction cell during collision-induced dissociation vibrationally excite the peptides causing them to fragment at the amide bonds (Figure 1.8).[36] A ladder of sequence ions results in which the mass difference between the consecutive ion signals indicates the amino acid at that position in the sequence. A variety of predicted ion types can be produced during the fragmentation process in which the charge is either retained on the C-terminus to produce y-type ions or on the N-terminus to produce b-type ions. Determination of the peptide sequence from the MS/MS spectrum requires the interpretation of whether or not the ions originate from the N- or C-terminus. It has been shown that the position of basic amino acid residues (e.g., lysine and arginine) within the peptide decides the type of ion that is formed.[35] If arginine or lysine is present at the N-terminus, then b-type ions are

typically prominent, and if they are present at the C-terminus then y-type ions generally dominate the spectrum. If these basic residues are present near the middle of the peptide then a mixture of both types of ions may be observed. Under low-energy collisions c, x, and z fragment ions are rarely observed.

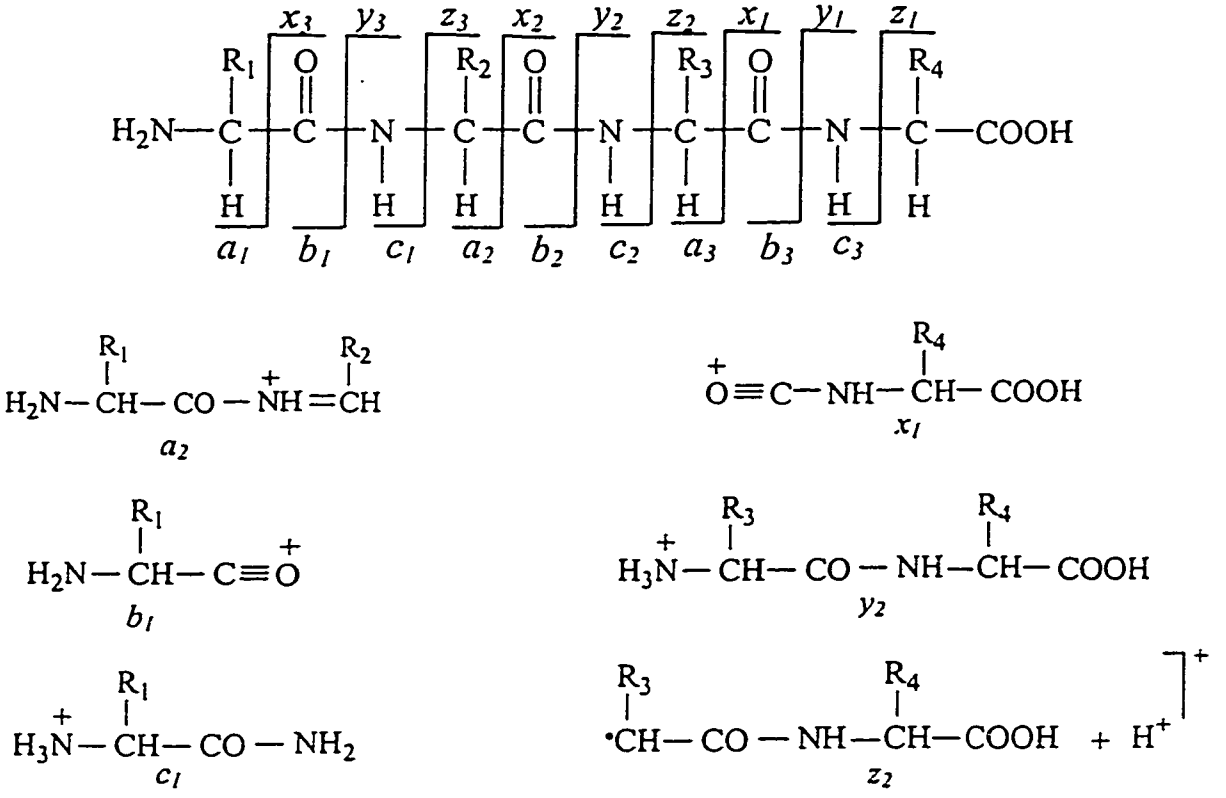

Figure 1.8 Characteristic peptide fragment ions in tandem mass spectrometry.

A short stretch of amino acids (two or three residues) together with the peptide mass and the position of the sequence tag in the peptide are sufficient to identify a protein from protein and nucleotide sequence databases such as SEQUEST.

1.5.3 Database Searching

The large-scale genome sequencing effort has led to the establishment of extensive databases containing the predicted sequences of proteins along with those

determined experimentally for known proteins. These databases are constantly growing and being updated. There are numerous computer algorithms (e.g., SEQUEST, ProteinProspector, and EMBL's PeptideSearch) available both commercially and through the internet that search these databases using mass spectral data obtained from protein digests in order to identify the protein of interest. These algorithms offer many variables that can be adjusted by the operator in order to reduce the number of 'hits' obtained. These include mass tolerance for the parent peptide mass and its fragment ions, the number of 'errors' (unidentified masses) that can be tolerated, the choice of the proteolytic enzyme used, the presence of chemical modifications such as phosphorylation or carboxyamidomethylation, the species source of the protein, the type of mass spectrometer used, and the databases searched. Scoring algorithms such as MOWSE (for peptide mass mapping) are used to indicate the degree of fit between the 'database hits' and the experimentally determined data.

1.6 Capillary Zone Electrophoresis (CZE)

Since its introduction CZE has become an important tool for the analysis of a wide range of molecules. The inherent characteristics of capillary zone electrophoresis include small sample size requirement (nl), high analysis speed, separation efficiency, low solvent consumption, and high recovery.[37] Because of the versatility of this separation technique, it has been used successfully in the separation and analysis of a wide range of substances including drug metabolites, peptides and proteins, carbohydrates, inorganic ions, and DNA.[38]

In CZE a fused-silica capillary column with an internal diameter ranging from 25-100 μm is filled with an electrolytic buffer containing the sample analytes and placed between two buffer reservoirs (Figure 1.9). An electric field (typically 300 V/cm) is established across the capillary length resulting in the migration of the charged particles towards the detector. Analyte species are separated due to differences in charge, size, and shape. The migration velocity of ions through the capillary is determined by the electroosmotic flow of the buffer solution and the electrophoretic velocity of the individual ions.

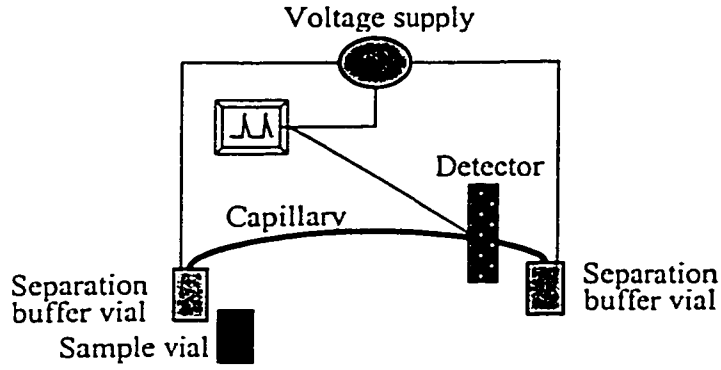

Figure 1.9 Schematic diagram of capillary electrophoresis instrumentation.[39]

When a charged particle is exposed to an electric field (E), it encounters a force which is proportional to the electric field strength and the charge on the ion (q). The resulting movement of the particle is opposed by the frictional forces that are proportional to the velocity of the particle (v), the hydrodynamic radius of the particles (r), and the medium viscosity (η). The electrophoretic mobility (μ_e) of the particle is given by:

$$\mu_e = \frac{q}{6\pi\eta r} \qquad [4]$$

while the overall velocity of the ion is the product of the electrophoretic mobility and the applied electric field.

Electroosmotic flow (EOF) is the result of the electric double layer that develops at the capillary/solution surface (Figure 1.10). In fused-silica capillaries, the silanol groups are negatively charged for pH > 2.6. The second layer of the electric double layer is formed by the attraction of positive ions from the buffer to the negative surface of the capillary. A portion of these positive buffer ions is firmly held to the capillary surface by electrostatic forces and forms what is known as the Stern layer. In the presence of the electric field, the surrounding diffuse layer will move towards the appropriate electrode carrying solvent molecules with it. Electroosmotic flow produces a nearly flat flow profile and therefore does not contribute to band broadening the way that hydrostatic flow does in liquid chromatography. The EOF velocity (v_{eof}) is given by the Helmholtz-Smoluchowski equation:

$$v_{eof} = \frac{\varepsilon \zeta}{\eta} E \qquad [5]$$

where ε is the dielectric constant of the electrolyte and ζ is the potential drop between the Stern layer and the bulk solution. EOF is typically measured using a neutral analyte that has no electrophoretic mobility and therefore will only be carried through the capillary by the electroosmotic flow. Positive species move through the capillary at a velocity greater than the EOF due to their electrophoretic attraction to the negative electrode. Neutral species travel with the EOF, while negative species are repulsed by the negative electrode and move at rates slower than the EOF.

Sample is injected into the capillary by either hydrodynamic or electrokinetic means. In hydrodynamic injection, a pressure difference is applied across the capillary while the capillary is immersed in the sample. This type of injection is dependent on the injection time, capillary dimensions, applied pressure, and sample viscosity. In electrokinetic injection, a voltage is applied across the capillary while one end of the capillary is in the sample reservoir and the other is in the buffer reservoir. The amount of sample injected is dependent on the electrophoretic mobility of the analyte species, the conductivity of the sample solution, and the electroosmotic flow.

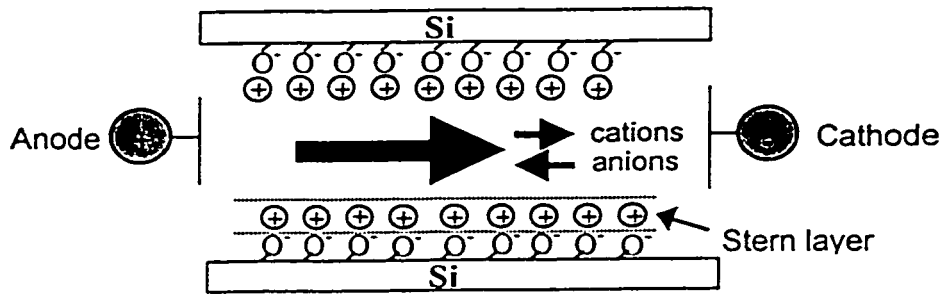

Figure 1.10 Schematic diagram showing the phenomenon of electroosmotic flow.

As discussed earlier, the formation of the electric double layer is a vital element in establishing the electroosmotic flow and the mobility of the ions through the capillary. Unfortunately, any electrostatic or hydrophobic interactions between the analyte and the capillary wall will result in peak tailing and a loss in sensitivity. For proteins and peptides, this is particularly problematic since these molecules contain various hydrophobic and charged sites. This problem can be remedied by covalently altering the surface of the capillary such that these interactions are no longer possible. In the CZE analyses performed in this study, the capillary was modified with the

positively charged coating [(acryloylamino)propyl]trimethylammonium chloride (BCQ) which reverses the direction of the electroosmotic flow thereby requiring the reversal of the applied voltage polarity. These conditions are also conducive with separation using acidic buffers and thus facilitates coupling to electrospray mass spectrometry.

1.6.1 Sensitivity Enhancement for Capillary Electrophoresis

Trace level analysis by CZE has been restricted by poor detection limits. The short optical pathlengths (typically ~ 50 μm internal diameter) used with ultraviolet-visible (UV-Vis) detection results in limits of detection on the order of 10^{-4} to 10^{-6} M.[40,41,42] Sensitivity can be enhanced using alternative detectors such as laser-induced fluorescence or electrochemical detection. However, these detectors are only useful with analytes that have the required detection characteristics. On-line sample concentration techniques involving the injection of increased sample amounts without sacrificing separation efficiency have also been investigated for the improvement of CZE sensitivity. Sample stacking, in the form of isotachophoresis and field amplification, as well as on-line chromatographic packing has been used to enhance sensitivity.[40,42,43,44] Field amplification methodology was utilized for the purposes of sample concentration in CZE experiments carried out in this study due to its ease of use, compatibility with the instrumentation, and ability to enhance sensitivity by up to several hundred-fold over conventional CZE.[44]

Field amplification involves the introduction of a large sample plug (typically half the volume of the capillary) using hydrodynamic injection. By reversing the polarity

and direction of the applied field, the sample is focused at the inlet end of the capillary, and the sample buffer is discarded into a waste vial. When the observed current has reached 80-90% of the separation current, the polarity is reversed to effect zone electrophoresis separation toward the detector. With amine coated capillaries, a negative voltage is applied at the inlet end during separation since the direction of electroosmotic flow is reversed (anodal EOF). As a result, the anions as well as the sample buffer are mostly removed into the inlet buffer reservoir prior to the polarity reversal. This method has been shown to improve the limit of detection by at least one order of magnitude over that observed with conventional stacking methods.[44]

1.7 Surface Plasmon Resonance Optical Sensors

Understanding biological processes at the molecular level involves the areas of structural characterization and functional investigation. The development of surface plasmon resonance (SPR) for biological applications has revolutionized the study of biomolecular interactions. SPR is a very sensitive technique for the real-time monitoring of these interactions without having to label the biomolecules for detection. In addition, molecules such as proteins, peptides, nucleic acids, or carbohydrates do not need to be purified prior to analysis but can be studied directly within the crude cellular extracts. The development of the commercial SPR instrument has led to the widespread use of this technique for immunological analyses, studies of protein-protein interactions, concentration measurements, epitope mapping, the determination of affinity constants, and the measurement of binding kinetics.[45,46]

This technique involves the excitation and propagation of charge-density oscillations (plasma waves) at the interface of two media of opposite dielectric constants, such as metal and water. The commercial instrument (Biacore) for SPR analyses involves directing light of a fixed wavelength through a glass prism onto a glass surface covered with a thin gold film (Figure 1.11). The other surface of this glass sensor chip forms one wall of a micro-flow cell. One interactant (e.g, antibody) is immobilized in a dextran matrix on this side of the chip (opposite to the gold film) exposed to the flow cell. The sample containing the other interactant (e.g., antigen) is then injected over the immobilized surface in a controlled flow. Biomolecular interactions cause a change in the refractive index of the immobilized surface, which in turn affects the surface plasma resonance. SPR causes a reduction in the intensity of the reflected light observed at specific wavelength and angle combinations which is detected by linear arrays of charge-coupled devices (CCDs). As a result, interactions at the immobilized surface are measured continuously as changes in the SPR (measured in response units—RU). The change in response observed with interactions is related to the change in the mass concentration of the surface layer. The response is generally the same for all proteins and peptides, therefore, variation in response is a function of the interaction properties of the molecule immobilized on the surface and the sample analyte as well as the amount of analyte binding.

The progress of an interaction is monitored such that the binding of an analyte produces an increase in signal with time, while the dissociation of the interaction can be monitored as a decrease in signal when the sample is replaced by a continuous flow of buffer. The immobilized surface can be regenerated and generally reused up

to 100 times depending on the stability of the immobilized ligand. Detection limits in the picomolar range are typical with only microliter (25-150) quantities of sample and 1-5 μg of the immobilized ligand being required.[45,46]

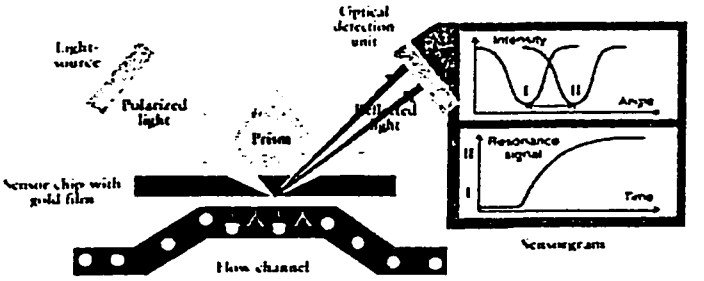

Figure 1.11 Schematic diagram showing how the phenomenon of surface plasmon resonance is used for the measurement of intermolecular interactions.[47]

The speed, reproducibility, low sample consumption, and ability to analyze samples in crude preparations make this technique ideal for studying immunoaffinity binding. Either the antibody or antigen can be immobilized on the dextran matrix while the sample is passed over the surface to determine the affinity constant, necessary elution conditions, antibody or antigen concentration, to probe the activity of the antibody, or for epitope mapping. A major limitation of this method in all applications is a low sensitivity to low molecular weight species. Therefore, the surface concentration of these small molecules must be large in order to facilitate detection.

1.8 Summary

The use of immunoaffinity extraction for the purification of a variety of molecules from various biological and environmental sources continues to grow. The current

trend in this field, however, involves the interfacing of immunoaffinity chromatography with other chromatographic techniques as well as with on-line detection. Mass spectrometry is an ideal tool to use with immunoaffinity extraction because of its sensitivity, resolution, and sequencing capacity for the identification and characterization of the selected proteins.

An immunoaffinity matrix involving anti-*c-myc* mouse monoclonal IgG1 antibody was developed and used in conjunction with mass spectrometry for the selective preconcentration of wild-type and recombinant single chain antibodies from *E. coli* extracts and subsequent identification of point mutations. The developed methodology was also used for the selection and identification of the *c-myc* peptide from human and fetal bovine sera at ng/mol concentrations. In addition, extraneous sera and *E. coli* proteins eluted from the immunomatrix were identified using mass spectrometry followed by database searching.

Chapter 2 Experimental Procedures

2.1 Chemicals and Materials

Fused-silica capillary was purchased from Polymicro Technologies (Phoenix, AZ) and Teflon tubing from LC Packing (San Francisco, CA). The wash buffer reagents such as ß-alanine, sodium deoxycholate, tween, nonidet P-40, and 1-*O*-Octyl-β-D-glucopyranoside as well as trifluoroacetic acid (TFA), ethanolamine, dimethyl pimelimidate (DMP), HEPES, imidazole, male human serum (type AB) and fetal bovine serum were all purchased from Sigma (St. Louis, MO). Ammonium bicarbonate, acetonitrile, sodium borate, sodium azide, guanidine hydrochloride, and ethylenediaminetetraacetic acid (EDTA) were obtained from Fisher Scientific (Hampton, NH). Hydrochloric acid, formic acid, acetic acid, citric acid, acetone, ethanol, sodium hydroxide, sucrose, magnesium chloride, sodium chloride, calcium chloride, nickel chloride, β-mercaptoethanol, and PBS salts were purchased from BDH Inc. (Darmstadt, Germany). Eppendorfs were obtained from Diamed Lab Supplies Inc. (Mississauga, ON). All matrices used for MALDI-MS were obtained from Aldrich (Milwaukee, WI). Distilled and deionized water was prepared from a UHQ water filtration system (USF Elga, Lowell, MA). All pH measurements were obtained using an Accumet Basic pH meter (Fisher Scientific).

For protein digestion, the trypsin was purchased from Promega (Madison, WI) while the endoproteinase Glu-C was obtained from Boehringer Mannheim (Laval, PQ). Reduction and alkylation of the protein was achieved using DL-dithiothreitol and iodoacetamide (Sigma).

For the modification of the fused silica capillary, [(Acryloylamino)propyl]-trimethylammonium chloride (BCQ) was purchased from Chemische Fabrik Stockhausen

(Krefeld, Germany) while the 7-oct-1-enyltrimethoxysilane was obtained from United Chemical Technologies Inc. (Bristol, PA). N,N,N',N'-Tetramethylethylenediamine (TEMED) was purchased from Aldrich, and ammonium persulfate was obtained from Sigma.

Standard protein and peptide mixtures were prepared for use in the development of the affinity selection procedures. All these standards were purchased from Sigma. The standard peptide mixture consisted of an equimolar solution of *c-myc* peptide, [Glu^1]-fibrinopeptide B, bradykinin, angiotensin II, and [Gln^{11}]-amyloid β-protein fragment 1-16. The standard protein mixture consisted of an equimolar solution of scFv antibody, β-lactoglobulin A, α-lactalbumin, lysozyme, and bovine serum albumin (BSA).

Mouse ascites fluid containing the monoclonal anti-*c-myc* (mouse IgG1 isotype) antibody was grown in-house according to published protocols[10] and purified using Protein A chromatography (Section 2.2). The scFv mutants were produced in-house by site-directed mutagenesis, and most were received as the shock buffer periplasmic extracts of *E. coli*. The *c-myc* peptide was synthesized in-house using standard FMOC solid phase synthesis. The 9E10 (anti-*c-myc*) peptide was purchased from BabCO (Richmond, CA).

2.2 Antibody Purification

The anti-*c-myc* antibody was purified from frozen mouse ascites fluid using protein A chromatography. After thawing, 4 ml of the ascites fluid was diluted three-fold in 20 mM phosphate buffer (pH 7) and centrifuged for 20 minutes at 10,000 rpm to remove any lipids. The HiTrap protein A column (Pharmacia Biotech, Baie d'Urfé, PQ) was connected to an HPLC pump system (LKB Bromma 2150, Bromma, Sweden) for the delivery of solutions, and a LKB Bromma 2151 variable wavelength absorbance detector was used to monitor sample application and elution (280 nm). After equilibration of the protein A column with

the phosphate buffer, the ascites supernatant was applied at a flow rate of 0.8 ml/min. The column was then washed with the phosphate buffer until baseline absorbance was observed. Elution of the antibody was achieved with the application of 0.1 M citric acid buffer (pH 3). The pH of the collected antibody was adjusted to 6 with 0.2 M Tris buffer (pH 8), and the concentration was determined by absorbance spectrophotometry. The antibody was then dialyzed against PBS buffer. All solutions were filtered through a 0.45 μm membrane before injection on the protein A column.

2.3 Antibody Coupling to Solid Phase

A variety of solid phase supports were used in the development of the anti-*c-myc* IgG1 immunomatrix. Each matrix involved different coupling methods for immobilization of the antibody onto the solid support. The coupling conditions for the immunomatrices investigated are described in the following sections.

2.3.1 Amine Coupling with 1,1'-Carbonyldiimidazole Activated Beads

Reacti-gel was purchased from Pierce (Rockford, IL) as a 6% crosslinked agarose gel activated with 1,1'-Carbonyldiimidazole. For antibody coupling, 500 μl of the gel slurry (~ 250 μl of gel) in acetone was placed in a 1.5 ml eppendorf tube and centrifuged to pellet the gel. The supernatant was removed using a pasteur pipette, and the pellet was then washed three times with 1.3 ml of 7:3 acetone:deionized water, 3:7 acetone:deionized water, water alone, and finally with 0.5 M sodium phosphate (pH 7.5). After removal of the binding buffer, 618 μl of the antibody (810 μg/ml in PBS) was added and shaken with the gel for 15 hr at room temperature. The uncoupled antibody was then removed, and the gel pellet was washed three times with 1.3 ml of the phosphate buffer, deionized water, and 0.1 M

ethanolamine (adjusted to pH 7.5 with concentrated HCl). The gel was resuspended in the ethanolamine solution and shaken again for 15 hr at room temperature. In preparation for storage at 4°C, the gel was washed three times with 1.3 ml of PBS and resuspended in 0.02% NaN_3 (PBS). All centrifugation was done for 30 s at 3600 g (8000 rpm).

2.3.2 Solution Affinity Selection

In a 1.5 ml eppendorf tube, 50 µl of antibody (810 µg/ml) was mixed at room temperature for 1 hr with the standard protein or peptide mixture (~ 0.3-0.5 nmol of the *c-myc* component). The antibody complex was removed from the mixture via Centri•Spin gel filtration columns (swelled in PBS buffer) following the manufacturer's protocol (Princeton Separations, Adelphia, NJ). The fraction containing the immunocomplex was freeze-dried before the addition of 55 µl of 0.1 M formic acid. This selected component was then further purified (removal of salt and antibody) using C18 ZipTip disposable preconcentration tips (Millipore, Bedford, MA) (Section 2.11). Centri•spin-10, -20 and -40 gel filtration columns, having respective molecular weight cutoffs of 5, 25, and 100 kDa, were used.

2.3.3 Hydrazide Activated Gels and Oxidized Antibody Carbohydrate Moieties

This method of immobilization, using the CarboLink trial kit, was performed as described by the manufacturer (Pierce, Rockford, IL). In preparation for coupling, 130 µl of the antibody (0.8 mg/ml) was exchanged into the CarboLink coupling buffer (0.1 M sodium phosphate, pH 7.0) with the desalting column provided. The elution of the antibody from the column was monitored by absorbance spectrophotometry. The immunoglobulin solution was then added to 1 mg of sodium *Meta*-periodate and incubated at room temperature for 30 minutes. The oxidized sample was desalted using the desalting column and then combined

with 40 µl of the CarboLink beads in a 0.45 µm centrifugal filter unit with shaking at room temperature overnight. The uncoupled antibody was removed by centrifugation, and the immunomatrix was conditioned for selection with 200 µl of the Equilibration buffer (included with the kit) followed by 200 µl of PBS buffer. Following selection, the matrix was reactivated by washing with 800 µl of 1 M NaCl and stored in 0.05% NaN_3 in PBS at 4°C.

2.3.4 Immobilization of the Antibody to Protein G through Chemical Crosslinking

Protein G Sepharose 4 Fast Flow gel was purchased from Pharmacia Biotech preswollen in 20% ethanol. A gel slurry was prepared in a Millipore 1.5 ml, 0.45 µm Ultrafree-MC centrifugal filter unit by decanting the 20% ethanol solution and replacing it with PBS buffer in a ratio of ten parts buffer to one part settled gel. IgG1 antibody was then added to the settled gel at 2 mg antibody (in PBS) for every 1 ml of gel and allowed to bind to the protein G over a one hour incubation period at room temperature with mild shaking on a Fisher Vortex Genie 2. The non-retained antibody was removed, and the gel was washed twice with ten-fold volumes of 0.2 M sodium borate (pH 8.9). DMP was added to the antibody gel slurry in the above borate buffer to a final concentration of 20 mM and incubated for a period of 30 minutes. Following removal of the DMP solution, the gel was washed once with and resuspended in 0.2 M ethanolamine (pH 8) for a two hour incubation period. The ethanolamine solution was replaced by 0.02% NaN_3 in PBS, and the immunomatrix was stored at 4°C between uses. All solutions were removed by centrifugation at 3600 g (8000 rpm).

2.4 Antibody Quantitation

The concentration of immobilized IgG was determined indirectly by calculating the difference in total antibody applied for coupling and that remaining in solution (unbound IgG) upon termination of the coupling reaction. Absorbance spectrophotometry, surface plasmon resonance analysis, as well as capillary electrophoresis (Section 2.13) were all used to quantitate the anti-*c-myc* IgG.

2.4.1 Absorbance Spectrophotometry

Absorbance spectroscopy was performed on a Varian Cary 1 double beam UV-Vis spectrophotometer (Harbor City, CA) using quartz sample vials. The absorbance was measured at 280 nm assuming an extinction coefficient of 1.35 for a 1 mg/ml IgG solution with a 1 cm pathlength.[10]

2.4.2 Surface Plasmon Resonance Analyses

Quantitation of anti-*c-myc* IgG1 mouse monoclonal and scFv antibodies was carried out using a BIAcore 1000 biosensor system (Biacore Inc., Piscataway, NJ). For quantitation of the scFv in the *E. coli* periplasmic extracts, the anti-*c-myc* IgG was immobilized on research grade CM5 sensor chips (Biacore Inc.) at a concentration of 50 μg/ml using the amine coupling kit (Biacore Inc.) Approximately 6400 response units (RU) of IgG were immobilized under these conditions, where 1 RU corresponds to an immobilized protein concentration of ~ 1 pg/mm^2.[48] Ethanolamine was used to block any unreacted moieties on the chip surface. All measurements were performed in HEPES-buffered saline consisting of 10 mM HEPES, 150 mM NaCl, 3.4 mM EDTA (pH 7.4). ScFv preparations were diluted 40 to 80 times in the HEPES buffer for binding to the IgG surface. Analyses were carried out at

25°C with flow rates of 10 µl/min and a sample injection volume of 30 µl. Sample concentrations were determined using a standard curve obtained for a standardized scFv mutant antibody on the IgG surface.

The binding kinetics of the *c-myc* peptide/anti-*c-myc* IgG immunocomplex were determined by SPR. Monoclonal anti-*c-myc* IgG1 was immobilized on the sensor surface at a concentration of 50 µg/ml using amine coupling. Approximately 8400 RU of IgG were immobilized on the surface. All measurements were carried out in HEPES-buffered saline. Analyses were performed at 25°C with a flow rate of 5 µl/min and a *c-myc* peptide injection volume of 15 µl (2 µM). Rate constants were calculated by nonlinear fitting of the primary sensorgram data using the BIAevaluation 3.0 software (Biacore Inc.)[49]

For anti-*c-myc* IgG quantitation, polyclonal rabbit anti-mouse IgG1 was immobilized on the sensor chip at a concentration of 100 µg/ml using amine coupling. Approximately 7900 RU of rabbit IgG were immobilized under these conditions. All measurements were carried out in HEPES-buffered saline as mentioned above. Anti-*c-myc* IgG preparations were diluted 60 to 150 times in the HEPES buffer for binding to the rabbit IgG surface. All analyses were carried out at 25°C with a flow rate of 20 µl/min and an injection volume of 20 or 80 µl. A standard curve using standardized salmonella 155-4 IgG on the rabbit IgG surface was used for the determination of the IgG concentration in the samples.

2.5 Affinity Selection Protocol

Crosslinked antibody resin (~ 10 to 30 µl for selection from PBS buffer and either 30 or 90 µl for selection from sera) was equilibrated at room temperature and washed three times with a ten-fold volume of PBS buffer. The antibody bed was then incubated with the *c-myc*-

containing matrices (250 µl of varying concentrations unless otherwise stated) for one hour at room temperature with mild shaking. Following three deionized water washes, the selected analyte was eluted from the antibody by a 30-minute incubation with 0.1 M formic acid (50 µl). To ensure the complete elution of the selected components, the immunomatrix was washed three times with 250 µl of 0.1 M formic acid. All solutions were removed from the gel by centrifugation. Regeneration of the beads was achieved by washing with the binding buffer (PBS).

2.6 Periplasm Extraction of ScFv

E. coli cells were harvested by centrifugation with a GS-3 rotor at 8000 rpm for 15 minutes. The resulting pellet was resuspended in a tris buffer (50 mM tris-HCl, 0.8% NaCl (w/v) pH 8) and then centrifuged at 10,000 rpm for 15 minutes. The pellet was then resuspended in the sucrose extraction buffer (25% sucrose, 1mM EDTA, 10mM tris-HCl at pH 8.0) in a ratio of 1 g wet cell/2.5 ml buffer. The sucrose-extracted scFv antibody was retrieved by centrifugation at 10,000 rpm for 30 minutes. The pellet was resuspended in 4°C shock buffer (0.5 mM $MgCl_2$ and 10 mM tris-HCl at pH 8.0) and placed on ice for 15 minutes. A final centrifugation at 10,000 rpm for 15 minutes was performed to obtain the scFv-rich supernatant. Both the sucrose and shock extractions were analyzed by surface plasmon resonance optical detection for scFv content and stored at 4°C in 0.02% NaN_3. The cells were killed with Javex prior to disposal.

2.6.1 Immobilized Metal Affinity Chromatography (IMAC)

The *E. coli* periplasmic extract of the scFv wild-type antibody was dialyzed against 10 mM HEPES buffer, 500 mM NaCl (pH 7) (running buffer) and then centrifuged at 10,000

rpm for 15-30 min. The HiTrap IMAC column (Pharmacia Biotech), connected to an HPLC pump system, was prepared for use with 5 column volume rinses of deionized water followed by the application of a 5 mg/ml $NiCl_2 \cdot 6H_2O$ solution until the column was green in color. After equilibration with 5 column volumes of the running buffer, the sample was introduced at a flow rate of 2 ml/min. The column was then washed with the running buffer until baseline absorbance (280 nm) was observed. The His-tagged protein was finally eluted at 1 ml/min with 500 mM imidazole, 10 mM HEPES, 500 mM NaCl (pH 7). All solutions were filtered through a 0.45 μm membrane prior to injection onto the IMAC column.

2.7 Affinity Selection of *c-Myc* Peptide from Sera

The development of immunoaffinity extraction of *c-myc*-tagged molecules from complex matrices was carried out using both human and fetal bovine sera spiked with the *c-myc* peptide.

2.7.1 Fetal Bovine Serum

The pH of the fetal bovine serum (originally pH 7.9) was adjusted to 7.0 using 0.1 M HCl, and affinity selection was performed on both the basic and neutral *c-myc* spiked solutions. The *c-myc* peptide was spiked into the serum at a final concentration of 33 μg/ml, and 15 μl of this solution was applied to 5 μl of the non-crosslinked IgG-coated protein beads (2 mg IgG/ 1 ml beads). Affinity selection was then carried out according to the protocol outlined in Section 2.5 except that the selected peptide was eluted into 20 μl of the elution buffer compared to 50 μl used previously.

2.7.2 Human Serum

The serum was diluted five times and neutralized with 0.1 M HCl prior to spiking at various concentrations with the *c-myc* peptide. After centrifugation of the spiked serum solutions to prevent blockage of the 0.45 μm centrifugal units, immunoaffinity selection of the peptide was carried out according to Section 2.5.

For human serum purification prior to affinity selection, both the *c-myc* spiked serum and the serum alone were passed through either a Millipore Ultrafree-MC 10,000 or 100,000 nominal molecular weight limit (NMWL) centrifugal filtration unit at 9000 rpm (4500 g). The serum filtrate was spiked with the *c-myc* peptide, and affinity selection was subsequently carried out according to the method outlined in Section 2.5.

Precipitation of the serum proteins prior to affinity selection was also performed. To 1 ml of the undiluted serum was added 1 ml of acetonitrile in 50 μl aliquots with shaking. After centrifugation the supernatant was removed, freeze-dried, reconstituted in 300 μl of PBS buffer, and spiked to 1 μg/ml with the *c-myc* peptide. Precipitation from 250 μl of a 1 μg/ml *c-myc* spiked serum solution was carried out by adding 250 μl of acetonitrile in 25 μl aliquots with shaking. After centrifugation, the supernatant was freeze-dried and reconstituted in 250 μl of PBS buffer. Immunoaffinity extraction was then carried out according to Section 2.5.

A variety of wash buffers were used in an attempt to remove non-specific binding. These buffers were used prior to the deionized water rinses in the standard immunoaffinity selection method described in Section 2.5. A more detailed discussion of the frequency and types of buffers used is presented in Section 5.6.

Purification of the serum was also carried out by incubating the diluted serum solution with 200 µl of protein G resin. The resin was regenerated with a 1 minute application of 0.1% 1-*O*-Octyl-β-D-glucopyranoside buffer at 37 °C followed by re-equilibration with PBS buffer.

2.8 Gel Electrophoresis

Sodium dodecyl sulfate polyacrylamide gel electrophoresis (SDS-PAGE) was performed using either the Mini-Protean II (80 × 73 × 0.75 mm) or the Protean II xi (160 × 160 × 1 mm, Bio-Rad, Mississauga, ON) systems. All the chemicals and reagents for electrophoresis were purchased from Bio-Rad. The 10% SDS resolving gels were prepared from 40% acrylamide (w/v), 1.5 M 'lower' tris buffer (1.5 M tris base and 14 mM SDS adjusted to pH 8.8 with concentrated HCl) and deionized water in a 1:1:2 ratio. After degassing for ten minutes, polymerization of the acrylamide was initiated using 10% ammonium persulfate (w/v) and TEMED (0.7%:0.1% v/v), and the solution was poured into the cell placing a layer of water on the gel surface to ensure a level surface. After one hour, the separating gel was overlaid with a 5% SDS stacking gel prepared from 40% acrylamide, 'upper' tris buffer (0.5 M tris base and 14 mM SDS adjusted to pH 6.8 with concentrated HCl), deionized water in a 1:2:5 molar ratio and polymerized after degassing with 0.2%:1.5% TEMED and 10% ammonium persulfate. Protein samples were diluted one-to-one in conventional Laemmli buffer (19:1 Laemmli buffer:β-mercaptoethanol) and heated to 95°C for five minutes. The gels were run at 20°C using the following running buffer 25mM tris base, 2.4 mM SDS, and 192 mM glycine chilled to 4°C. Normal gels were run at a constant current of 10 mA while mini-gels

were run at a constant voltage of 200 V until the bromophenol blue tracking dye reached the bottom of the gels.

Gels were first washed three times with deionized water to remove running buffer and then stained with Coomassie-Blue G250 stain. Background stain was removed by washing several times with deionized water. Protein bands were then cut from the gel in preparation for digestion.

2.9 Preparation of Gel Electrophoresis Samples

The two SDS-PAGE gels discussed in Chapter 5 involve different samples. The origins and preparation of these samples are presented below.

2.9.1 Regular SDS-PAGE gel (Section 5.7)

Affinity selection was performed according to the method outlined in Section 2.5 using 90 µl of the crosslinked IgG resin. Prior to rinsing with deionized water, the immunomatrix was washed seven times with 250 µl of β-alanine buffer to remove non-specific binding components. The 0.1 M formic acid elution samples from two 10 µg/ml *c-myc* spiked serum affinity selections were combined with the corresponding first 250 µl formic acid wash of the immunomatrix (after elution). These combined selections were freeze-dried and reconstituted in 200 µl of deionized water. This stock solution was diluted two, four, ten, and twenty times. A 20 µl aliquot of each of these solutions was then further diluted with Laemmli buffer and applied to the gel. The method described above was also used for the selection of serum components from the serum alone using 90 µl of protein G resin in place of the immunomatrix.

2.9.2 Mini SDS-PAGE gel (Section 5.8)

The diluted human serum was passed through a 100 kDa NMWL filtration unit before being spiked to 0.1 μg/ml with the *c-myc* peptide. Affinity selection of the peptide from this spiked serum was then carried out according to the method outlined in Section 2.5 using 90 μl of the immunomatrix. For gel electrophoresis, the 0.1 M formic acid elution samples from four affinity selections were combined, freeze-dried and reconstituted in 20 μl of Laemmli buffer. This stock solution was then diluted two, five, and twenty times to prevent overloading of the gel. All four protein solutions were applied to the gel. For comparison with the selection lanes, the filtered human serum itself was also used. A 250 μl aliquot of the diluted human serum was passed through a 100 kDa filtration unit, freeze-dried and reconstituted in 20 μl of Laemmli buffer. This solution was then further diluted two, four, and ten times.

2.10 Protein Digestion

Protein digestion was performed either in-gel or in solution. Both trypsin and endoproteinase Glu-C were used as the proteolytic enzymes. The protocols used for the protein digestions are described below.

2.10.1 In-gel Protein Digestion

Excised gel pieces were placed in 1.5 ml eppendorf tubes and washed with 250 μl aliquots of 50% methanol/10% acetic acid until the Coomassie dye was no longer visible. To remove the acetic acid, the gel pieces were washed twice with 250 μl of 40% ethanol and then shrunk by adding acetonitrile (500 μl). After a few minutes, the solvent was removed

and the gel pieces were freeze-dried. At this point, storage of the samples is possible. Reduction of the gel-bound proteins was achieved by reswelling the gel pieces in 300 µl of 10 mM DTT (dissolved in 50 mM ammonium bicarbonate adjusted to pH 8.3 using ammonium hydroxide) and incubating at 56°C for one hour. After cooling, excess liquid was removed and replaced with 300 µl of 55 mM iodoacetamide in 50 mM NH_4HCO_3 (pH 8.3). Samples were incubated in the dark for one hour with periodic vortexing. Removal of the excess iodoacetamide solution was followed by shrinking the gel pieces with acetonitrile, reswelling them in 500 µl of 50 mM NH_4HCO_3, shrinking the pieces again, and finally freeze-drying them. The samples were then reswollen in 10 µl of 50 mM NH_4HCO_3 containing 20 µg/ml of trypsin. An extra 30 µl of bicarbonate buffer was added to each eppendorf to ensure complete coverage of the gel pieces. After incubation at 37°C for 15 hours, the reaction supernatant containing the tryptic peptides was transferred to clean microcentrifuge tubes. To further extract any peptides from the gel pieces, 100 µl of 5% acetic acid was added, and each tube was shaken at room temperature for 15 minutes. This step was performed twice combining the sample supernatants with the tryptic extract from above. The peptide extract samples were then freeze-dried and stored at -20°C until analysis. With all protein digestion mixtures, peptide mass profiles were obtained without any further sample preparation or clean-up prior to mass spectrometric analysis.

2.10.2 Solution Protein Digestion

Approximately 70 µg of affinity-purified scFv antibody was dissolved in 20 µl of denaturing buffer (6M guanidine hydrochloride, 0.1 M Tris-HCl adjusted to pH 8.5 with concentrated HCl) and incubated under argon with DL-Dithiothreitol (2 mM) at 37°C for two

hours. Alkylation with iodoacetamide (8 mM) was then performed in the dark under argon for one hour at 37°C. The reaction was quenched by the addition of 0.5 µl of β-mercaptoethanol. A buffer exchange into 50 mM ammonium bicarbonate was then performed by microdialysis using a 5000 molecular weight cutoff regenerated cellulose membrane (AmiKa Corp., Columbia, MD). The dialyzed sample was freeze-dried and reconstituted in 80 µl of tryptic buffer (0.1 M ammonium bicarbonate and 0.1 mM of calcium chloride, pH 8.00). A 50:1 substrate-to-enzyme ratio was used for the incubation of trypsin with the sample at 37°C for 15 hours. The solution was freeze-dried, reconstituted once in 50 µl of deionized water and subsequently evaporated to dryness in preparation for analysis.

2.10.3 Endoproteinase Glu-C Digestion

Approximately 20 µg of the wild–type scFv antibody was mixed with the enzyme in a 20:1 substrate-to-enzyme ratio. The sample was then diluted ten times in 0.1 M ammonium bicarbonate (pH 7.8) to a final volume of 50 µl and incubated for 15 hours at 37°C. The solution was freeze-dried and reconstituted in 20 µl of 0.05% formic acid in preparation for analysis.

2.11 Desalting Peptides

Desalting of tryptic and *c-myc* peptides was achieved using ZipTip pipette tips. These are 10 µL polypropylene pipette tips packed at the end with approximately 0.55 µL of C18 silica (200 Å, 15 µm). The tip is prepared for use by rinsing sequentially with 60 µl of methanol, 60 µl of 0.05% formic acid, 60 µl of 75% MeOH/ 0.05% formic acid, and 60 µl of the 0.05% formic acid solution. The sample is applied to the tip in 10-20 µl of 0.05% formic acid and passed through the tip at least ten times. The salts are removed by the application of

80-100 µl of 0.05% formic acid. The peptides are eluted in 5-6 µl of 75% MeOH/0.05% formic acid. This volume should be passed through the tip several times to ensure complete elution. Formic acid was sometimes replaced by acetic acid.

2.12 Matrix-Assisted Laser Desorption/Ionization Time-of-Flight Mass Spectrometry

MALDI-TOF mass spectra were obtained using a Voyager Elite-STR reflecting time-of-flight Biospectrometry Workstation (PerSeptive Biosystems, Framingham, MA) equipped with a nitrogen laser (337 nm). An aliquot of 1 µl of protein sample was mixed with 2.5 µl of 10 mg/ml 3,5-dimethoxy-4-hydroxycinnamic acid (sinapinic acid) dissolved in a 1:1:1 methanol/water/acetonitrile solution. One of the two following matrices was used for peptide analyses. An aliquot of 1 µl of sample was mixed with 2 µl of either 5 mg/ml α-cyano-4-hydroxycinnamic acid (α-CHCA) in 50% ACN/0.3% TFA or 0.2 M 2,5-dihydroxybenzoic acid (2,5-DHB) in MeOH. Of the matrix solution, 0.5 µl was applied to either a gold-plated or polished stainless steel MALDI sample stage and allowed to air-dry. A matrix sandwich was also used for some tryptic peptide samples in which 1 µl of 2,5-DHB matrix was applied to the MALDI probe and allowed to dry. A 1 µl volume of sample was then directly applied to this spot, dried and a second 2,5-DHB layer was applied on top.

Protein samples were analyzed in linear positive ion mode with an accelerating voltage of 25 kV, a pulse delay time of 225 ns, a grid voltage of 91% and guide wire voltage of 0.3%. Calibration was external to the samples using bovine insulin (MH^+ 5734.59 Da) and horse apomyoglobin dimer ($(2M + H)^+$ 33904.00 Da).

Peptide analysis was performed in either linear or reflectron positive ion mode. For linear mode, an accelerating voltage of 20 kV, a pulse delay time of 175 ns, a grid voltage of 94.5%, and a guide wire voltage of 0.05% were used. For reflectron mode acquisitions, an

accelerating voltage of 20 kV, a pulse delay time of 200 ns, a grid voltage of 72%, and a guide wire voltage of 0.1% were used. In both modes, calibration was applied externally using des-Arg^1-bradykinin (904.4681 Da, monoisotopic mass) and bovine insulin (5734.59 Da, average mass).

2.13 Capillary Zone Electrophoresis (CZE-UV)

CZE-UV experiments were performed on a Beckman P/ACE System 5000 (Fullerton, CA). Separation was achieved by applying +25 kV to the outlet end of a 47 cm × 360 μm o.d. × 50 μm i.d. BCQ-coated capillary. The separation buffer was 0.1 M formic acid and detection was set at 200 nm. The sample was injected hydrodynamically by pressurizing the sample vial (~ 0.5 psi) for 4 s resulting in typical injection volumes of ~ 5 nl.

On-line sample preconcentration was performed by pressure injection of samples prepared in water (15 s at 0.5 psi, ~ 15 nl). A voltage of –25 kV was applied to the outlet end resulting in the removal of water from the inlet end while the analyte was focused. When the current reached about 90% of the maximum separation value the polarity of the electrodes was physically switched and separation carried out under the conditions described above. For all CE experiments the samples were freeze-dried first and reconstituted in 30 μl of deionized water (this volume was measured on a balance) prior to analysis.

2.14 BCQ Capillary Coating

Bare fused silica capillary was covalently modified with BCQ according to the method of Bateman and coworkers.[50] A 2 meter length of capillary was rinsed sequentially with 1 M NaOH, deionized water, and methanol each for one hour at 20 psi and then treated with a

solution of 0.5% (v/v) 7-oct-1-enyltrimethoxysilane and 0.5% (v/v) glacial acetic acid in methanol overnight (~ 12 h) at 20 psi. The capillary was subsequently rinsed with methanol and deionized water each for 1 h at 20 psi. A solution of 0.2% (v/v) N,N,N',N'-Tetramethylethylenediamine (TEMED), 1.4% (v/v) aqueous ammonium persulfate (15% (w/v)), and 4% BCQ in deionized water was passed through the capillary for ~ 12 h at 20 psi. The capillary was flushed with deionized water for 1 h and stored in either water or subsequently flushed to dryness using nitrogen.

2.15 Immunoaffinity Chromatography

The IgG1 immobilized protein G beads were slurry packed into a 584 μm i.d. × 1588 μm o.d. plastic tubing (VG Biotech Fisons Instruments, Beverly, MA) using 20 psi of N_2. During packing, the tubing was dipped into the bead suspension while the slurry was shaken in an ultrasonic bath. A bed of approximately 2.5 cm, verified using a light microscope, was prepared using this packing technique. The packed plastic column was attached at both the outlet and inlet ends to a BCQ-coated 50 μm i.d. × 184 μm o.d. capillary using low dead volume butt connectors (Upchurch, Oak Harbor, WA) fitted with HPLC tubing frits (LC Packings).

After filling, the inlet end of the column was connected to either a Harvard syringe pump, using a 250 μl gas-tight syringe (Hamilton, Reno, NV), or a Crystal CE system (Thermo Capillary Electrophoresis, Franklin, MA) for the pressure delivery of filtered solutions. The flow rates of solutions through the column were estimated by measuring the volume collected from the outlet end over a period of time. A flow rate of 5 μl/min was used for the injection of all solutions applied to the column.

Equilibration of the packed column was achieved by rinsing with PBS buffer for 10 min. Antigen solutions were introduced into the column for 2 min followed by an incubation period of 20-60 min. Non-selected components were removed by a 10 minute wash with deionized water. The selected components were eluted from the column using 0.1 M formic acid. On-line mass spectral detection was performed using a triple quadrupole mass spectrometer. The off-line analyses used the same set-up except that 10 µl volumes of 0.1 M formic acid were collected directly from the outlet capillary. The pressures used were adjusted to achieve the desired flow rate (5 µl/min).

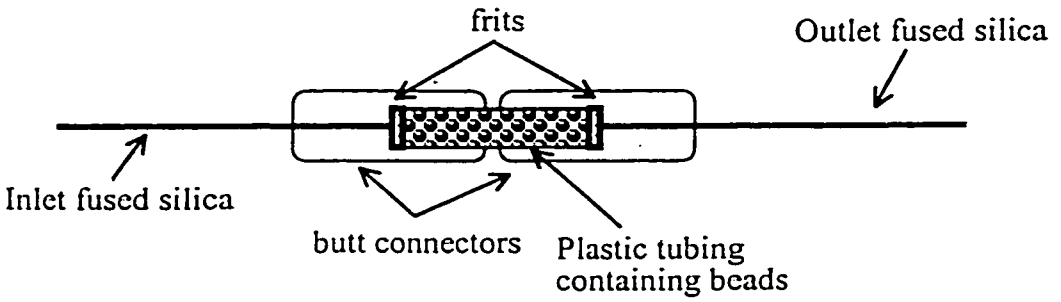

Figure 2.1 IAC column arrangement.

2.16 Concentration Study of *c-Myc* Selection from PBS using LC-MS

To ensure concentration accuracy, all *c-myc* peptide solutions were prepared by careful volumetric weighing on a balance from an original 470 µg/ml stock solution. The *c-myc* peptide alone was diluted in PBS buffer at concentrations varying from 1 µg/ml to 1 ng/ml. The affinity selection protocol outlined in Section 2.5 was followed except that a 35 minute incubation period of the *c-myc* solution with the immunomatrix was used while a 15 minute period was allowed for the elution buffer. The eluted samples were freeze-dried and reconstituted in approximately 20 µl of deionized water (this volume of water was

determined on a balance). It was felt that a shorter incubation period of 35 minutes could be used since the immunoaffinity chromatography study discussed in Section 3.8 showed very little difference between the amount of *c-myc* peptide selected when the selection period was varied from 20 to 60 minutes.

2.17 Nanoelectrospray Emitters

Nanoelectrospray gold-coated emitters, having an internal diameter of ~ 1 μm, were purchased from Micromass (Manchester, UK). In addition, emitters were also constructed by placing a platinum wire inside tapered glass tips (μTips, WPI, Sarasota, FL) having an internal diameter of ~ 1 μm. Nanoelectrospray was used to electroinfuse 1-2 μl of sample into a Micromass quadrupole time-of-flight mass spectrometer (Q-TOF). Mass spectral acquisition generally involved an ionization voltage of 1000-1200 V while the TOF acquisition range was set to m/z 300-2500.

2.18 LC-ESMS

LC experiments were carried out using a Hewlett Packard Series 1100 HPLC (Palo Alto, CA). Chromatographic separation was achieved using a 3 μm × 300 μm PEPMAP C18 column (LC Packings) with a 5-95% aqueous acetonitrile gradient (0.2% formic acid). A pre-column splitter was mounted before the injector to provide a flow rate of ~ 3 μl/min to the column.

Mass spectrometric experiments were conducted using an API 3000 LC-MS/MS system (Perkin-Elmer/Sciex, Concord, ON) and a Q-TOF mass spectrometer (Micromass). A conventional sheath flow configuration was employed using a sheath buffer of 50% methanol/1% acetic acid. For the triple quadrupole instrumentation, mass spectral

acquisition generally involved a dwell time of 3.5 msec per step of 1 m/z unit over the range m/z 500-1500 or 100 msec per channel for selected ion monitoring (SIM) experiments. On average, an ionization voltage of 4 kV was used. Collision-induced dissociation (CID) of ions selected by the first quadrupole was obtained using nitrogen as the collision gas at collision energies of 25-30 V. For MS/MS experiments on the API 3000, the fragment ions generated in the collision cell were mass analyzed by scanning the third quadrupole with a dwell time of 1 msec per step of 1 m/z unit over the range of m/z 50-1400.

LC-MS experiments with the Q-TOF instrumentation generally involved an ionization voltage of 4 kV. Conventional mass spectral acquisition was obtained by operating the first quadrupole in rf-only mode and pulsing the ions to the TOF analyzer at a frequency of 16 kHz. Collision-induced dissociation experiments were conducted using argon with collision energies of 25 to 30 V. Automatic program switching to MS/MS mode (data dependent switching) was executed such that when a signal having an intensity greater than a predetermined threshold value (10 counts) was detected in the survey scan (m/z 400-2000), CID was commenced. The program was then returned to scanning the quadrupole after three accumulations of MS/MS spectra of 1.5 sec each. This process allows both the parent ion mass measurement and sequence analysis to be performed concurrently.

2.19 Database Searching

Peptide mass and partial amino acid sequence searching were carried out with ProteinProspector (using the non-redundant database, NCBInr, compiled by the National Center for Biotechnology Information) developed by UCSF Mass Spectrometry Facility (http://prospector.ucsf). For peptide mass searches, monoisotopic peptide masses were

selected in the range of m/z 900-4000 with a mass tolerance of ± 0.500 Da and a protein molecular weight range of 1-300 kDa. A minimum of four peptide matches were required for a protein hit.

For partial amino acid sequence searching, the monoisotopic peptide mass as well as the fragment ion masses was entered with a tolerance of ± 1 Da and ± 0.60 Da respectively. A maximum of one unmatched ion mass was allowed for a protein hit. The peptide sequences found by the search program were compared with that determined from the MS/MS spectrum to further support the protein identification. All searches were restricted to human and mouse or *E. coli* species depending on the source of the tryptic peptides.

Chapter 3 Development of *c-Myc* Affinity Selection

3.1 *c-Myc* Epitope

The myc oncogene (v-*myc*) was first identified as the transforming sequences of the avian myelocytamatosis viruses, which cause a variety of "neoplasms" in chickens.[51] Interestingly, normal genes, homologous with the v-*myc* sequence, have been identified in many eukaryotic genomes including that of humans. Most of the work on the *myc* gene family has focused on three members—c-*myc*, N-*myc*, and L-*myc*—all of which have been involved in the formation of human carcinomas (for example: Burkitt's lymphoma and breast, nasopharyngeal, hepatocellular carcinomas).[52]

The human proto-oncogene *c-myc* encodes an unstable transcription factor phosphoprotein (typical half-life of 30 min) that is involved in the regulation of cell proliferation.[53] The Myc protein, in complex with its protein partner Max, binds to promoter components and regulates the expression of genes needed for cell cycle progression and cellular proliferation. In many tumor types, however, the expression of the Myc protein is often observed at elevated levels.[54] The instability of the Myc protein prevents its accumulation in normal cells; however, it is believed that cancer-associated and transforming mutations within the transcriptional activation domain of the protein may result in its stabilization. In keeping with the role of Myc in normal cell growth, its elevated levels may result in the oncogenic conversion of the cell. The actual mechanism by which the Myc protein is involved in the formation of the various human cancers is still not understood.

From the nucleotide sequence of the human *c-myc* gene, a 439-amino acid protein with a molecular mass of 48 kDa is expected.[51,55] In order to characterize the actual gene product, the synthetic peptide approach was used to develop antibodies specific for the Myc protein.

This method involves the synthesis of peptides whose amino acid sequences are determined from the DNA sequence of the gene of interest. The synthetic peptides are then are used as immunogens to raise antibodies that cross-react with the whole gene product. Consequently, the murine anti-*c-myc* IgG1/κ antibody 9E10, recognizing the *c-myc* tag "EQKLISEEDLN", was produced (Figure 3.1). This antibody was then used to detect the 62 kDa Myc phosphoprotein from human cell lysates. Since then, this anti-*c-myc* antibody has been used extensively in cancer research for detecting and studying the distribution of the Myc protein in normal and malignant cells.

It was later discovered that the *myc* tag could also be genetically fused to non-Myc proteins and still be recognized by the anti-*c-myc* antibody. As a result, the epitope peptide of the anti-*c-myc* antibody has been used as a detection tag for a variety of recombinant fusion proteins expressed in numerous systems such as *E. coli* (see Chapter 4) and *Saccharomyces cerevisiae*.[56] Because of the involvement of the Myc protein in human malignancies and the extensive use of the *myc* tag for immunodetection and immunoextraction of recombinant proteins, a procedure involving an anti-*c-myc* immobilized matrix was developed for the purification and concentration of *c-myc*-tagged proteins from various complex matrices. In order to maximize the antigen selection and ensure mass spectral detection, the development of this immunomatrix and the corresponding immunoaffinity methodology was carried out using the *c-myc* peptide.

Variable Light chain:

CDR-1

1 DIVLTQSPAF FGCISRQRAT ISCRASESVD NYGFSFMNWF

CDR-2

41 QQKPGQPPKL LIYAISNRGS GVPARFSGSG SGTDFSLNIH

CDR-3

81 PVEEDDPAMY FCQQTKEVPW TFGGGTKLEI KRAVA

Variable Heavy Chain:

CDR-1

1 QVQLQESGGD LVKPGGSLKL SCAASGFTFS HYGMSWVRQT

CDR-2

41 PDKRLEWVAT IGSRGTYTHY PDSVKGRFTI SRDNDKNALY

CDR-3

81 LQMNSLKSED TAMYYCARRS EFYYYGNTYY YSAMDYWGQG

121 ASVTVSSAKTT

Figure 3.1 The sequence of the light and heavy variable domains of the anti-*c-myc* IgG1 mouse monoclonal antibody. CDRs are shown in the boxed regions.[56]

3.2 Antibody Immobilization

A fundamental aspect of immunoaffinity chromatography involves the immobilization of a specific antibody onto an inert, solid support. The numerous methods that are used for the immobilization of antibodies to the solid phase can be divided into three main categories: activated beads, protein A/G beads, and activated antibodies. All these methods use commercially available matrices that have been chemically modified to contain reagents that bind specifically to antibodies. In the activated antibody method, however, the chemical activation of both the immunoglobulin and the support is necessary for covalent attachment.

Choice of coupling method is antibody-specific and trial-and-error is often involved in the development of a successful immobilization method for affinity selection. All three types of immobilization listed above were investigated for the preparation of the anti-*c-myc* IgG1 immunomatrix.

3.3 *c-Myc* Peptide

It should be noted that initially a commercially available *c-myc* peptide, having the sequence CEQKLISEEDL (MH^+ 1306.6 Da), was used in the development of the affinity selection methodology. It was found by MALDI-MS, however, that a peptide having a mass of 2610.2 Da was present in addition to the 9E10 *c-myc* peptide both before and after affinity selection. It is believed, from the observed mass and the fact that it was affinity-selected by the anti-*c-myc* antibody, that this peptide is a dimer of the *c-myc* peptide with linkage between the monomers occurring through a disulfide bond (via the cysteine residues of the peptide). To differentiate the commercial from the in-house synthesized *c-myc* peptide, the commercial peptide will be referred to as the 9E10 *c-myc* peptide.

The limit of detection by MALDI-MS for the 9E10 *c-myc* peptide dimer in PBS was found to be 7 μg/ml, while the limit of detection for the *c-myc* peptide in deionized water was determined to be 0.2 μg/ml. CE-UV analysis of the *c-myc* peptide using the preconcentration method had a limit of detection of 1 μg/ml while CE-UV without using preconcentration had a limit of detection of 12 μg/ml.

3.4 Antibody Immobilization on Activated Beads

The activated matrix, Reacti-Gel, was the first immunosorbent evaluated (Section 2.3.1). With this resin, immobilization occurs through the reaction of a free amino group on the antibody with the imidazolyl carbamate of the Reacti-Gel to form a stable, uncharged *N*-alkylcarbamate (Figure 3.2). Reacti-Gel provides a cheap, mechanically stable matrix (up to 100 psi) that involves relatively mild coupling conditions as well as resulting in an immunomatrix that is free of nonspecific binding.[57]

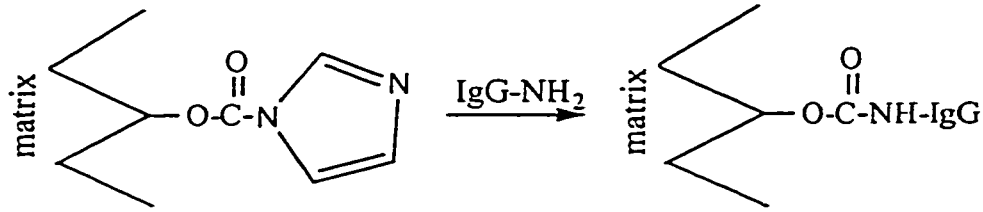

Figure 3.2 Covalent immobilization of antibody on Reacti-Gel matrix.[57]

Affinity selection of the 9E10 *c-myc* peptide was carried out from a non-complex matrix (30 μg/ml PBS buffer) using the Reacti-Gel preparations. The immunomatrix was washed two to three times with 200 μl of PBS buffer prior to the introduction of the elution buffer. MALDI-MS of the elution buffer fraction (reconstituted in 10 μl of deionized water) showed no peptide signal (Figure 3.3A). The non-retained portion, however, showed a weak signal for the 9E10 *c-myc* dimer (Figure 3.3B). The poor signal intensities may be a result of the PBS buffer present in these samples. As a result, these samples were desalted using the ZipTip pipette tips, freeze-dried, and reconstituted in 10 μl of deionized water for MALDI-MS analysis (Section 2.11). Again, no peptide signal was observed in the desalted elution fraction (Figure 3.4A). However, strong signals were observed for the 9E10 *c-myc* monomer and dimer in the non-retained fraction (Figure 3.4B).

It was estimated, using absorbance measurements (Section 2.4.1), that approximately 80% of the IgG input was being retained on the activated beads. Assuming no loss of antibody activity upon immobilization, it was determined that the maximum binding capacity of the immunomatrix for the peptide was approximately 3.6 μg. Therefore, a maximum concentration of 360 μg/ml can be expected for the peptide selected by the immunomatrix. However, from Figure 3.3A it is apparent that less than 0.07 μg of peptide was selected from the 4 μg applied (estimated limit of detection for this peptide in PBS buffer by MALDI-MS).

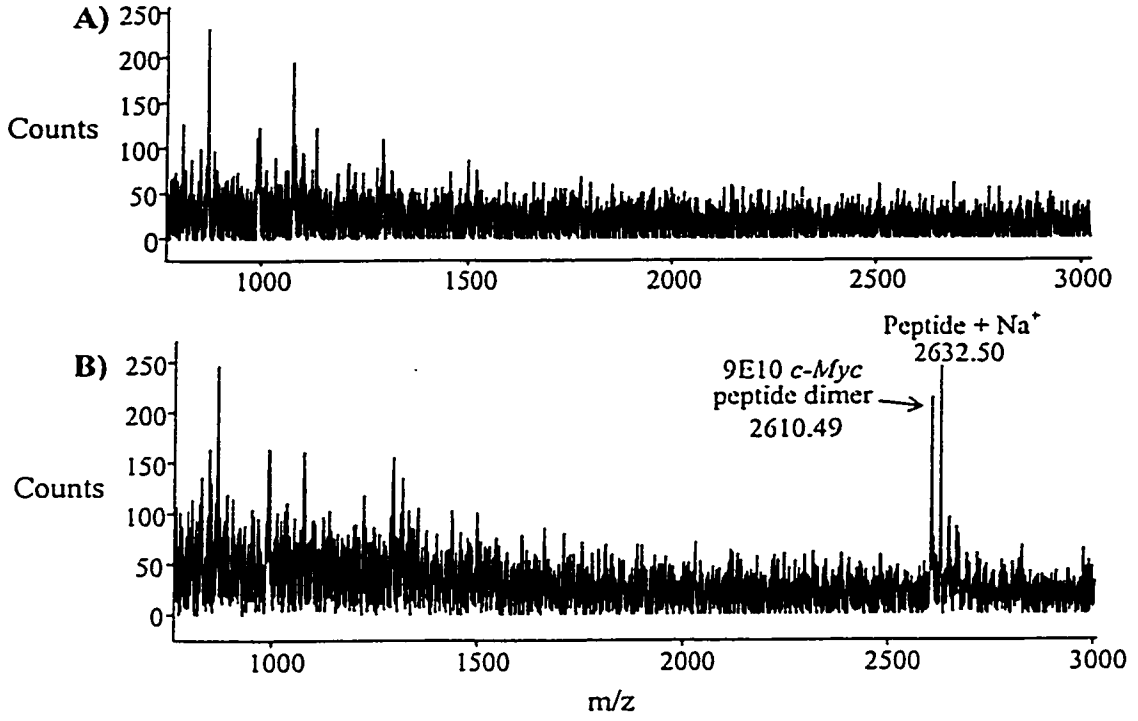

Figure 3.3 MALDI-MS of the 9E10 *c-myc* peptide (prior to desalting) A) affinity-selected using the Reacti-Gel immunomatrix and B) not retained by the immunomatrix during the affinity selection.

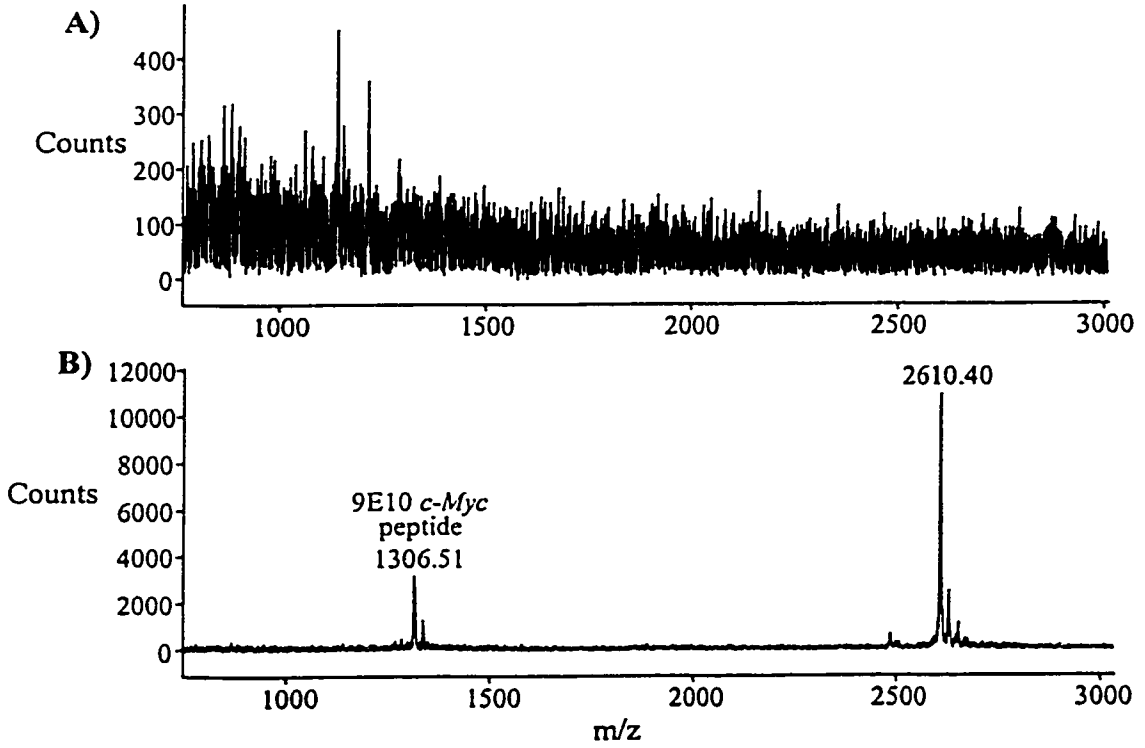

Figure 3.4 MALDI-MS of the samples shown in Figure 3.3 after desalting.

Interestingly, the MALDI-MS of the desalted non-retained fraction (Figure 3.4B) indicates that most of the peptide was not retained by the immunomatrix and was being removed before the application of the elution buffer. It is most likely that the poor selection observed was due to the inactivation of the antibody during the immobilization process. It is in the nature of the coupling of the IgG with Reacti-Gel to suffer some loss of activity in the bound antibody.[58] Binding of the IgG with the matrix occurs randomly through primary amino groups; therefore, coupling can occur near or on the antigen-binding site or the antibody can be oriented such that its activity is intact, but it cannot physically bind an antigen. The presence of several lysines, two of which are found in the complementarity determining regions, in the primary sequence of the anti-*c-myc* IgG heavy and light chain variable domains (Figure 3.1) confirms the potential for inactivation through antigen-binding site coupling. In addition, as with most commercially available activated supports, Reacti-Gel contains an excess of activation groups such that multi-site attachment of the antibody is certain. As a result, an immunomatrix that is largely inactive (approximately 1-30% of the theoretical antigen binding efficiency) is produced.

3.5 Antigen Capture in Solution

To avoid the problems encountered with solid-phase coupling, antigen capture in solution was explored (Section 2.3.2). Using this method, it can be expected that the times for reaching equilibrium will be shorter because the antibodies are not bound thereby speeding up the kinetics of binding.[10] In addition, the antigen binding efficiency of the antibodies is not sacrificed due to harsh coupling conditions or improper orientation of the binding site.

Selection using this method involved incubating the IgG antibody with the *c-myc* antigen in PBS buffer for one hour. To remove the immunocomplex from the non-selected proteins and peptides, gel filtration in the form of Centri•Spin columns was employed. These columns are typically used for the fast and efficient purification of proteins and peptides from smaller molecules such as salts and nucleotides. The columns are purchased as a dry gel thereby allowing for hydration in the buffer of choice. However, in the separations discussed here the gels were hydrated in PBS buffer to ensure that the immunocomplex was not disrupted upon application to the resin. This resulted in a high salt background for the selected *c-myc* peptide or protein thereby requiring post-selection desalting. Separation occurs via centrifugation for two minutes with an expected retention of > 98% of salts and a recovery of > 70%.[59] Three different Centri•Spin products were utilized: Centri•Spin-10, -20 and -40. Each unit is used for the purification of proteins with molecular weights ≥ 5, 25, and 100 kDa respectively.

From MALDI-MS analyses, it was observed that a successful purification of the *c-myc* peptide was achieved using the Centri•Spin-10 and -20 units followed by desalting (Figures 3.5 and 3.6). These units could not be used, however, for the purification of larger antigens such as scFv (MW ~ 27 kDa, see Chapter 4) since the molecular weight cutoff of the gels was limited to 25 kDa.

Centri•Spin-40 units were designed to purify proteins with a molecular weight ≥ 100 kDa, which in theory is ideal for the separation of the IgG-scFv complex from any non-selected proteins. The IgG-scFv complex, having a combined molecular mass of approximately 180 kDa, should pass directly through the filtration unit upon the first centrifugation, while the proteins having molecular weights less than 100 kDa would be

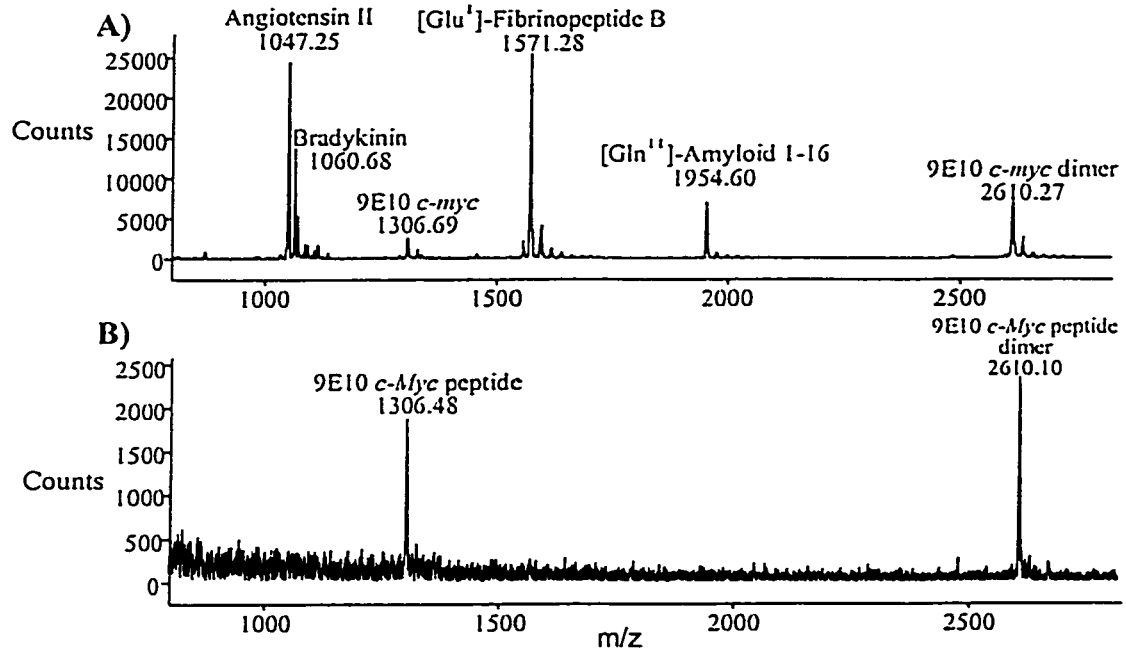

Figure 3.5 MALDI-MS of A) the standard peptide mixture in PBS buffer prior to affinity selection and purification using a Centri•Spin-10 column and B) the desalted affinity-selected 9E10 *c-myc* peptide purified using the Centri•Spin-10 column.

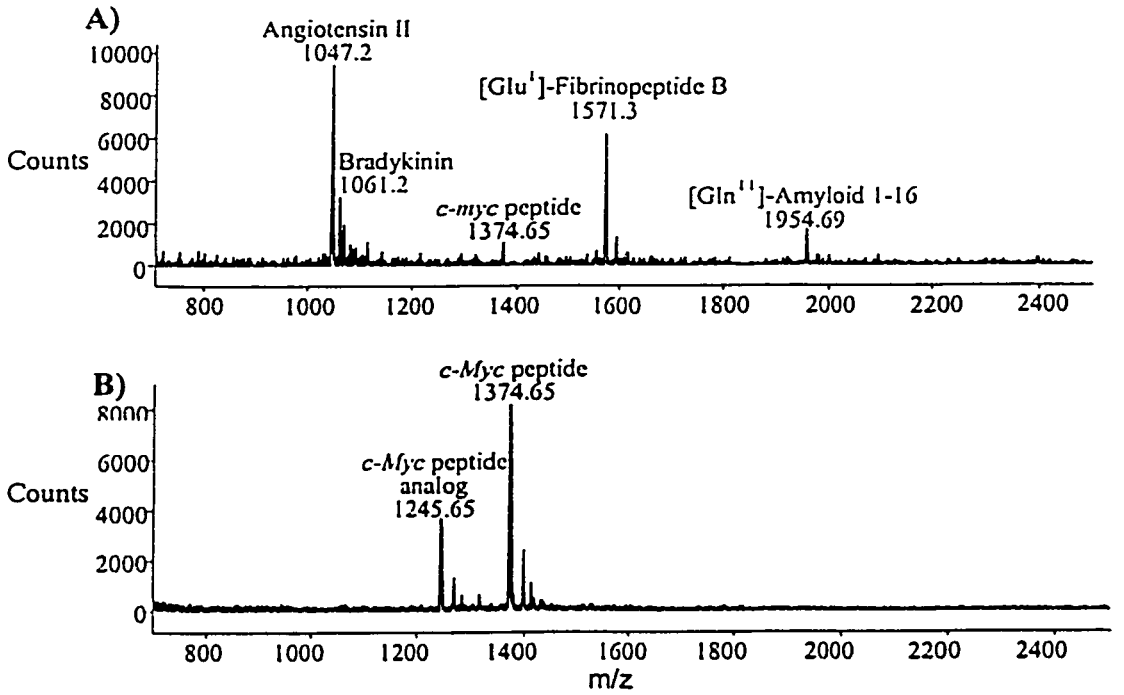

Figure 3.6 MALDI-MS of A) the standard peptide mixture in PBS buffer prior to affinity selection and purification by the spin column and B) the desalted affinity-selected *c-myc* peptide purified using a Centri•Spin-20 column.

retained by the gel. Unfortunately, the quality of the Centri•Spin-40 units proved to be poor. These units were hard to work with due to the long hydration times required and the difficulty in removing the interstitial fluid. The larger pore size of the resin resulted in a weaker gel that often collapsed when subjected to centrifugation and also greatly diminished the separation efficiency. As a result, MALDI-MS of the Centri•Spin-40 fractions showed the presence of several proteins, in addition to the selected scFv (Figure 3.7). To verify that the observation of these proteins was due to poor separation and not the result of non-specific binding to or selection by the antibody, the Centri•Spin-40 columns were used to purify the IgG-*c-myc* peptide complex from the standard peptide mix (Figure 3.8). Unlike the Centri•Spin-10 and –20 units (Figures 3.5 and 3.6), all the standard peptides were observed along with the affinity-selected *c-myc* peptide after purification with the Centri•Spin-40 unit (Figure 3.8). Therefore, it was confirmed that the poor separation capacity of the Centri•Spin-40 column was responsible for the presence of the extraneous proteins observed in the column purification of affinity-selected scFv (Figure 3.7). The poor separation efficiency of these units is probably due to the difficulties in removing the interstitial fluid (excess removal resulting in gel bed cracks or insufficient removal) as well as the large pore size of the beads.

Finally, using the Centri•Spin columns for the separation of the IgG-antigen complex from non-selected matrix components results in a sample containing the affinity-selected molecule along with the antibody. As a result, another clean-up is required prior to further sample manipulation (e.g., tryptic digestion or analysis) in order to remove the antibody. In view of the significant technical difficulties found in the optimization of this affinity selection method, no further development was deemed warranted.

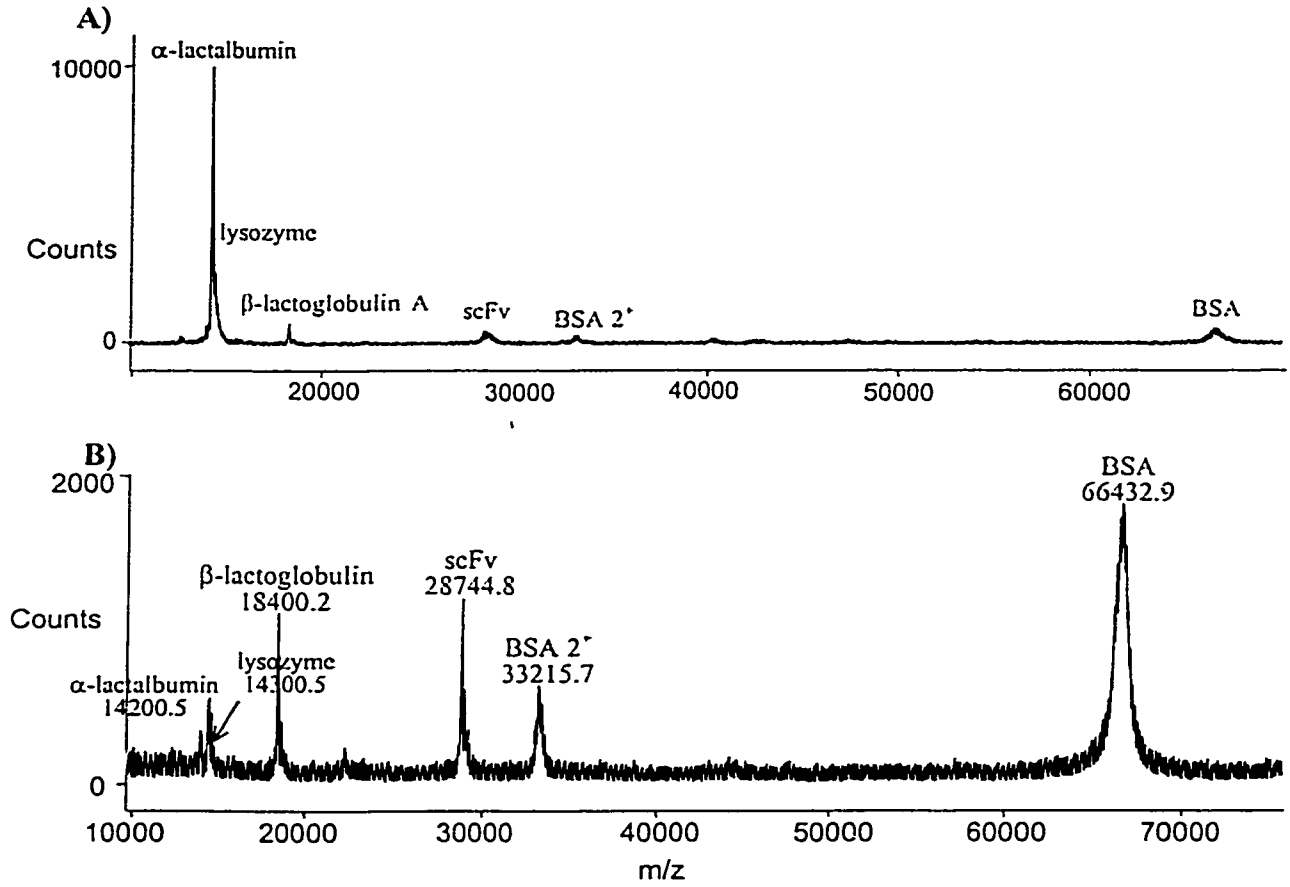

Figure 3.7 MALDI-MS of A) the protein mixture in PBS buffer prior to affinity selection and purification with the Centri•Spin-40 column and B) the affinity-selected scFv after purification with the spin column.

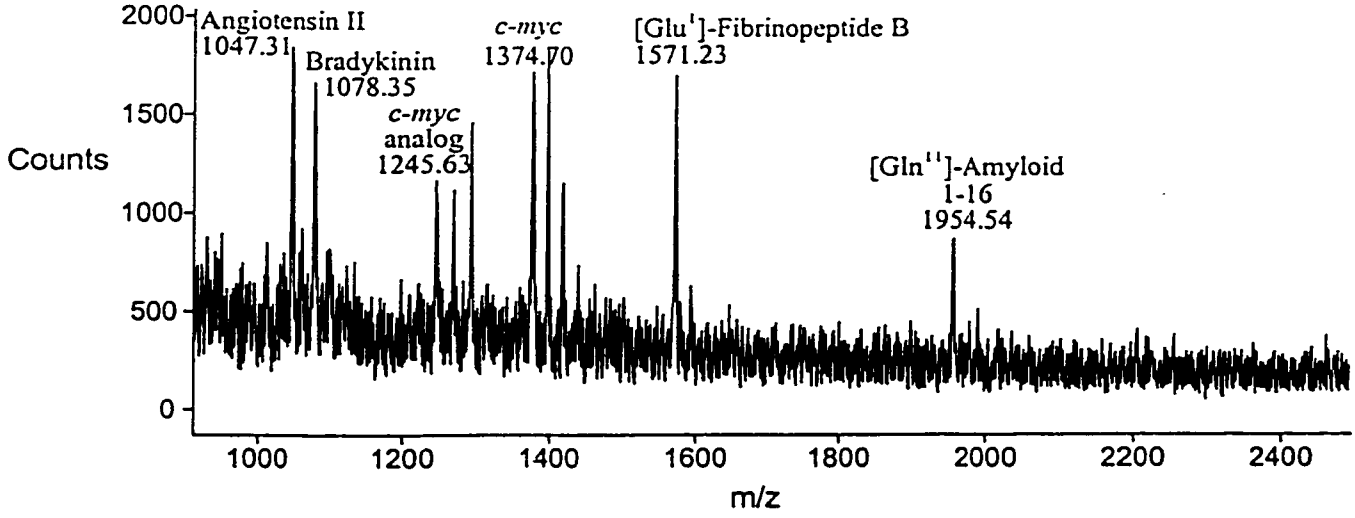

Figure 3.8 MALDI-MS of the standard *c-myc* peptide mixture after purification with the Centri•Spin-40 column (sample was not desalted).

3.6 Immobilization through Antibody and Matrix Activation

The next approach, also known as oriented coupling,[58] involves the immobilization of the antibody to a matrix via its Fc domain. The CarboLink Gel kit was used for this purpose (Section 2.3.3). With this method, sodium periodate is used to oxidize vicinal hydroxyl groups of the IgGs' carbohydrate moieties to aldehydes which then react with hydrazide groups on the matrix to form hydrazone bonds (Figure 3.9). Since the carbohydrates are usually located on the Fc domain of the antibody and no other groups within the antibody will react with the hydrazide, an oriented coupling can be expected. The CarboLink kit contains a solid-support matrix that has a long 23-atom spacer arm (R in Figure 3.9) to reduce steric hindrance.

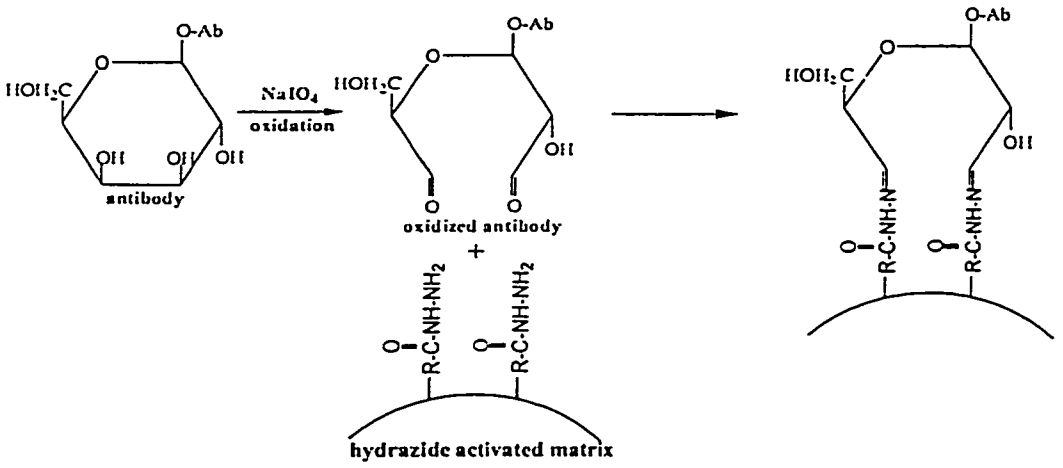

Figure 3.9 Antibody immobilization using a hydrazide-activated gel.[60]

Absorbance measurements of the oxidized antibody applied to the hydrazide matrix and the unbound antibody showed that approximately 48.0 ± 0.1% of the IgG was retained on the matrix. According to Hoffman and O'Shannessy, this level of coupling can be expected for monoclonal antibodies.[61] Like polyclonal antibodies, monoclonals may not be highly glycosylated. Also, any carbohydrate side chains present might have been altered such that

periodate oxidation is rendered difficult or that the size of the oligosaccharide chain and steric hindrance of adjacent residues makes this reaction impractical. In addition, the optimal pH for oxidation and binding of the antibody is dependent upon the immunoglobulin. It is known that aldehyde groups at high pH will react with amino groups to form Schiff bases. This reaction leads to intermolecular crosslinks of the antibodies and therefore a loss of antigen binding activity.[62] However, carrying out the oxidation and binding steps under acidic conditions (pH 5) slows the Schiff base side reaction down resulting in a higher yield of hydrazone bonding. It should be noted that this acidic environment may result in some denaturing of the antibody leading to a loss of binding activity of the immunomatrix. The extent of glycosylation of the anti-*c-myc* IgG was not determined for this method, nor was the oxidation and binding pH optimized (a pH of 7 was used according to the manufacturer's instructions).

Affinity selection of the *c-myc* peptide from PBS buffer was achieved; however, MALDI-MS showed that the levels of selection were far lower than expected (Figure 3.10). The prepared immunomatrix was calculated to have a maximum binding capacity for the *c-myc* peptide of 0.9 μg, while 0.75 μg of the peptide was applied. Assuming complete selection and elution, the maximum concentration of the peptide in 30 μl of the elution buffer should be 25 μg/ml, which is obviously not the case when compared to a 25 μg/ml standard of the peptide (Figure 3.11). However, the signal observed seems to suggest that the concentration is closer to the limit of detection for the peptide by MALDI-MS of 0.2 μg/ml. Desalting of the sample was not required since the immunomatrix was rinsed with deionized water prior to the application of the elution buffer.

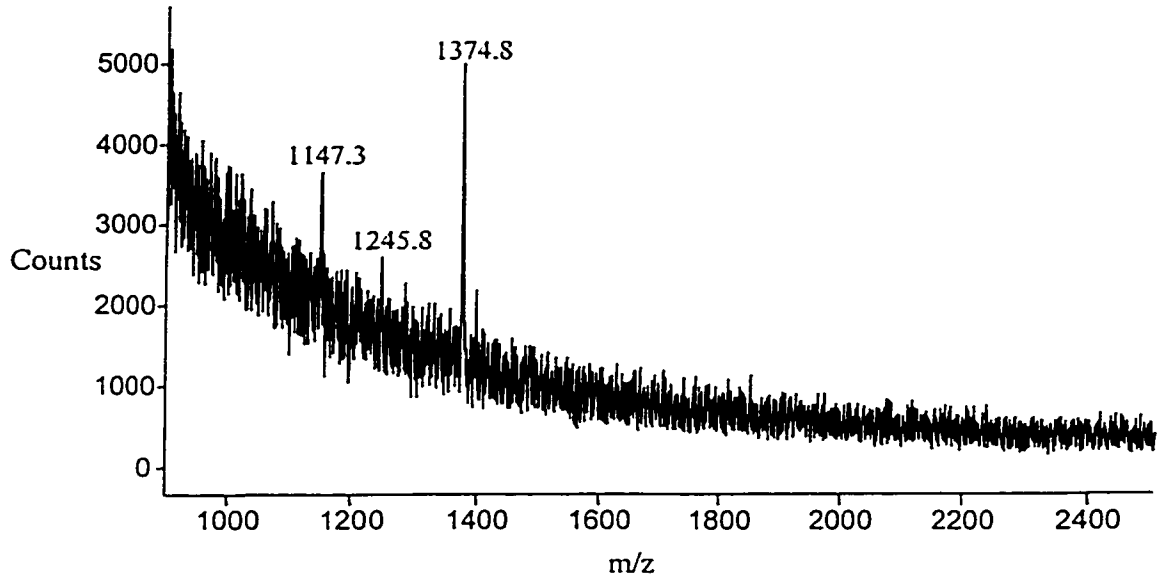

Figure 3.10 MALDI-MS of *c-myc* peptide affinity-selected using the CarboLink immunomatrix.

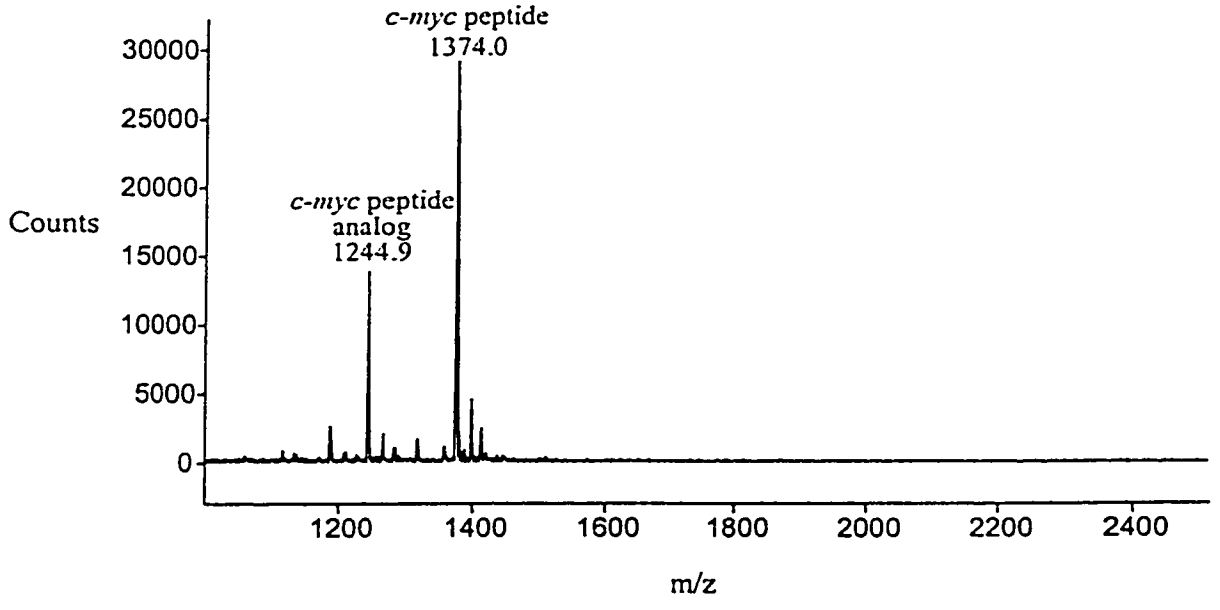

Figure 3.11 MALDI-MS of *c-myc* peptide in deionized water (25 μg/ml).

Considering that 50 μg of IgG was bound to the matrix, the affinity selection observed was poor. This may be due to excessive oxidation of the antibodies or to coupling through carbohydrate moieties near the antigen-binding site, thereby reducing activity. A study by Orthner and coworkers showed that monoclonal antibodies immobilized to agarose matrices via antibody carbohydrate residues still suffer from limited antigen binding.[60] This effect may be present for the CarboLink immobilization of the IgG antibody and could explain the poor selection efficiency observed here. Consequently, this method was not developed further due to its inherently poor coupling efficiency.

3.7 Immobilization of Antibody to Protein G through Crosslinking

Finally, protein G beads were used for the site-directed immobilization of IgG onto a solid-phase matrix (Section 2.3.4). Protein G is a bacterial cell wall protein isolated from group G streptococci that binds specifically to the Fc region of immunoglobulin (Ig) G. The protein is purchased already immobilized on sepharose beads. Protein G is known to have a stronger binding affinity for mouse IgG1 compared to that of protein A, as a result protein G beads were chosen.

There are a number of advantages related to this form of coupling. First, since the antibodies bind to protein G through their Fc domain, the antigen-binding site is oriented correctly for maximum interaction with the antigens. The coupling conditions used are mild, thereby minimizing any denaturing and subsequent inactivation of the antibodies. Also, the binding capacity of the resin used (Pharmacia Biotech protein G sepharose 4 fast flow gel) is high with a total capacity of six mg of mouse IgG per ml of drained gel.[63] It was determined by surface plasmon resonance analysis (Section 2.4.2) that 99 ± 1.3% of the input IgG was

retained on the resin resulting in a concentration of two mg of properly oriented IgG per ml of beads.

This coupling method, however, has a number of limitations. First, uncoupled protein G sites can interact with proteins or antibodies that may be present in the antigen preparation. This limitation is often encountered when antigen solutions originate from mammalian biological extracts. Chapters four and five will discuss this matter further.

Another obstacle encountered with protein G coupling is related to the fact that the antibody binds under physiological conditions to protein G through non-covalent interactions. A decrease in the pH of the surrounding solution, as used with antigen elution, results in the simultaneous elution of the antibody. However, this can be desirable if frequent replacement of the antibodies on the immunomatrix is needed. This method does require the use of large amounts of antibody (2 mg per ml of beads) and generally needs longer conditioning time prior to subsequent affinity selection. Covalent immobilization can be achieved using a crosslinker such as dimethyl pimelimidate (DMP). DMP is a homobifunctional imidoester that reacts with primary amine groups to form stable covalent bonds without affecting the overall charge of the protein. DMP was chosen because of its stability and its relative ease of use. The antibody was coupled to the protein G prior to crosslinkage to sepharose beads in order to ensure proper orientation of the antigen-binding site. With crosslinking, however, there is a risk of inactivating the antibody through intramolecular crosslinkage or by modification of the active site. With the covalent immobilization of the mouse anti-*c-myc* IgG1 to protein G, it is believed that any loss of activity is minimal. The lifetime of the crosslinked resin is on the order of two months

depending on the amount of use. The application of this immunomatrix for affinity selection will be discussed in Chapters four and five.

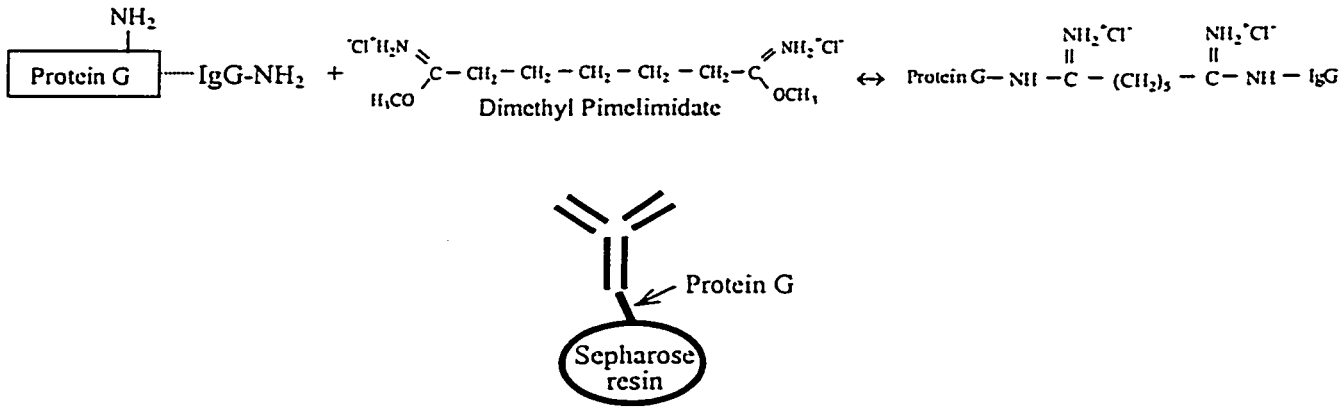

Figure 3.12 Immobilization of antibody to protein G through the crosslinker dimethyl pimelimidate.

3.8 Development of Immunoaffinity Chromatography with On-Line Mass Spectral Detection

Immunoaffinity chromatography (IAC) generally involves the adsorption of antigens onto an immobilized antibody column, followed by the release and detection of the selected antigens. By using an immunoaffinity column coupled to mass spectrometry, antigens can be selected and subsequently identified with minimal user interaction. The advantages of using on-line detection for analytical applications include the potential for automation as well as a reduction in sample handling. In addition, as with general affinity selection, this technique can be expected to be relatively simple and fast with good precision.

Preliminary studies using IAC and on-line mass spectral detection were carried out with the anti-*c-myc* IgG (Section 2.15). A variety of small-scale columns were used to pack the immunoaffinity beads; however, it was found that teflon tubing offered better advantages in terms of ease of use, relatively large capacity, in addition to facilitating the handling of minute amounts of solvents and buffers with minimal leakage. A column bed of

approximately 2.5 cm was packed into the teflon tubing with an estimated bed volume of 7 μl. At 2 mg of IgG per ml of beads, it is estimated that for this volume 0.19 nmols of antigen-binding sites are present. Therefore, the IAC column is expected to have a maximum binding capacity of 256 ng for the *c-myc* peptide.

As discussed in Section 2.15, the antigen solution was applied to the column over a two minute period followed by an incubation time ranging from 20 to 60 minutes. Preliminary studies using CE-UV indicated that an incubation time greater than 20 minutes for selection was unnecessary. After the 20 minute incubation period, 15 ng of peptide was eluted in 30 μl (Figure 3.14), while after 60 minutes 18 ng was eluted (Figure 3.15). In contrast to the affinity selection using the gel slurry, elution of the selected peptide in the above experiments was carried out by passing 30 μl of the acid buffer through the column without an incubation period. Consequently, an experiment was performed in which the elution buffer was introduced into the column for two minutes followed by a 25 minute incubation period. A 45 minute incubation period was allowed for peptide selection. Figure 3.16 shows an increase in the amount of peptide eluted from the affinity column (33.4 ng) in the first 10 μl volume of formic acid. In the second 10 μl volume only 6.7 ng was detected (Figure 3.17). Analysis of the deionized water rinse showed that 25.9 ng of the estimated 70-80 ng of applied peptide was not selected by the column (Figure 3.18). Figure 3.16 seems to indicate that allowing an incubation time for the elution of the peptide does affect the amount of peptide eluted. In addition, on-line mass spectral detection of the peptide was only successful when this method was used. Figure 3.16 also shows that the selected *c-myc* component was found in the first 10 μl volume of the elution buffer.

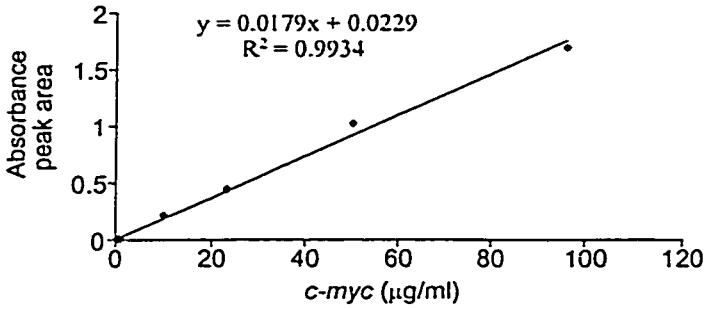

Figure 3.13 Preconcentration CE-UV calibration curve for *c-myc* peptide.

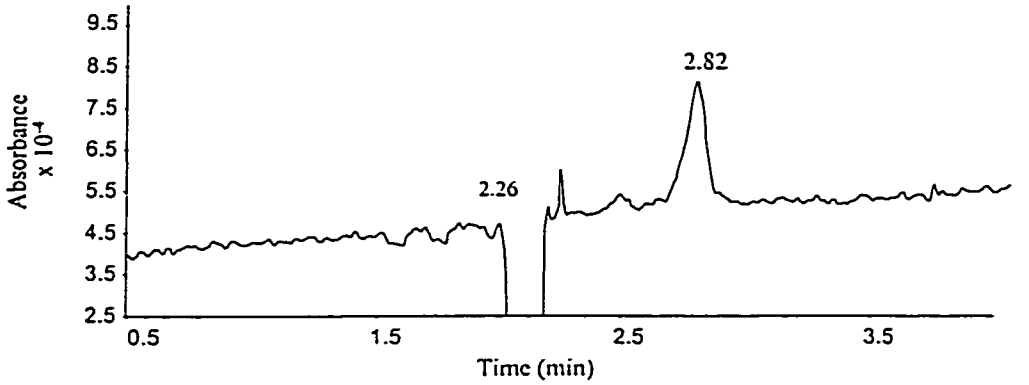

Figure 3.14 Preconcentration electropherogram of the *c-myc* peptide eluted from the immunoaffinity column after a 20 minute incubation of the sample with the column (15 ng selected).

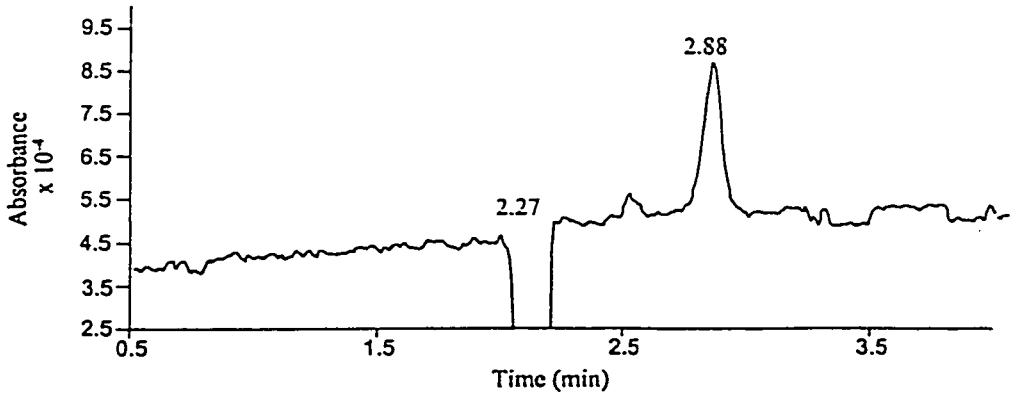

Figure 3.15 Preconcentration electropherogram of the *c-myc* peptide eluted from the immunoaffinity column after a 60 minute incubation of the sample with the column (18 ng selected).

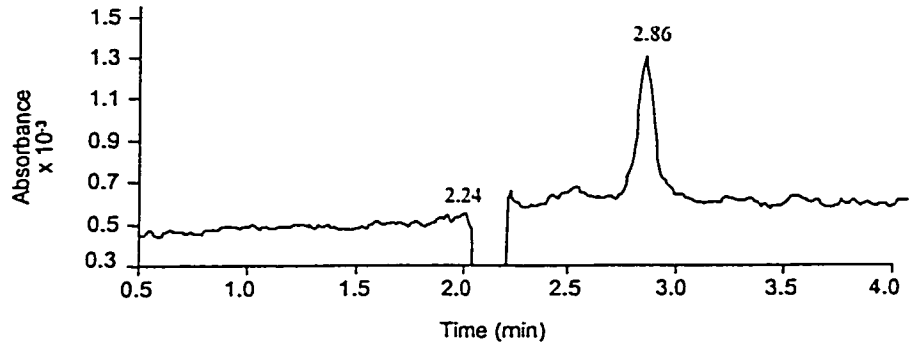

Figure 3.16 Preconcentration electropherogram showing the first 10 µl of elution buffer removed from the immunoaffinity column after a 25 minute incubation with the elution buffer (a 45 minute incubation of the sample with the column was allowed).

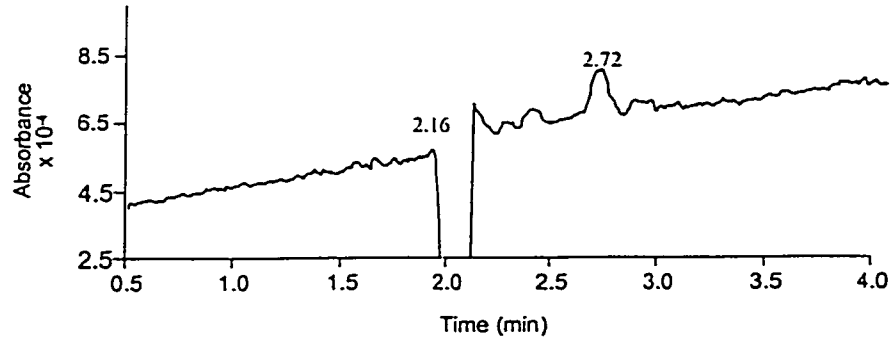

Figure 3.17 Preconcentration electropherogram showing the second 10 µl of elution buffer removed from the immunoaffinity column after a 25 minute incubation with the elution buffer (a 45 minute incubation of the sample with the column was allowed).

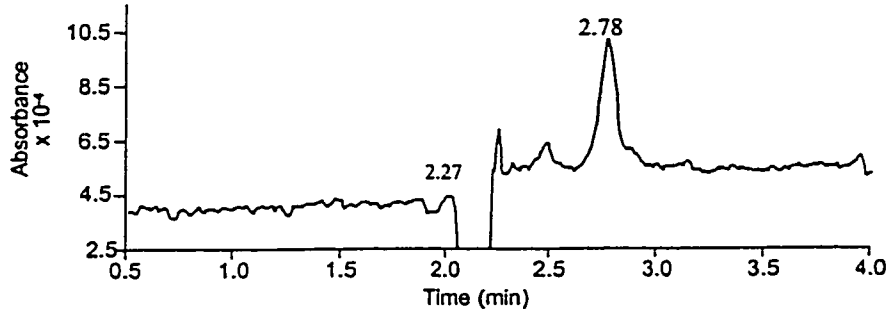

Figure 3.18 Preconcentration electropherogram showing the amount of applied *c-myc* peptide not retained by the immunoaffinity column (26 ng) after a 45 minute incubation of the sample with the immunomatrix).

The direct coupling of IAC to electrospray mass spectrometry was attempted on a number of occasions with the *c-myc* peptide (Figure 3.19). However, the signals observed were far weaker than expected. The mass spectrum of the peptide on-line affinity selection shows two weak *c-myc*-related peptides at m/z 688.0 and m/z 574.0 for the corresponding doubly-protonated molecules (Section 5.3 discusses the MS/MS characterization of these peptides). The method used for this selection was the same as that of the 45 minute incubation off-line selection discussed previously. Therefore, a peptide concentration of 3.3 μg/ml was expected in the first 10 μl eluted from the column. Figure 3.20 shows the mass spectrum of the *c-myc* peptide at a concentration of 1 μg/ml in 0.1 M formic acid infused directly into the mass spectrometer. A comparison of Figures 3.19 and 3.20 shows that the signal observed in the on-line selection of the peptide was far below that of a 1 μg/ml peptide solution.

The poor signal intensities observed may be due to difficulty in obtaining a constant flow rate compatible with the electrospray conditions. The presence of the acidic buffer and subsequent oclusion of the capillary column due to protein precipitation is one possible explanation accounting for these difficulties. In addition, the lack of uniformity found with the packing in the column may have affected the stability of the flow. The instability of the elution buffer flow rate directly affects the electrospray sensitivity.

The on-line affinity selection proved to be a lot less sensitive and efficient than originally expected. Automation of the on-line selection is very difficult with the present system because of the instability of the flow of the elution buffer through the column. In addition, automation is also limited by the fact that the column cannot be directly interfaced with the mass spectrometer during the application of the samples, wash solution (DIW), and

regeneration buffer (PBS) since the instrument cannot be exposed to these high salt solutions. Due to the logistics constraints and the required time for effective selection and elution of the antigen (approximately 90 minutes cycle time), on-line antigen preconcentration was not explored further. As a result, off-line affinity selection (not column-packed) was investigated for the selective enrichment of the *c-myc* peptide and scFv antibodies from complex matrices.

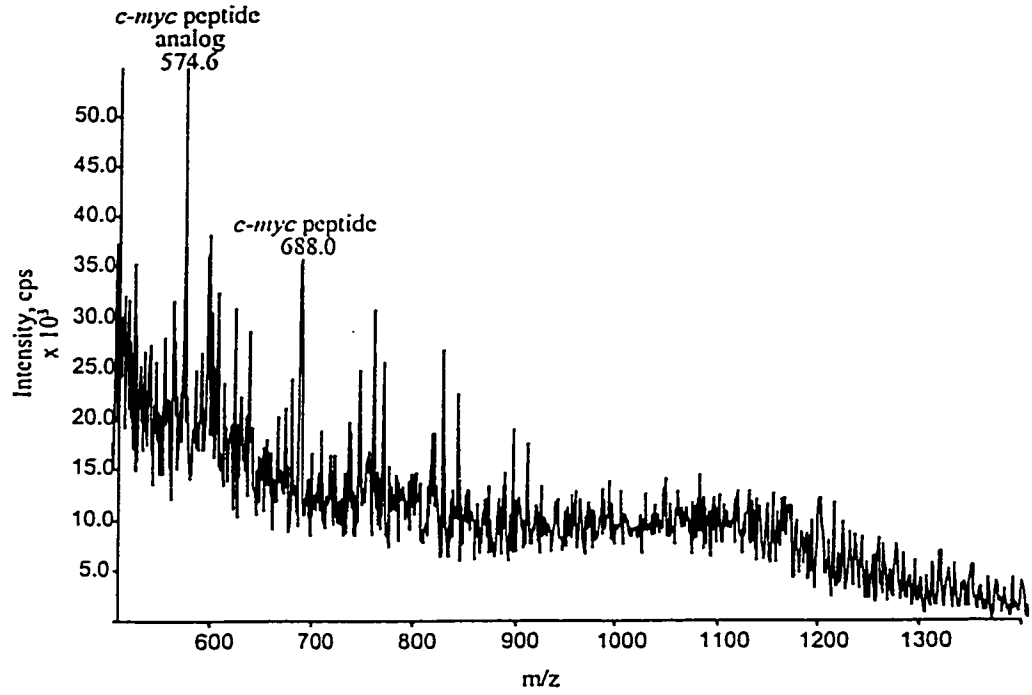

Figure 3.19 Electrospray mass spectrum of on-line *c-myc* immunoaffinity selection from PBS buffer.

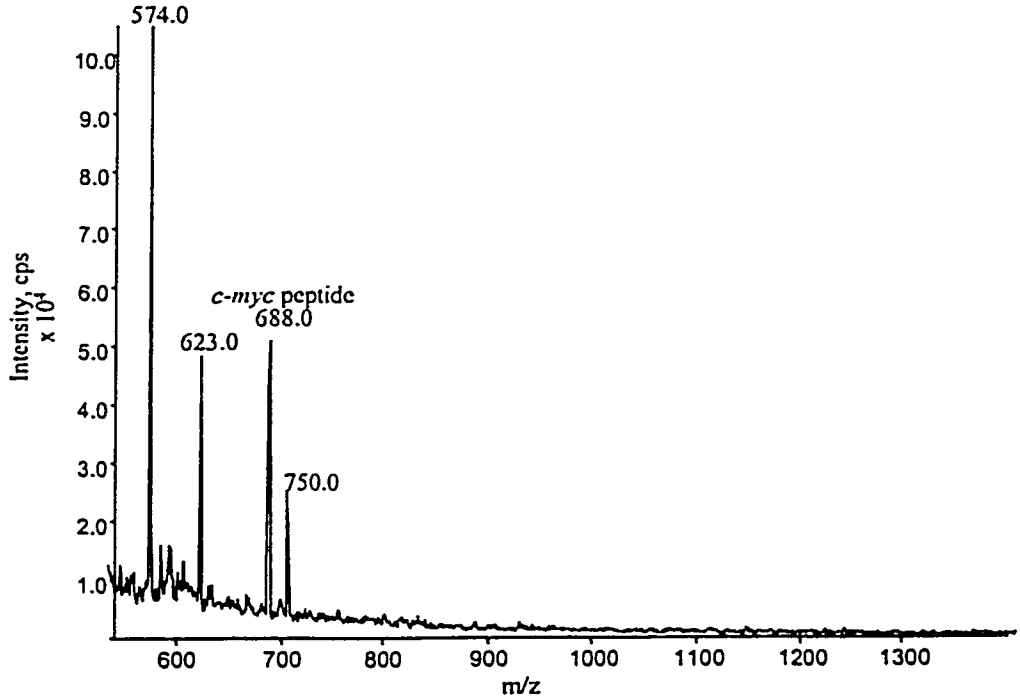

Figure 3.20 Electrospray mass spectrum of 1 μg/ml *c-myc* peptide in 0.1 M formic acid. M/z 574, 623, and 705 are all analogs of the *c-myc* peptide present in original synthetic mixture (Section 5.3 discusses the characterization of these analogs.

Chapter 4 Affinity Selection for the Enrichment of Single Chain Antibodies (scFvs)

4.1 Single Chain Antibodies

Single chain antibodies (scFvs) are recombinant proteins composed of immunoglobulin variable light (V_L) and heavy-chains (V_H) joined by a linker peptide of appropriate length and flexibility. These 30 kDa antibodies, which are expressed in *Escherichia coli*, offer many advantages in immunotherapy and *in vivo* diagnostics due to their shorter clearance times, reduced immunogenicity, and relative ease of production and manipulation when compared to the larger intact antibody or proteolytic Fab' or $F(ab')_2$ fragments.[64] Expression plasmids can be designed so that the scFv gene is preceded by a membrane protein A (ompA) secretory signal to favor its secretion into and extraction from the periplasm of *E. coli*. These plasmids can also be tailored to contain nucleotide sequences encoding peptide segments recognized by specific antibodies thus enabling purification and detection of these polypeptides by immunological methods.

Affinity purification was used to selectively enrich both wild-type and mutant scFvs specific for the blood group A antigen from the periplasmic extract of *E. coli*. The presence of the *c-myc* peptide (EQKLISEEDLN) localized at the C-terminal segment of the scFv (Figure 4.1) allowed for affinity purification using the anti-*c-myc* IgG antibody. A gene encoding this scFv antibody was assembled according to Mackenzie and coworkers.[65]

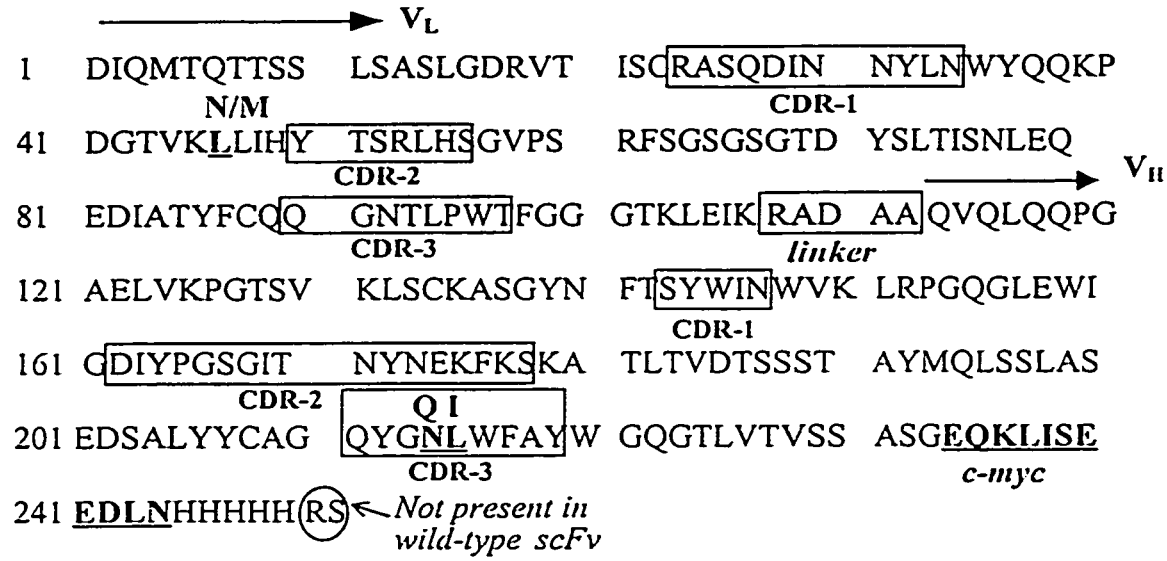

Figure 4.1 Sequence of the human blood group A scFv antibody showing the heavy (V_H) and light chain (V_L) domains, linker region, *c-myc* tag, and CDR mutation sites.

4.2 Identification of Mutation Sites in Human Blood Group A scFv Antibodies

In an attempt to increase the affinity of the scFv antibody for human blood group A antigens, the scFv sequence was modified in or near the complementarity-determining regions of the variable chains. The identification of the mutation sites within the scFv mutants was accomplished by the selective enrichment of the antibodies from the shock buffer periplasmic extract of *E. coli* using the crosslinked protein G immunomatrix followed by tryptic digestion of the purified protein and LC-MS/MS of the resulting peptides.

Several mutant scFvs were affinity-purified (Section 2.5) and analyzed using mass spectrometry. The effectiveness of affinity enrichment for a mutant scFv protein is illustrated in Figure 4.2. The MALDI-MS spectrum corresponding to 1 µl of the original 500 µl *E. coli* extract is shown in Figure 4.2A. As indicated, the *E.*

coli periplasmic extract contains several hundred proteins, including the expressed scFv product and buffer salts, which complicate the interpretation of the MALDI-MS spectrum. In contrast, the MALDI-MS spectrum of the affinity-selected fraction of the extract described above showed predominantly a single protein component of the expected molecular weight (Figure 4.2B). In a separate set of experiments, this affinity selection procedure was evaluated for a number of scFv antibodies comprising single point mutations. Table 4.1 summarizes the results obtained for the mutant scFvs and compares the observed and expected molecular masses.

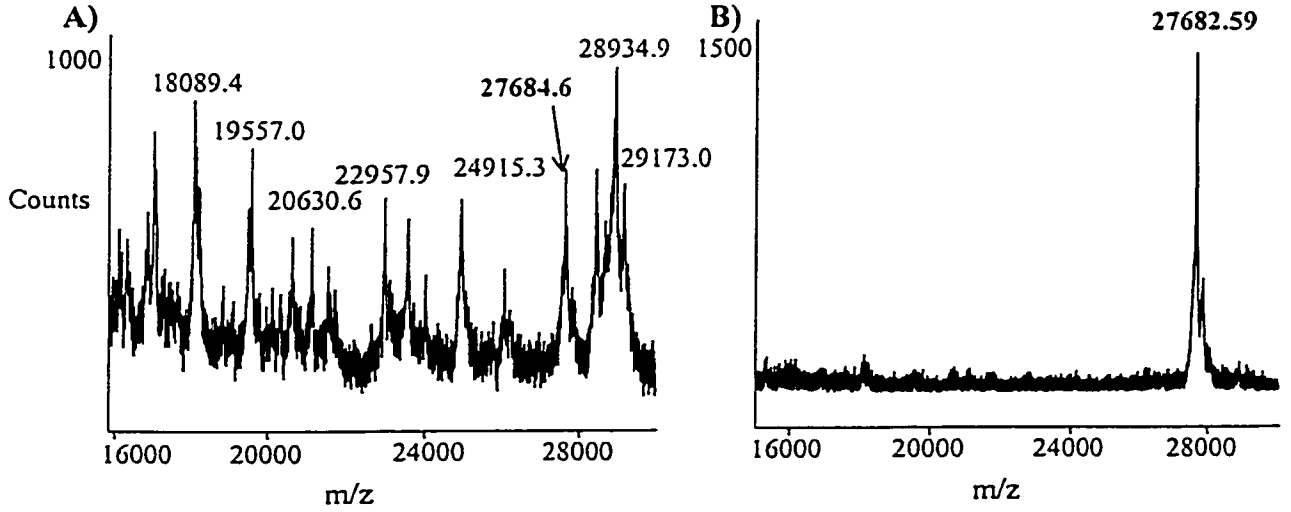

Figure 4.2 MALDI-TOF MS showing scFv mutant L46N, N214Q, L215I (# 1) A) in the shock buffer periplasmic extract of *E. coli* (scFv 570 µg/ml) and B) affinity-selected (estimated 270 µg/ml).

BGA scFv		Mass Calculated (Da)	Mass Observed (Da)
Wild-type		27423.45	27423.20
1	L46N N214Q L215I	27681.69	27682.59
2	N214Q	27680.75	27680.50
3	L46N	27667.66	27667.60
4	L46M	27684.76	27683.30

Table 4.1 Calculated and observed masses (MALDI-MS) for Blood group A scFv wild-type and mutant proteins.

Following purification, all the proteins listed above, except the L46M mutant, were digested using trypsin (Section 2.10.2). MALDI-MS was used initially for the rapid analysis of the tryptic peptides generated (Figures 4.3 and 4.4 and Tables 4.2 and 4.3). In all the digests the peptide T46-53 containing the mutation site L46N was observed; however, the tryptic peptide containing both the N214Q and L215I mutations was only barely detected in the corresponding MALDI-MS of the first and second mutant scFvs (Figure 4.4). Unfortunately, both these mutations are found on a large tryptic peptide—(K)180 ATLTVDTSSS TAYMQLSSLA SEDSALYYCA GQYG**QI**WFAY WGQGTLVTVS SASGEQK 236(L) (sequence shown for the mutant #1)—having a calculated molecular weight of 6139.72 (MH^+) for the mutant and 6125.29 (MH^+) for the wild-type. Because of the size of this peptide, the MALDI matrix sinapinic acid, which is suitable for the analysis of high molecular weight species, was also used with the tryptic digest; however, the peptide was not observed. In addition, several different solvents were used for the MALDI-MS analysis, and the peptide was observed only in those having an acid or organic component (5% acetic acid or 30% acetonitrile and 0.01% trifluoroacetic acid). It is possible that the peptide may not be fully recovered due to poor solubility, adsorption on the surface of the eppendorf, poor ionization efficiency, or incomplete proteolytic digestion. However, the MALDI-MS of the digest showed no large peptides that could possibly be related to the incomplete digestion of the protein in the vicinity of the mutant tryptic peptide. It is noteworthy that the presence of the 6139.32 Da peak in the MALDI spectrum of the mutant #1 indicates a 14 Da difference from the wild-type 180-236 peptide in agreement with the mutation from asparagine to glutamine.

Tryptic Peptides Observed		Theoretical Mass (Da)	Theoretical Tryptic Peptide Position
Peak #	Mass (Da)		
1	735.431	735.38	(R)19 VTISCR 24(A)
2	852.547	852.47	(R)54 LHSGVPSR 61(F)
3	1002.67	1002.57	(K)46 LLIHYTSR 53(L)
4	1617.87	1617.75	(K)237 LISEEDLNHHHHH 249(<)
5	1835.99	1835.88	(K)136 ASGYNFTSYWINWVK 150(L)
6	2335.41	2335.26	(R)109 ADAAQVQLQQPG AELVKPGTSVK 131(L)
7	2482.36	2482.20	(R)25 ASQDINNYLNW YQQKPDGTVK 45(L)
8	2491.52	2491.36	(K)108 R 131(L)
9	2777.59	2777.39	(K)151 LRPGQGLEWIGD IYPGSGITNYNEK 175(F)
10	3465.83	3465.76	(R)25-45 LLIHYTSR 53(L)
11†	4301.83	4301.81	(R)25-53 LHSGVPSR 61(F)
12†	4537.71	4537.88	(R)62 FSGSGSGTDYSLTISNLEQED IATYFCQQGNTLPWTFGGGTK 103(L)
13†	4597.06	4597.10	(K)136-175(F)

Table 4.2 Tryptic peptides of the scFv wild-type protein as observed by MALDI-MS (Figure 4.3). † indicates that the average mass was observed for this peptide.

Tryptic Peptides Observed		Theoretical Mass (Da)	Theoretical Tryptic Peptide Position
Peak #	Mass (Da)		
1	1003.60	1003.53	(K)46 NLIHYTSR 53(L)
2	1774.02	1773.85	(K)237 LISEEDLNHHHHHR 250(S)
3	1836.04	1836.98	(K)136 ASGYNFTSYWINWVK 150(L)
4	1910.03	1910.91	(>)1 DIQMTQTTSSLSASLGDR 18(V)
5	2482.44	2482.20	(R)25 ASQDINNYLNW YQQKPDGTVK 45(N)
6	2491.56	2491.36	(K)108 RADAAQVQLQQPG AELVKPGTSVK 131(L)
7	2777.45	2777.39	(K)151 LRPGQGLEWIGD IYPGSGITNYNEK 175(F)
8†	4537.91	4537.88	(R)62 FSGSGSGTDYSLTISNLEQED IATYFCQQGNTLPWTFGGGTK 103(L)
9†	6139.32	6139.72	(K)180 ATLTVDTSSSTAYMQLSS LASEDSALYYCAGQYGQIWFAYWGQ GTLVTVSSASGEQK 236(L)

Table 4.3 Tryptic peptides of the scFv mutant #1 antibody as observed by MALDI-MS (Figure 4.4). † see Table 4.2.

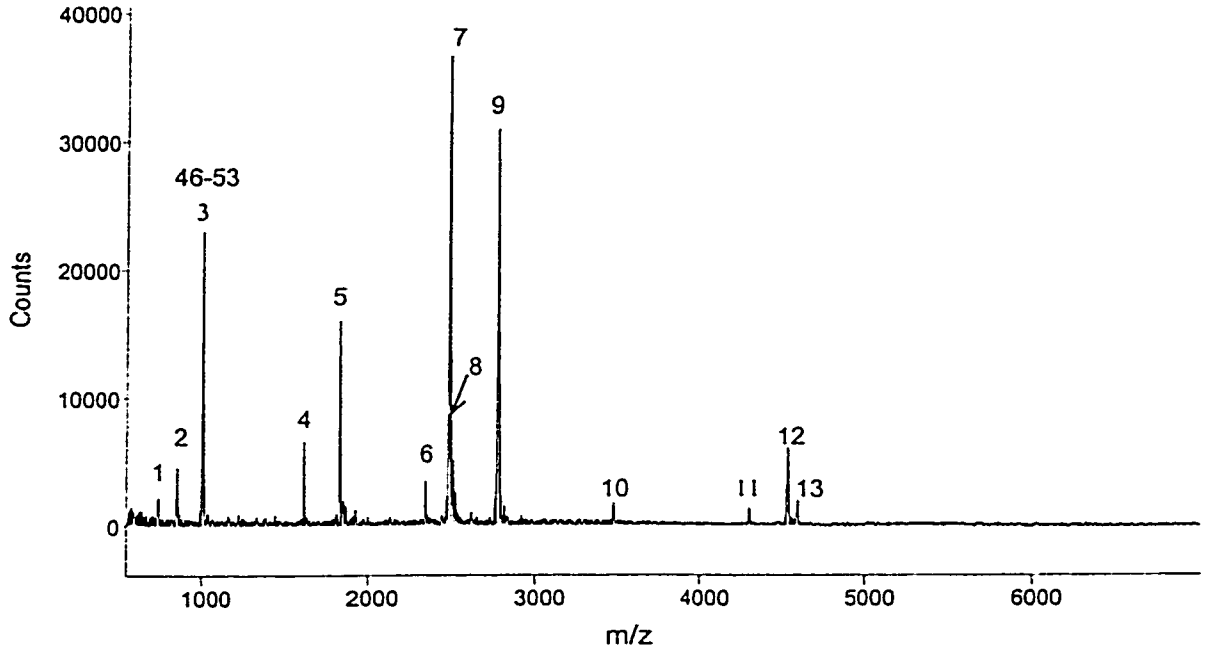

Figure 4.3 MALDI-MS of the scFv wild-type tryptic digest. See Table 4.2 for mass assignments.

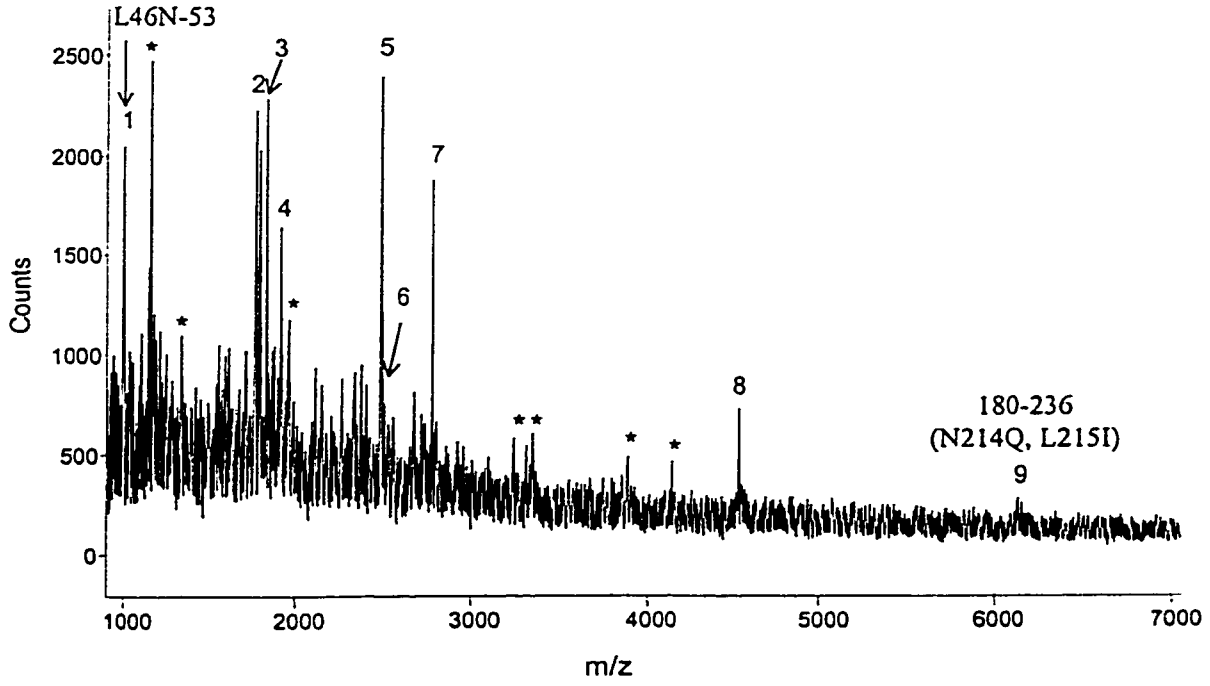

Figure 4.4 MALDI-MS of the mutant #1 tryptic digest showing the two mutant tryptic peptides (1 and 9). See Table 4.3 for mass assignments. * indicates those peptides not identified from the tryptic digest of the mutant protein.

Peptide identification and sequencing was performed using LC-MS/MS on the tryptic digest of the #1 scFv mutant as well as the wild-type protein. The L215I site of mutation could not be confirmed by mass spectrometry as the amino acids leucine and isoleucine are isobaric. Figure 4.5 and Tables 4.4 and 4.5 show the assignment of the tryptic peptides of the wild-type and #1 mutant scFv antibodies as observed by LC-MS. In both digests the tryptic peptide T46-53 containing the mutation L4-6N was observed and further characterized using combined LC-MS/MS. However, the tryptic peptide containing the N214Q and L215I mutations was not detected for either protein. The size of this peptide and the fact that it is largely hydrophobic may result in its being retained on the C18 PEPMAC column and therefore slowly eluted. As a result, the mutation N214Q could not be confirmed by LC-MS/MS sequencing.

Digestion of these proteins was also performed using Endoproteinase Glu-C ; a serine protease that cleaves only at the carboxyl side of glutamic acid residues. Unfortunately, this digestion results in a relatively large and hydrophobic peptide containing the mutations (202-234 MH^+ 3621.63 Da). Incomplete digestion of the protein was observed. As a result, this peptide was not detected by MALDI-MS.

MS/MS sequencing to confirm the N214Q and L215I mutations was also attempted on the intact reduced and alkylated scFv protein. Since these mutations were found at the C-terminal of the protein, it was anticipated that MS/MS sequencing would be possible. Unfortunately, the size of the protein and the presence of anti-*c-myc* antibody from the affinity enrichment (purification was executed before

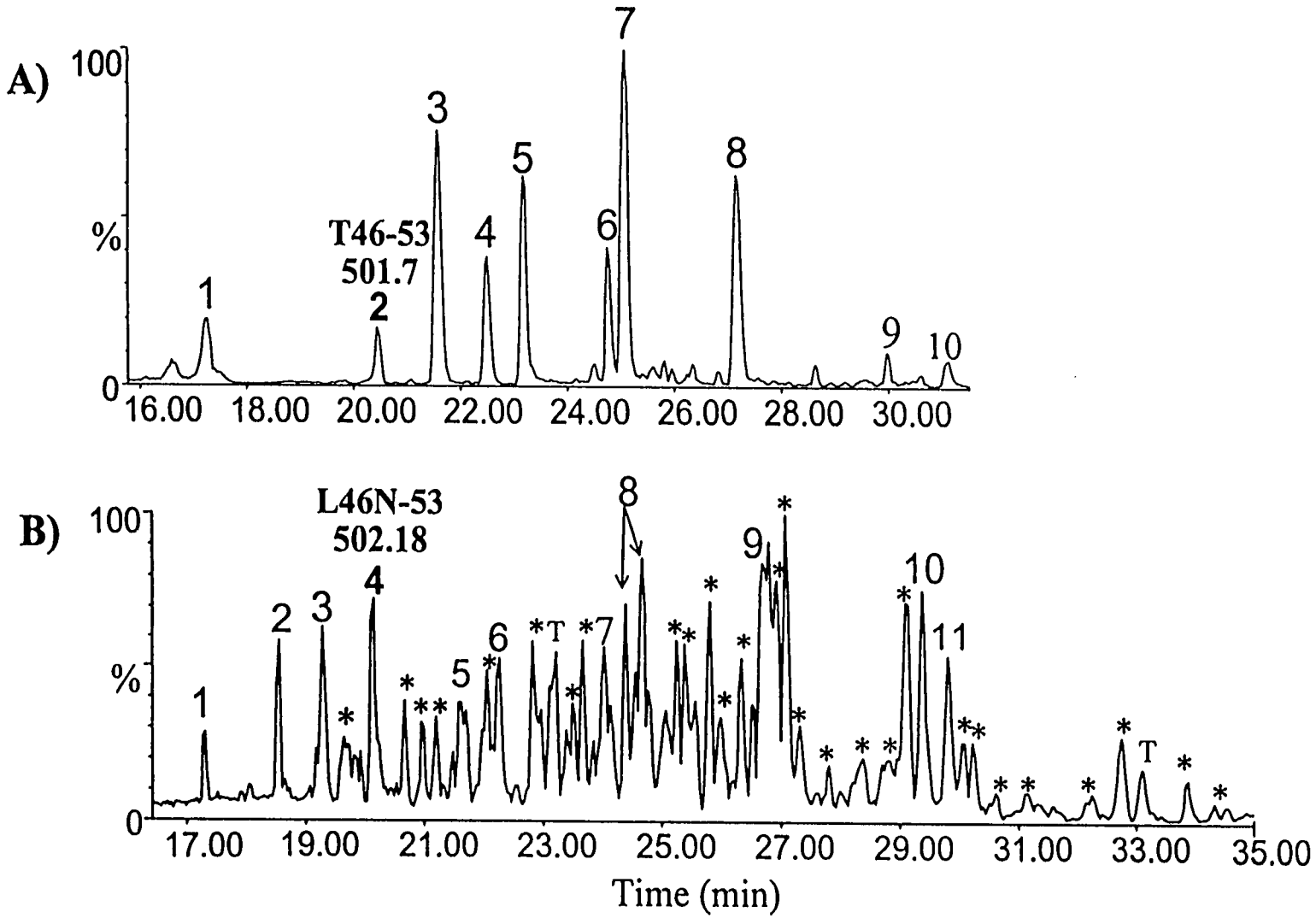

Figure 4.5 LC-MS reconstructed ion chromatograms of A) scFv wild-type and B) mutant tryptic digests showing the 46-53 tryptic peptide chosen for MS/MS characterization.
* indicates non-scFv tryptic peptides while T indicates peptides resulting from trypsin autolysis.

crosslinked protein G immunomatrices were used) resulted in no sequence information.

Tryptic Peptides Observed			Theoretical Mass (Da)	Theoretical Tryptic Peptide Position
Peak #	Rt (min)	Mass (Da)		
1	17.26	1617.7	1617.75	(K)237 LISEEDLN HHHHH 249(<)
2	20.44	1002.4	1002.57	(K)46 L LIHYTSR 53(L)
3	21.56	2491.0	2491.36	(K)108 RADAAQVQLQQP GAELVKPGTSVK 131(L)
4	22.51	2334.85	2335.26	109-131
5	23.17	1926.5*	1910.91	(>)1 DIQMTQTTS SLSASLGDR 18(V)
6	24.75	1910.6	1910.91	1-18
7	25.07	2481.6	2482.2	(R)25 ASQDINNYLN WYQQKPDGTVK (L)45
8	27.15	2776.8	2777.39	(K)151 LRPGQGLEWIGD IYPGSGITNYNEK 175(F)
9	29.96	1835.6	1835.88	(K)136 ASGYNFTSY WINWVK 150(L)
10	31.12	4534.4	4535.06	(R)62 FSGSGSGTDYSLT ISNLEQEDIATYFCQQG NTLPWTFGGGTK 103(L)

Table 4.4 Tryptic peptides observed by LC-MS (Q-TOF) of scFv wild-type protein (Figure 4.5A). *oxidized methionine. All masses shown are monoisotopic.

Tryptic peptides observed			Theoretical Mass (Da)	Theoretical Tryptic Peptide Position
Peak #	Rt (min)	Mass (Da)		
1	17.31	852.34	852.47	(R)54 LHSGVPSR 61(F)
2	18.55	735.3	735.38	(R)19 VTISCR 24(A)
3	19.29	502.3	502.32	(K)104 LEIK 107(R)
4	20.13	1003.3	1003.53	(K)46 N LIHYTSR 53(L)
5	21.58	2490.8	2491.36	(K)108 RADAAQVQLQ QPGAELVKPGTSVK 131(L)
6	22.26	2334.9	2335.26	109-131
7	24.03	1910.6	1910.91	(>)1 DIQMTQTTSS LSASLGDR 18(V)
8	24.66	2481.6	2482.20	(R)25 ASQDINNYLNW YQQKPDGTVK (L)45

9	26.72	2776.9	2777.39	(K)151 LRPGQGLEWIGDI YPGSGITNYNEK 175(F)
10	29.37	1835.6	1835.88	(K)136 ASGYNFT SYWINWVK 150(L)
11	29.80	4534.3	4535.06	(R)62 FSGSGSGTDYSLT ISNLEQEDIATYFCQQGN TLPWTFGGGTK 103(L)

Table 4.5 Tryptic peptides observed by LC-MS (Q-TOF) of affinity-purified scFv mutant protein L46N, N214Q, L215I (#1) (Figure 4.5B).

It is apparent from the chromatogram (Figure 4.5B) and the MALDI-MS spectrum of the mutant scFv tryptic digest (Figure 4.4) that a number of unexpected peptides were observed (labeled with an asterisk). These peptides were not observed with the wild-type scFv since this protein was purified by immobilized metal affinity chromatography (IMAC) using the penta-His tag on the C-terminus of the protein (Figure 4.1) and not by affinity selection. The identification of these extraneous components was attempted using MS/MS sequencing of several of the peptides followed by database searching. Section 4.3 will discuss this aspect further.

Figures 4.6 and 4.7 show the MS/MS spectra obtained from the 46-53 tryptic peptides for both the wild-type and mutant scFv proteins. For each spectrum, b and y fragment ions were generated providing a complete sequence coverage for each peptide. It was therefore confirmed that the amino acid 46 had been changed from a leucine in the wild-type to an asparagine in the mutant protein.

4.3 Identification of Extraneous *E. coli* Proteins Co-Selected with the scFv Antibodies

The LC-MS of the scFv mutant tryptic digest (Figure 4.5B) showed a number of unexpected peptides in addition to those from the digestion of the mutated protein. In

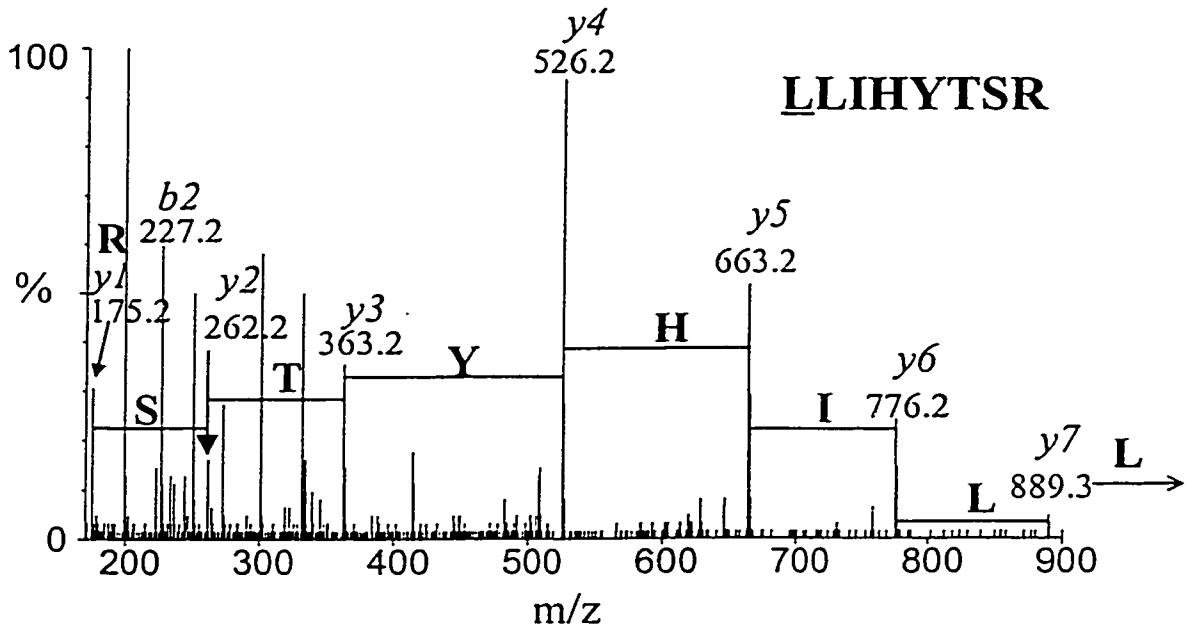

Figure 4.6 LC-MS/MS sequencing of the scFv wild-type 46-53 tryptic peptide.

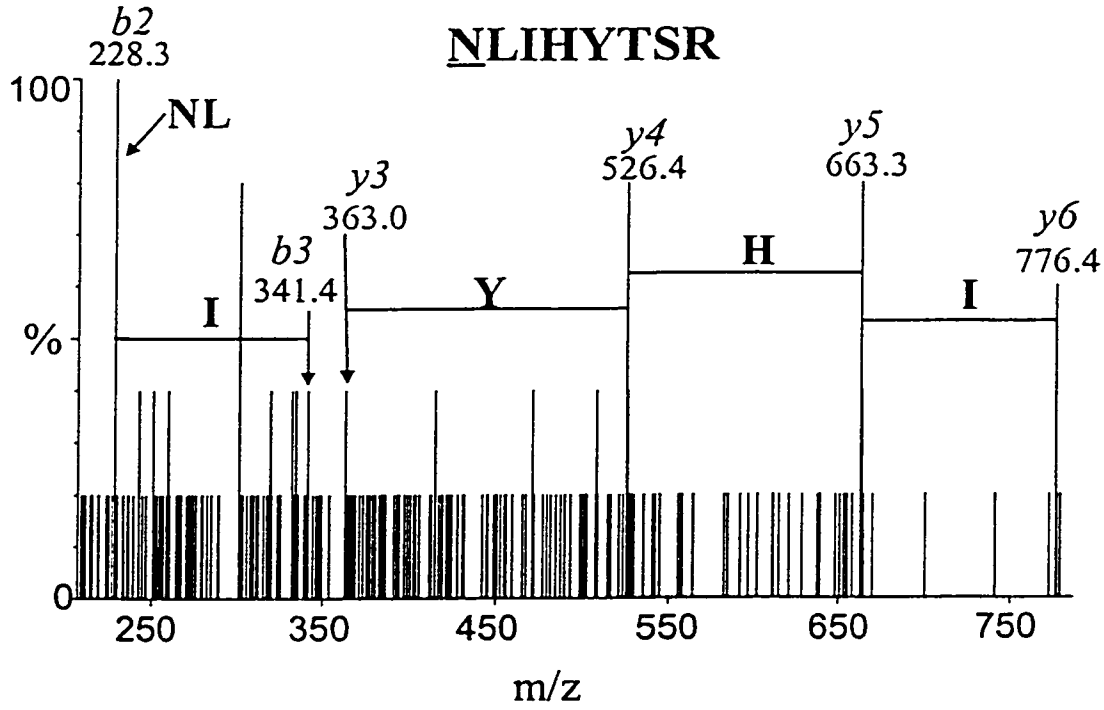

Figure 4.7 LC-MS/MS sequencing of the scFv mutant 46-53 tryptic peptide identifying the mutation of L46⇒N46.

order to identify these unexpected components, LC-MS/MS, using the data dependent MS/MS function of the Q-TOF mass spectrometer, was performed. Partial sequence information plus the mass of the corresponding peptide was used to conduct database searching. Table 4.6 shows the sequence tags obtained by MS/MS and the corresponding proteins identified using the ProteinProspector database searching tool.

It is believed that the extraneous tryptic peptides observed in the LC-MS (Figure 4.5B) are the digestion products of *E. coli* proteins (Table 4.7). To ensure that the peptides observed were not the product of non-specific or chymotryptic cleavage of the scFv mutant or the mouse IgG antibody, the sequences of both these proteins were searched using the ProMac program for matches with the peptide masses and respective sequence tags shown in Table 4.6. None of the above listed peptides could be matched to peptide segments of either the scFv mutant or the anti-*c-myc* antibody.

Mass (Da)	Sequence Tag	Tryptic Peptide Identified	Protein Identified
1100.2	YADMLAM	(K)YADMLAMSAK	•Tryptophanase 41936 •Tryptophanase (L-tryptophan indole-lyase) (TNase) 401195 •Tryptophanase 290556
1343.6	GAEQLYL	(R)GAEQIYIPVLIK	
1794.5	YTLPT	(K)NIFGYQ YTIPTHQGR	
2781.1	MVAFS*Y	(K)MVAFSNYFFDTT QGHSQINGCTVR	
3342.1	VQYLVD	(R)IAQVQYLVDG LEEIGVVCQQAG GHAAFVDAGK	
2395.0	PAQALA	(K)LLPHIPADQF PAQALACELYK	•Tryptophanase (L-tryptophan indole-lyase) (TNase) 401195 •Tryptophanase 290556
1069.4	VFTLADK	(R)EFVFTIADK	•Carbohydrate phosphotransferase II 1361020 •Putative tagatose 6-phosphate kinase 1 2507030
1250.4	FNDSLLDLR	(R)TGFNDSLLDIR	
2155.0	EQELL	(R)EAIFALAQI EQELIAPENR	
2550.1	PLA	(K)IHLDASMSCAGD PIPLAPETVAER	

1171.4	VGEEVELV	(K)VGEEVEIVGIK	•Elongation factor Tu 59-263 223399 •Protein chain elongation factor EF-Tu (duplicate of tufB) 538596 •Elongation factor EF-Tu (duplicate of tufA) 119201
1961.8	A**LDSYL	(K)ILELAG FLDSYIPEPER	
1409.6	FDSLM	(K)SPAFD SIMAETLK	•Periplasmic oligopeptide-binding protein precursor 1742032 •Periplasmic oligopeptide-binding precursor 585619 •Oligopeptide binding protein precursor 96309
1885.9	HLPF	(R)SVMIDASHL PFAQNISR	•Tagatose-bisphosphate aldolase 1 2506174 •Carbohydrate phosphotransferase II 1361019

Table 4.6 The sequence tags obtained by LC-MS/MS of the scFv mutant tryptic digest (Figure 4.5B) and the corresponding proteins identified from database searches with the sequence tags and respective tryptic peptide masses. * amino acids in the sequence not identified from the MS/MS spectrum. L refers to either leucine or isoleucine amino acid residues.

Proteins	Molecular Mass (Da)	% Sequence Coverage
Tryptophanase 41936	52732.7	93/471 19.7%
Tryptophanase (L-tryptophan indole-lyase) (TNase) 401195	52773.8	114/471 24.2%
Tryptophanase 290556	53410.5	114/476 23.9%
Carbohydrate phosphotransferase II 1361020	42346.4	63/378 16.7%
Putative tagatose 6-phosphate kinase I 2507030	47109.0	63/420 15.0%
Elongation factor Tu 59-263 223399	22645.0	28/205 13.7%
Protein chain elongation factor EF-Tu (duplicate of tufB) 538596	43283.8	28/394 7.1%
Protein chain elongation factor EF-Tu (duplicate of tufA) 119201	43313.8	28/394 7.1%
Periplasmic oligopeptide-binding protein precursor 1742032	43092.1	13/377 3.4%

Periplasmic oligopeptide-binding protein precursor 585619	60899.2	13/543 2.4%
Oligopeptide-binding protein precursor 96309	60902.2	13/543 2.4%
Tagatose-bisphosphate aldolase 1 2506174	31071.5	17/286 5.9%
Carbohydrate phosphotransferase II 1361019	31075.5	17/286 5.9%

Table 4.7 *E. coli* proteins identified by database searching to be present in the selection of the scFv mutant from the *E. coli* periplasmic extract. The percentage of their respective sequences covered by the sequence tags identified is also shown.

Interestingly, one tryptic peptide was found to be common to only two of the tryptophanase proteins. L-tryptophan indole-lyase and tryptophanase #290556 contain the tryptic peptide 372(K)LLPHIPADQFPAQALACELYK(V)392 (2395.0 Da) while the corresponding peptide in tryptophanase #41936 contains threonine (T) and glycine (G) in place of alanine (A) and glutamine (Q) resulting in a peptide of mass 2354.2 Da. This latter peptide was not observed in the digest, indicating that the tryptophanase #41936 protein may not be present at all. Since there are so few sequence variations among these three proteins, there are very few peptides that illustrate these differences therefore making it difficult to determine if one or all of these proteins are present. Unfortunately, from the MS/MS analysis these unique peptides could not be identified. For the other proteins shown in Table 4.6, sequence similarity was also observed within each group. Therefore, it is also possible that only one of the proteins shown is present.

MALDI-MS of the affinity-enriched scFv mutant showed the presence of several weak peaks with masses less than that of the mutant (Figure 4.8). None of these masses match those shown for the proteins identified from LC-MS/MS analysis. It is

therefore most likely that these proteins are the degradation products of the scFv mutant since foreign proteins that are produced in *E. coli* are generally unstable.[66] It is also possible, however, that some or all of the extraneous proteins identified in the database searching (Table 4.7) are present in the *E. coli* periplasm as fragments of their whole structure and therefore have a lower molecular weight than expected. Interestingly, in the MALDI-MS of the affinity-selected mutant, no proteins having a molecular mass greater than that of the mutant (27.7 kDa) were observed. These extraneous proteins may be present at concentrations lower than the limit of detection by MALDI-MS or may be suffering from discrimination effects resulting in their having an ionization efficiency lower than of the scFv mutant. As a result, these proteins were only observed by LC-MS as their respective digestion products.

Using the European Bioinformatics Institute's Blitz (bic sw) Compugen's Smith and Waterman algorithm, the proteins in Table 4.7 were searched for sequence similarity with the *c-myc* tag.[67] This homology tool involves searching the Trembl and SwissProt databases with the manually entered *c-myc* peptide sequence. Since all the proteins under investigation were found in these databases, an homology between the *c-myc* peptide and a portion of any one of these proteins could be expected if present. For these searches, a maximum of three amino acid omissions or replacements and a maximum of five total sequence variations were permitted. In addition, a manual search was carried out using the ProMac software in which each individual protein sequence of Table 4.7 was searched for homology with a variety of two to three amino acid combinations of the *c-myc* peptide (eg., EQK or EK etc). No

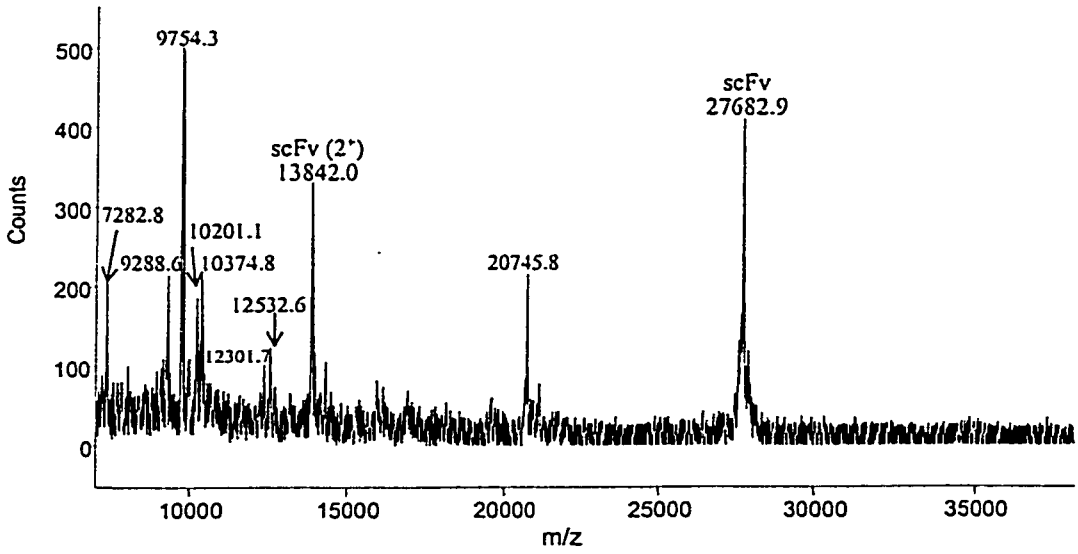

Figure 4.8 MALDI-MS of affinity-selected scFv mutant #1.

Human *c-myc*	AEEQKLISEE DLLRKRREQL KHKLEQLRNS CA
Mouse *c-myc*	ADEHKLTSEE DLLRKRREQL KHKLEQLRNS GA
Chicken *c-myc*	SDEHRLIAEK EQLRRRREQL KHKLEQLRNS RA
Chicken v-*myc*	SDEHKLIAEK EQLRRRREQL KHNLEQLRNS RA

Figure 4.9 Sequence of the human *c-myc* (amino acids 408-439) synthetic peptide immunogen selected by the anti-*c-myc* IgG antibody and the homologous mouse and chicken *myc* sequences.[68] The *c-myc* epitope sequence is underscored.

Human *c-myc* (235-245)	PEPLVLHEETP
Sigma Factor (62-72)	ADDLMLAENTA

Figure 4.10 The *c-myc* epitope of the MYC-X-5/1 monoclonal antibody and the cross-reactive epitope on the sigma factor of *E. coli*.[66]

sequence homology was found between any of the proteins shown in Table 4.7 and the *c-myc* peptide, suggesting that these proteins were not immunoaffinity-selected via a contiguous peptide sequence homologous to the *c-myc* tag.

One of the problems that is often incurred when monoclonal antibodies are used for immunoaffinity purification is that of cross-reactions.[10] These reactions are only seen for a subset of antibodies and involve the binding of the antibodies to other antigens through shared or homologous epitopes. A study by Evan and coworkers showed that the monoclonal anti-*c-myc* IgG antibody did not cross-react with any of the homologous peptide immunogens (mouse and chicken *myc* peptides) investigated and was specific only to the *c-myc* peptide (Figure 4.9).[68] Siegel and coworkers, however, found that the 9E10 monoclonal anti-human *c-myc* antibody used by Evan and coworkers in the previous study cross-reacted with a murine *c-myc* peptide (Figure 4.9–ADEHKLTSEK) as well as the murine *c-Myc* protein.[69] This cross-reactivity between the 9E10 antibody and the mouse *c-Myc* protein was also found by Mai and Martensson.[70] Interestingly, Ikegaki and coworkers found that an anti-*c-myc* monoclonal antibody (MYC-X-5/1), recognizing a human *c-myc* epitope (not the *c-myc* epitope used in this study), cross-reacted with two subunits of *E. coli* RNA polymerase as well as the murine *Myc* protein, all having epitopes homologous to the *c-myc* immunogen (Figure 4.10).[66] Therefore it is possible that the anti-*c-myc* IgG antibody is cross-reacting with the *E. coli* proteins identified in this study through an homologous epitope formed by a noncontiguous or contiguous amino acid sequence thereby resulting in their selection.

The observation of these extraneous proteins may also be the result of non-specific binding to the protein G resin used in the immunomatrix. Binding to protein G is not immunological in nature and therefore does not occur with the specificity observed with immunoaffinity complexes. As a result, the proteins may be retained by the available protein G sites and eluted along with the mutant scFv upon the application of the acidic elution buffer. Non-specific binding of the *E. coli* proteins to the scFv mutant or to the IgG antibody may also be occurring, resulting in their co-elution with the affinity selection fraction. It is unlikely that these proteins are being affinity-selected by the scFv antibody itself since these proteins are not observed when the antibody is purified by other methods (IMAC purification).

Chapter 5 Affinity Selection of the *c-Myc* Peptide

5.1 Introduction

Method development of the immunoaffinity enrichment of the *c-myc* peptide and scFv antibodies was carried out from non-complex matrices such as PBS buffer. However, for real samples such as tissue culture media, the matrices are complex having many components in addition to the *c-myc* peptides or proteins. As a result, immunoaffinity selection of the *c-myc* peptide from more complex media was investigated. This antigen was spiked into both fetal bovine and human sera and subsequently isolated using immunoaffinity purification.

5.2 LC-ESMS of the Affinity-Selected *c-Myc* Peptide from a Non-Complex Matrix

A study was conducted in order to determine the sensitivity of the LC-ESMS method for the detection of the *c-myc* peptide from a non-complex matrix (PBS buffer) (Sections 2.16 and 2.18). This was done to establish a benchmark against which serum selections could be compared. Both quadrupole time-of-flight (Q-TOF) and triple quadrupole (API 3000) instruments were used for this study. Figures 5.2 and 5.3 show plots of the LC-MS peak area (using both instruments) observed for the affinity-selected *c-myc* peptide (m/z 687.8) versus the amount of peptide originally applied to the immunomatrix. As expected, these graphs indicate that the amount of peptide selected increases linearly with the amount applied to the beads (equal volumes of increasing peptide concentrations were used). However, both plots show a departure from linearity at high concentration of the antigen peptide (250 ng application). The immunomatrix used for the affinity selections in this study was

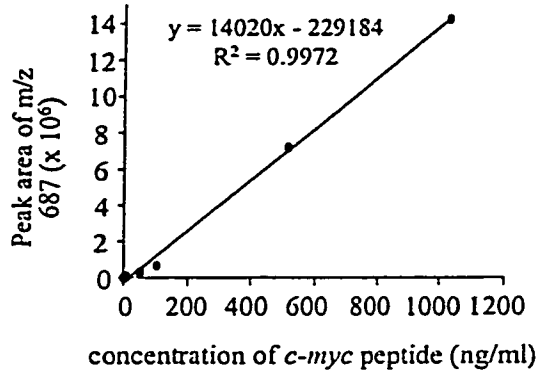

Figure 5.1 Calibration curve for *c-myc* (in DIW) using LC-ESMS (triple quadrupole).

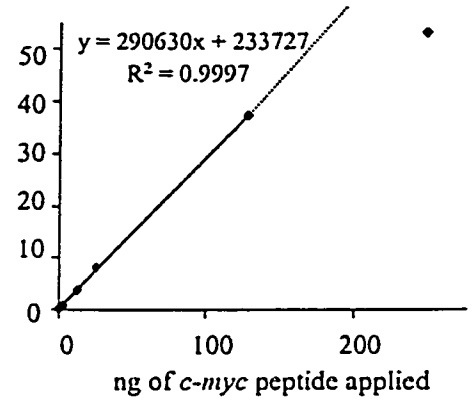

Figure 5.2 Affinity selection calibration curve by LC-ESMS (triple quadrupole).

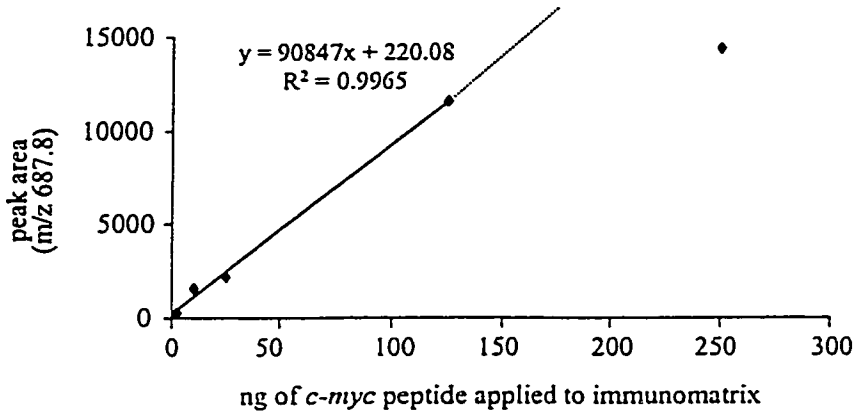

Figure 5.3 Affinity selection calibration curve using LC-ESMS (Q-TOF).

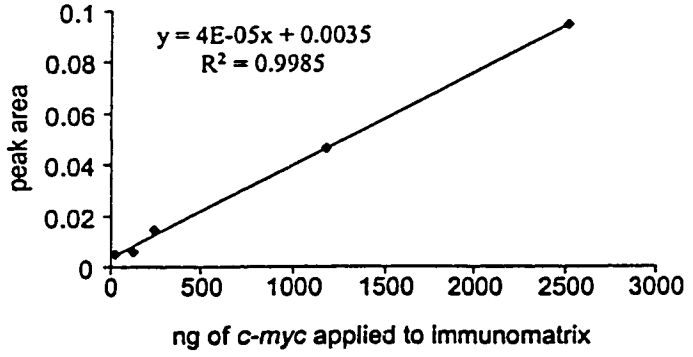

Figure 5.4 Affinity selection calibration curve using CE-UV (preconcentration).

calculated to have 2.3 x 10^{-9} mols of available antigen-binding sites thereby having a maximum *c-myc* selection capacity of 3.2 μg. Therefore, it is unlikely that the observed non-linearity is a result of the saturation of the immunomatrix binding sites when only 7.8% of the maximum *c-myc* binding capacity was applied (250 ng). On the other hand, if the entire 250 ng of *c-myc* that was applied to this immunomatrix was affinity-selected and eluted into a 20 μl volume, a concentration of 12.5 μg/ml would be produced. It is, therefore, highly possible that the mass spectral detector was being saturated resulting in the observed non-linearity. To verify this, the concentration study was carried out using the CE-UV preconcentration method (Section 2.13). Figure 5.4 shows that the amount of *c-myc* peptide selected and eluted does increase linearly over the applied analyte concentrations (25-2600 ng). This linearity was even observed with higher application quantities than used with the LC-MS study (e.g., 250 ng) thereby confirming that saturation of the mass spectrometer detector was occurring with this applied amount.

Using the calibration curve from LC-MS (Figure 5.1), the amount of *c-myc* peptide selected from the PBS buffer was calculated. Table 5.1 and Figure 5.5 show that an increase in the concentration of the peptide solution applied to the immunomatrix gave rise to a linear increase in the total amount selected. However, it was noticed that lower antigen recovery was observed as the concentration of the *c-myc* peptide was increased. For example, an applied antigen amount of 1.25 ng resulted in a recovery of 74.4%, whereas this value was only 39.5% for 128 ng of applied *c-myc* peptide. The observed decrease in percentage recovery with increasing antigen concentration is most likely due to the rapid dissociation of the antigen from

the antibody during the incubation and washing of the immunomatrix. Affinity selection is an equilibrium process in which the antigen can dissociate from and bind to the antibody several times throughout the course of the selection. The dissociation rate of the *c-myc* peptide from the anti-*c-myc* IgG was determined by surface plasmon resonance analysis to be 1.54×10^{-3} s^{-1}, indicating a relatively fast dissociation of the antigen from the antibody.[10] However, at a high antibody-to-antigen ratio it is highly probable that upon dissociation the antigen will be recaptured by an available immunoglobulin. As the concentration of the antigen is increased the amount of free antibody decreases resulting in a reduced probability of recapture. As a result, the percentage recovery decreases with increasing antigen concentration while the total amount of antigen selected increases. It is noteworthy that for a concentration of 1 ng/ml, a recovery value exceeding 100% was observed, suggesting a non-linearity behavior for the corresponding applied amount of antigen solution.

Concentration of *c-myc* peptide in PBS buffer (ng/ml)	**Amount Applied (ng)**	**Amount Affinity-Selected (ng)**	**% Recovery**
1.0	0.25	0.75	300.0
5.0	1.25	0.93	74.4
10.0	2.5	1.55	62.0
51.0	12.8	5.62	43.9
103.0	25.8	11.67	45.2
511.0	127.8	50.52	39.5

Table 5.1 Amounts of the *c-myc* peptide applied and selected by the anti-*c-myc* immunomatrix as determined by LC-ESMS (triple quadrupole).

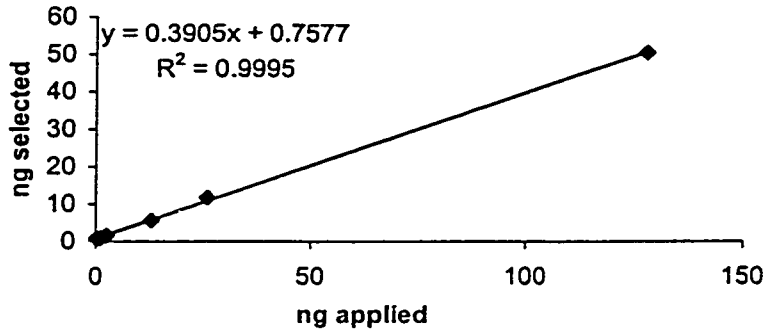

Figure 5.5 LC-MS showing the amount of *c-myc* selected vs. the amount applied to the immunomatrix.

5.3 Mass Spectral Analysis of the Synthetic *c-Myc* Peptide

Interestingly, the mass spectrum of the affinity-selected synthetic *c-myc* peptide from PBS buffer showed not only the *c-myc* peptide at m/z 688.0 (MH^+ 1375), but also two other peaks at m/z 574.0 (MH^+ 1147) and 623.0 (MH^+ 1245) (Figure 5.6). MS/MS analyses of the corresponding precursor ions (Figures 5.8 and 5.9) indicated similar sequences to that of the *c-myc* peptide (GEQKLISEEDLN), whereby the 1147 Da component was consistent with a peptide missing the two C-terminal amino acids leucine and asparagine (GEQKLISEED) and the 1245 Da component missing the first glutamic acid (GQKLISEEDLN) of the *c-myc* sequence.

The mass spectrum of the *c-myc* peptide mixture prior to affinity selection showed all three of the above components with the doubly-charged ions m/z 623 and 688 present in a nearly equal ratio, whereas the doubly-protonated ion m/z 574 was the most prominent (Figure 5.7). However, the mass spectrum of the affinity-selected mixture (Figure 5.6) shows a different intensity profile, whereby the *c-myc* peptide is the most prominent component followed by the truncated C-terminus peptide (m/z 623) and the truncated N-terminus peptide (m/z 574). This differential selection is not totally unexpected as binding efficiency of the monoclonal CDRs can be affected

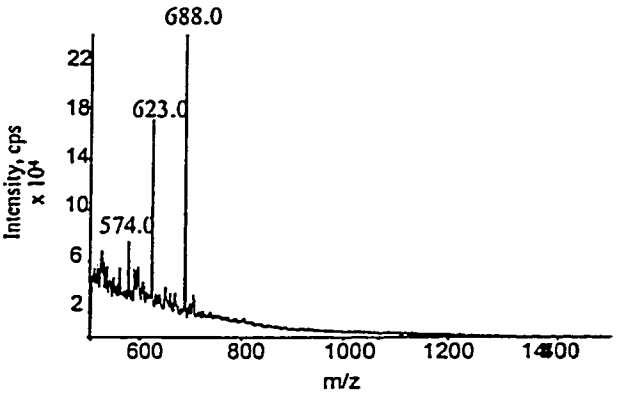

Figure 5.6 Electrospray mass spectrum of *c-myc* affinity selection from PBS buffer.

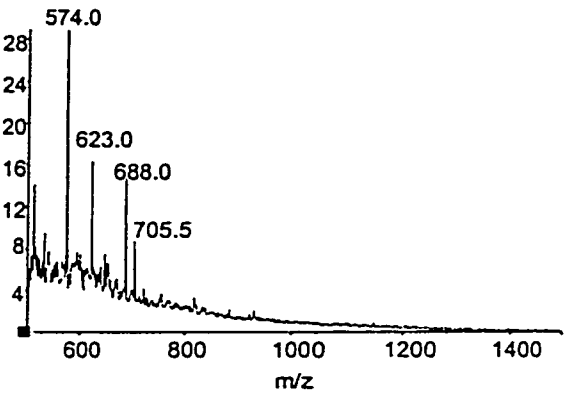

Figure 5.7 Electrospray mass spectrum of *c-myc* peptides in DIW (no affinity selection).

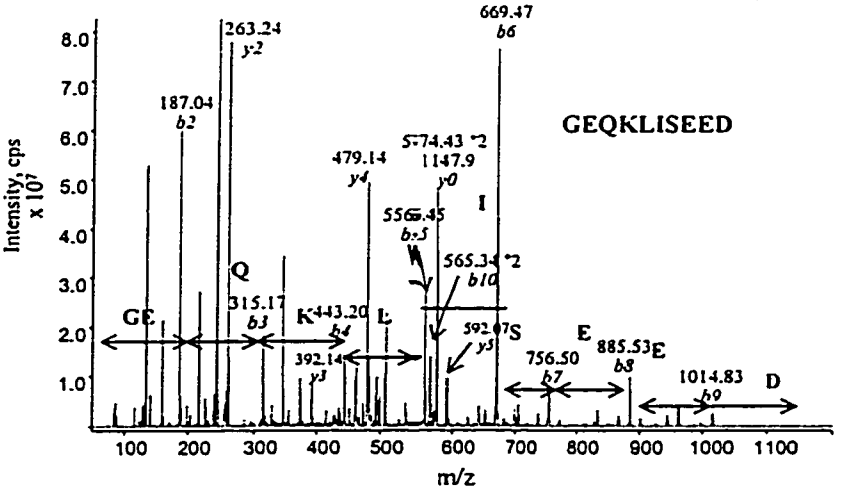

Figure 5.8 MS/MS sequencing of m/z 574 *c-myc* peptide.

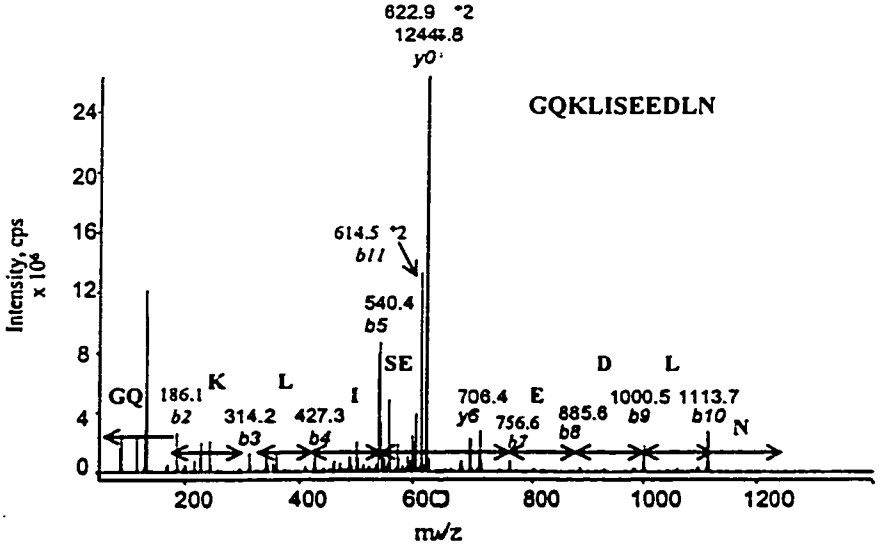

Figure 5.9 MS/MS sequencing of m/z 623 *c-myc* peptide.

by these truncated antigens compared to that of the original *c-myc*. From the poor selection of the 1147 Da peptide it appears that the C-terminal leucine and asparagine residues are more important for the antigen binding than that of the N-terminal glutamic acid since the selection of the 1245 Da peptide still occurs to a large extent (Figures 5.6 and 5.7).

Interestingly, the singly charged ion m/z 705 was not observed in the mass spectrum of the affinity-selected components (Figures 5.6 and 5.7). This could be explained by its poor binding efficiency to the antibody thus resulting in significantly lower selection compared to the *c-myc* peptide analogs. Based on the observed mass, this peptide is believed to have the following sequence SEEDL or ISEED and would not be expected to be selected to any significant extent since this peptide is missing 58% of the *c-myc* peptide sequence.

The presence of these three peptides is a result of side reactions during the synthesis of the *c-myc* peptide. Chromatographic purification of the synthetic product, unfortunately, did not remove these *c-myc* analogs. It should also be noted that the 1245 Da peptide was observed in the MALDI-MS of the affinity-purified *c-myc* solutions, but the 1147 Da peptide could not be detected in either the standard or affinity-selected *c-myc* solutions (Figure 5.10). It was therefore assumed that, if present, this peptide was at a concentration lower than the limit of detection by MALDI-MS. Such discrimination effects between MALDI and electrospray ionization are not unexpected as hydrophobic and surface activities of some peptides render them significantly more detectable in one technique over the other.

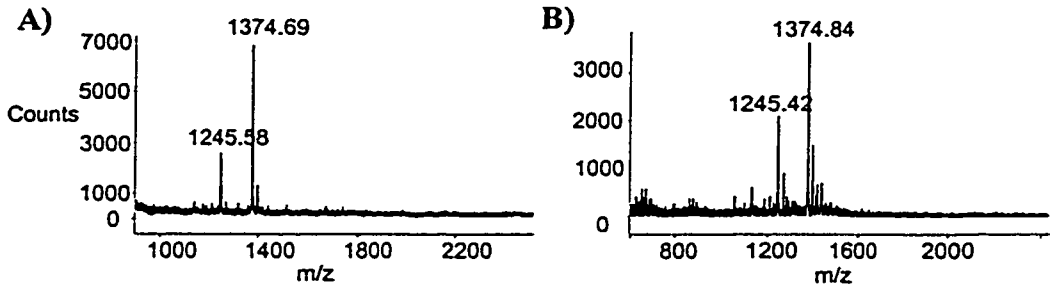

Figure 5.10 MALDI-MS of the *c-myc* peptide A) affinity-selected and B) 300 μg/ml in DIW (no affinity selection).

5.4 Affinity Selection of the *c-Myc* Peptide from Fetal Bovine Serum

Selection of the *c-myc* peptide from a complex matrix was first carried out using fetal bovine serum spiked to 33 μg/ml with the antigen (Section 2.7.1). Prior to selection, the pH of the serum was 7.9, slightly more basic than the optimal pH for antigen binding (pH 7). The pH of the serum was adjusted to 7 using 0.1 M HCl, and affinity selection was performed on both the basic and neutral *c-myc* spiked solutions. An approximate two-fold increase in signal of the *c-myc* peptide (MH^+ 1374.7 Da) was observed with selection from the neutralized serum over that of the more basic serum (Figure 5.11). A more efficient selection is expected at pH 7 since the physiological pH ensures the integrity of the antibody tertiary structure required for binding the *c-myc* epitope. Therefore, the sera used for all the affinity selections discussed in this chapter were neutralized to pH 7 prior to spiking the solution with the peptide. In addition, these selections were also performed using male human serum (type AB) as the matrix since it more closely mirrored the complex composition of the human tissue culture media.

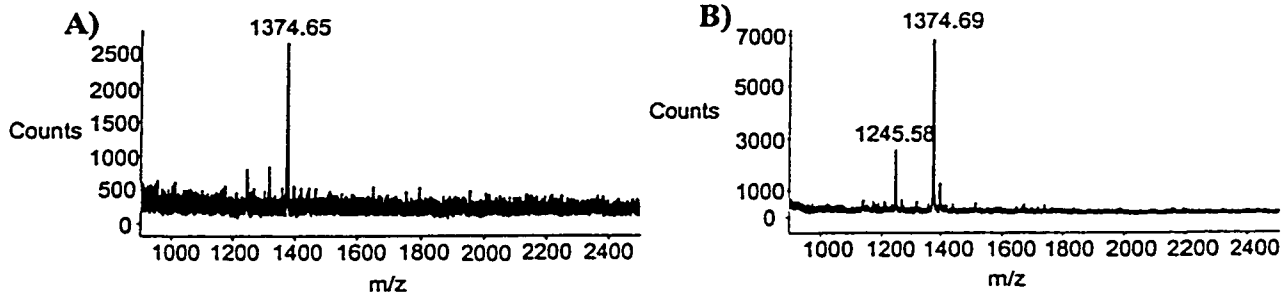

Figure 5.11 MALDI-MS of the affinity-selected *c-myc* peptide from fetal bovine serum A) pH 7.9 and B) pH 7 (both 20 µl of 0.1 M FA).

5.5 Affinity Selection of the *c-Myc* Peptide from Human Serum

As described in Section 2.5, affinity selection was performed using a 0.45 µm Ultrafree-MC centrifugal filter unit. It was found that the application of the human serum solutions to these units resulted in a blockage of the membrane thereby hampering centrifugation. To remedy this problem the human serum was diluted five times prior to spiking with the *c-myc* peptide and then centrifuged for several minutes at 3600 g (8000 rpm) to remove any particulate that could block the centrifugal unit.

The lowest concentration of *c-myc* peptide selected from the PBS buffer that was detected by LC-MS (Q-TOF) was 10 ng/ml. The limit of detection for selection of the peptide from human serum was, however, ten times higher than that observed for the non-complex matrix (100 ng/ml) (Figure 5.12). An increase in the limit of detection is expected for the serum selection since the complexity of this matrix would slow the kinetics of binding and result in a decrease in the amount of *c-myc* peptide selected in the incubation time allowed. However, from Figure 5.12 it appears that this increase in detection limit may also be due to the selection of other components. Automated LC-MS and LC-MS/MS switching was attempted on several of the peaks observed in Figure 5.12, but these proteins could not be identified

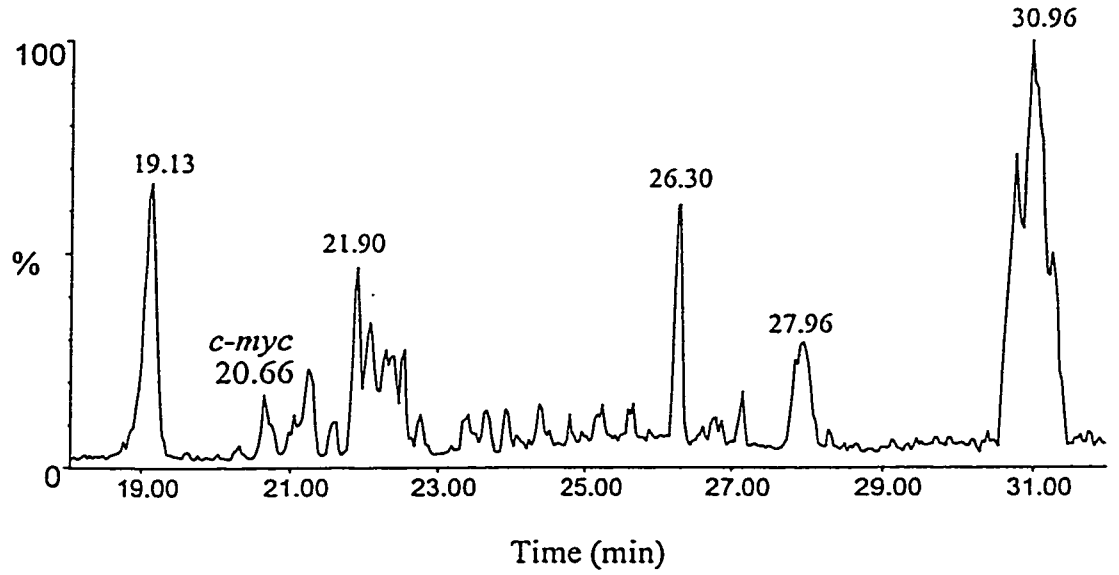

Figure 5.12 LC-MS reconstructed ion chromatogram showing affinity selection of the *c-myc* peptide from human serum (100 ng/ml).

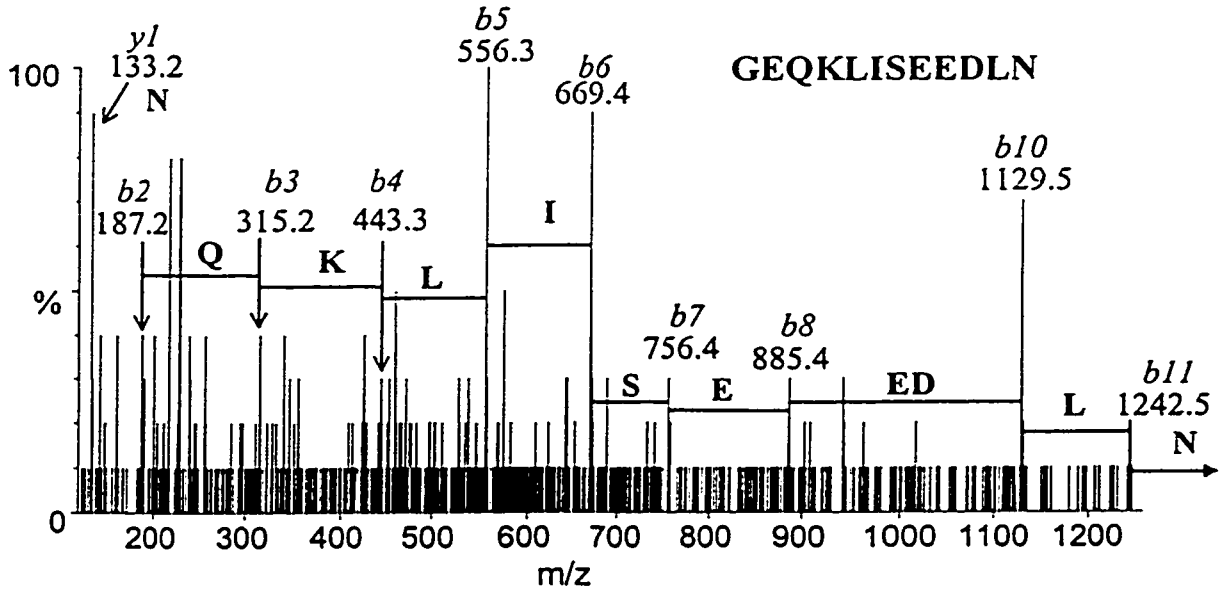

Figure 5.13 LC-MS/MS identifying the 20.66 min peak (m/z 687.8) shown in Figure 5.12 as that of the *c-myc* peptide.

through database searching due to the poor sequence tags obtained. The *c-myc* peptide was found at 20.7 min, and the corresponding MS/MS spectrum confirmed its identity (Figure 5.13).

5.6 Removal of the Extraneous Human Serum Components

It was initially postulated that the components observed in Figure 5.12 were serum peptides and proteins that were captured non-specifically either by the antibody or the protein G of the immunomatrix and were not effectively removed by the three deionized water rinses. As a result, a series of wash systems were investigated to remove these components (Section 2.7.2). CE-UV was used to monitor the presence of these components in the elution buffer as well as in the various rinses.

At first the number of deionized water rinses was increased to 12 (250 μl per rinse) in an attempt to remove the serum components. Electropherograms of the components from a 10 μg/ml *c-myc* spiked serum that were not retained by the immunomatrix as well as the water washes showed that a large amount of the serum proteins was eluted in the non-retained portion and in the first two water washes (Figure 5.14 A-C). No protein was observed in any of the water washes carried out subsequently (Figure 5.14D). The electropherogram of the affinity-selected sample, on the other hand, showed two large peaks that were not visible in the electropherograms of the non-retained sample or the water washes (Figure 5.15). Neither peak can be attributed to the *c-myc* peptide since the maximum concentration of the peptide after selection (8.3 μg/ml if complete selection and elution) would be

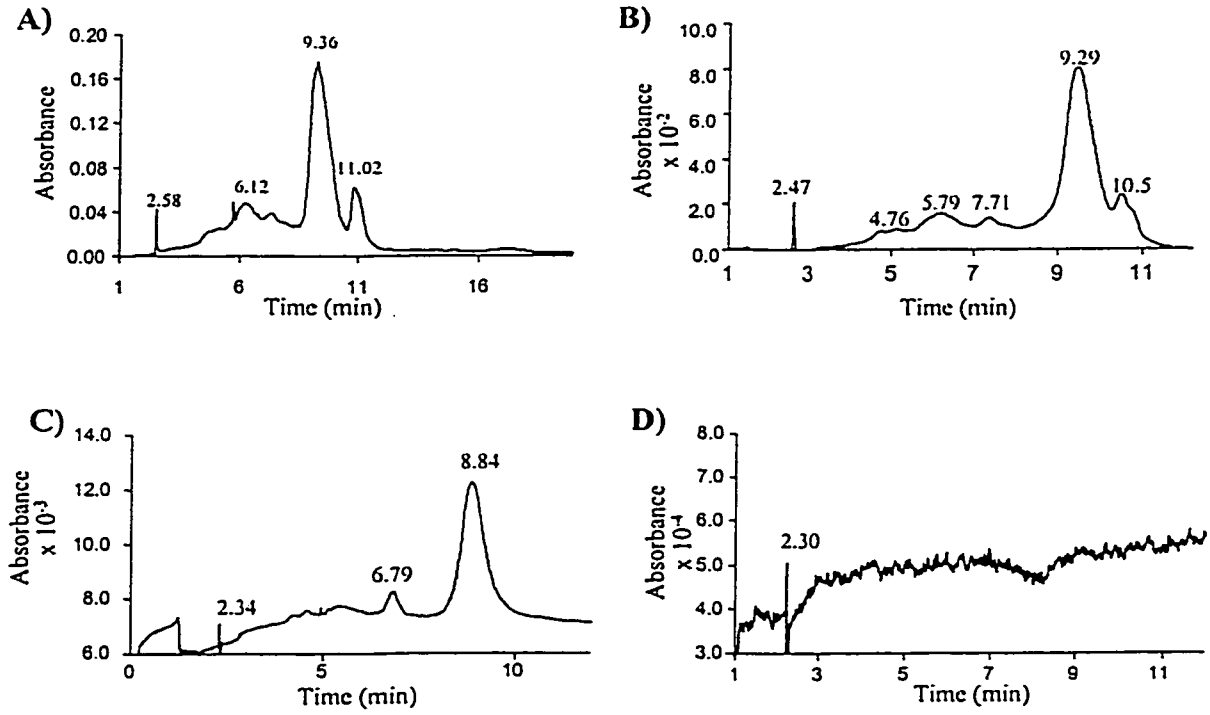

Figure 5.14 Electropherograms showing A) non-retained peptide and protein, B) first, C) second, and D) third deionized water washes for affinity selection from a 10 μg/ml spiked serum solution.

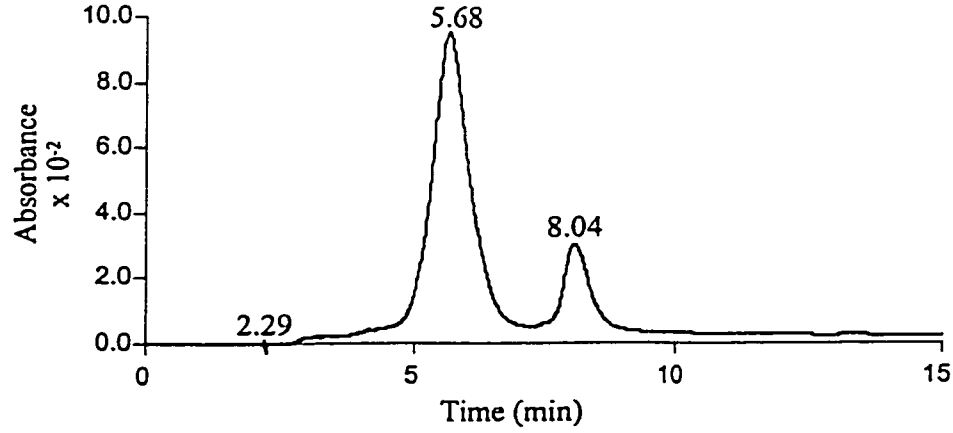

Figure 5.15 Electropherogram showing the serum proteins selected along with the *c-myc* peptide from a 10 μg/ml spiked human serum solution.

significantly less than the limit of detection for this CE-UV method (12 μg/ml). In addition, the observed migration time for the *c-myc* peptide using the above CE-UV conditions is three minutes. The fact that only two major peaks were observed in the affinity selection electropherogram (Figure 5.15) as compared to the more congested electropherogram of the non-retained portion (Figure 5.14A), and the absence of these peaks in the latter water washes (Figure 5.14D) indicates that these proteins might be selected. Nonetheless, several other wash systems were used in an attempt to remove these proteins.

Because of the large quantity of protein selected together with the *c-myc* peptide (Figure 5.15), protein carryover between selections was suspected. As a result, the immunomatrix was rinsed three times with 250 μl of the formic acid elution buffer followed by regeneration with PBS buffer. CE-UV of these formic acid washes showed that the extraneous proteins observed in Figure 5.15 were completely eluted by the third wash (Figure 5.16). In addition, affinity selection of the *c-myc* peptide from PBS buffer using the regenerated immunomatrix showed no serum components (Figure 5.17).

Affinity selection was then carried out on the human serum in the absence of the *c-myc* peptide to ensure that the serum components were not simply complexing with the peptide resulting in their simultaneous selection. The electropherogram of the sample eluted from the immunomatrix still showed two major components thereby confirming that the presence of the serum proteins was not the result of binding to the affinity-selected *c-myc* peptide (Figure 5.18).

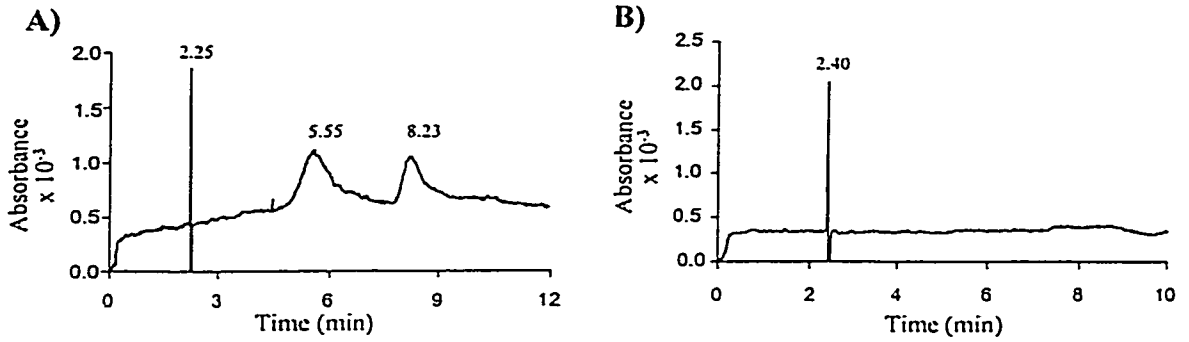

Figure 5.16 Electropherograms showing the formic acid washes of the immunomatrix during regeneration: A) second and B) third 250 µl formic acid washes.

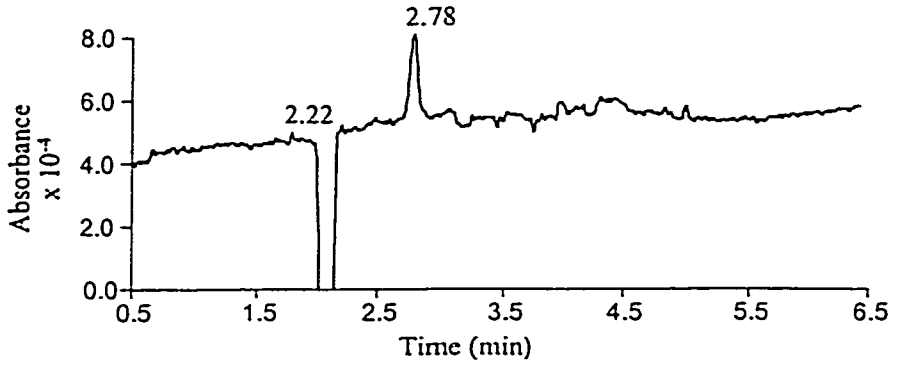

Figure 5.17 Affinity selection of the *c-myc* peptide from a 1 µg/ml PBS buffer solution using a regenerated immunomatrix (preconcentration CE-UV).

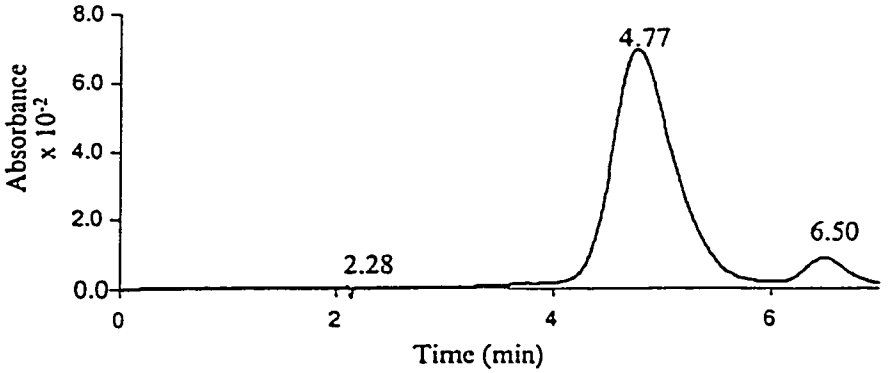

Figure 5.18 Affinity selection eluent of control human serum (CE-UV preconcentration). (Migration times are shorter as a result of the preconcentration method used).

To remove serum proteins and peptides that were non-specifically bound to immunomatrices Dalluge and Sander rinsed the immunomatrix with three column volumes of a 25 mM β-alanine, 125 mM acetic acid (pH 3.8) buffer.[3] Schneider and coworkers used a three buffer system in the following sequence: (i) 0.5M NaCl, 0.05 M Tris-HCl, pH 8.2, 1 mM EDTA, 0.5% Nonidet P-40; (ii) 0.15 M NaCl, 0.05 M Tris-HCl, pH 8.2, 0.5% Nonidet P-40, 0.1% SDS; (iii) 0.15 M NaCl, 0.5% sodium deoxycholate (two washes).[71] Finally, Hornshaw used a 0.5% Tween rinse.[72] All of the above wash systems were used in an attempt to eliminate the serum proteins present in the *c-myc* eluent.

MALDI-MS was used to determine if affinity selection of the *c-myc* peptide was still occurring in the presence of the varying wash systems tested. With the three buffer wash scheme the *c-myc* peptide was not detected by MALDI-MS, while only one broad serum protein peak was detected in the electropherogram of selection from 1 μg/ml spiked serum (Figure 5.19). The MALDI spectrum of the affinity-selected *c-myc* peptide from a 1 μg/ml spiked serum solution after ten β-alanine rinses showed a very weak signal for the corresponding peptide (Figure 5.20A). Interestingly, the electropherogram of the selected peptide (Figure 5.20B) showed a protein peak that was approximately four times smaller in abundance (based on peak area measurement) compared to that found with the three buffer elution method (Figure 5.19). CE-UV analysis of the ten β-alanine washes showed that the removal of most of the serum proteins by this buffer was achieved by the seventh rinse (Figure 5.21).

When the 0.5% Tween was used to wash the immunomatrix, the MALDI-MS spectrum of the affinity-selected *c-myc* peptide from a 1 μg/ml spiked serum solution

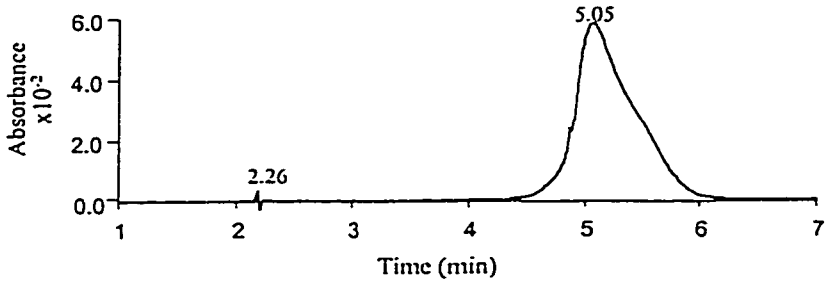

Figure 5.19 Affinity selection eluent from a 1 μg/ml *c-myc* spiked serum solution using the three buffer wash system.

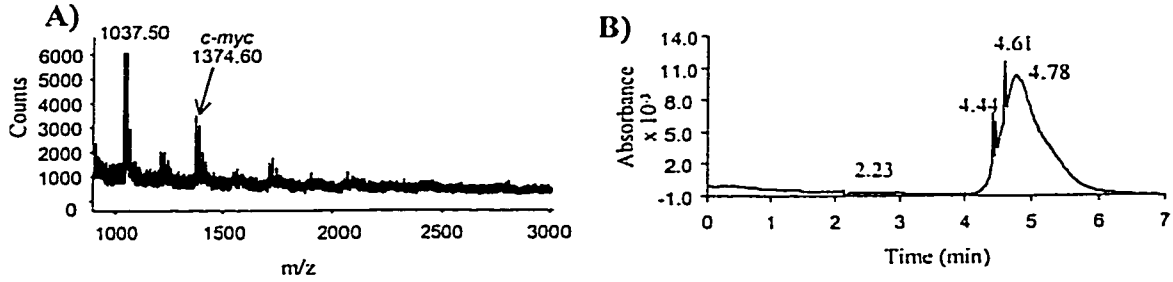

Figure 5.20 A) MALDI-MS of the *c-myc* peptide affinity-selected and B) electropherogram of the serum proteins present with affinity selection from a 1 μg/ml human serum solution after ten β-alanine washes.

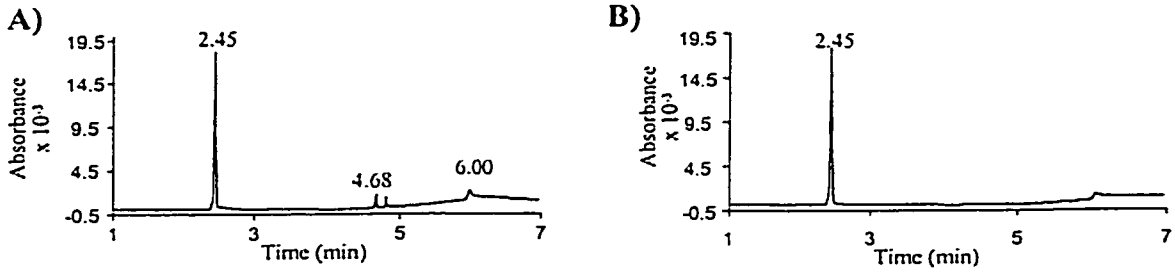

Figure 5.21 Serum proteins removed from the immunomatrix after the A) sixth and B) seventh β-alanine rinses.

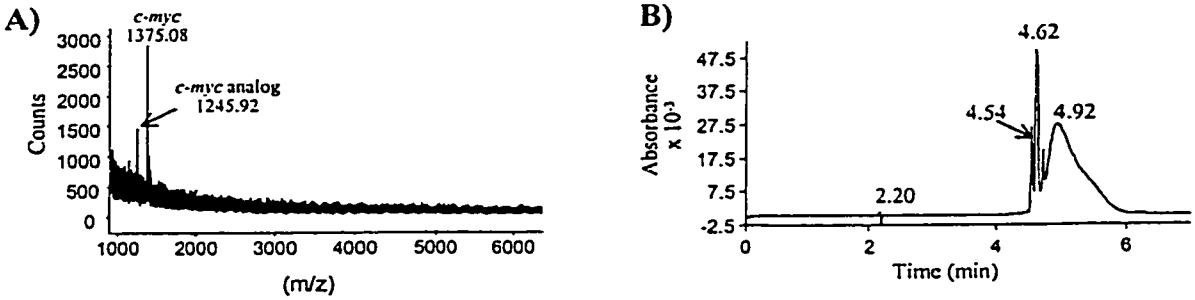

Figure 5.22 A) MALDI-MS of the *c-myc* peptide affinity-selected and B) electropherogram of the serum proteins present with affinity selection from a 1 μg/ml human serum solution after five washes of the immunomatrix with 0.5% Tween.

showed a stronger *c-myc* peak than observed previously with the β-alanine buffer (Figure 5.22A). The corresponding electropherogram (Figure 5.22B) was similar to that for the β-alanine wash; however, the abundance of the corresponding peak was approximately twice of that observed in Figure 5.20B. The number of washes with 0.5% Tween was varied from five to ten times, though no significant difference in the affinity selection and removal of the serum proteins was observed.

The surfactants and organic solvents in these wash systems would most likely disrupt the affinity complex between the antibody and the *c-myc* peptide, thereby resulting in the premature elution of the peptide in the washes. Since affinity selection is an equilibrium process, the peptide may leach from the antibody during the numerous washes of the immunomatrix. None of the washing schemes discussed above effectively removed the serum proteins observed in the selection of the peptide. This further supports the proposal that these proteins are being selected as opposed to a random binding. Among the different wash systems investigated, the β-alanine wash was found to be the best since affinity selection of the peptide was maintained while the largest amount of serum protein was removed.

Finally, precipitation of the serum prior to the addition of the *c-myc* peptide was investigated as a means of removing serum proteins. To the undiluted serum was added 1 ml of acetonitrile in 50 μl aliquots with shaking. After centrifugation the supernatant was removed, freeze-dried, and reconstituted in 300 μl of PBS buffer. Affinity selection of the *c-myc* peptide at 1 μg/ml from this solution showed a strong signal by MALDI-MS with no serum protein detected by CE-UV (Figure 5.23). Precipitation of the spiked serum was then investigated by the addition of 250 μl of

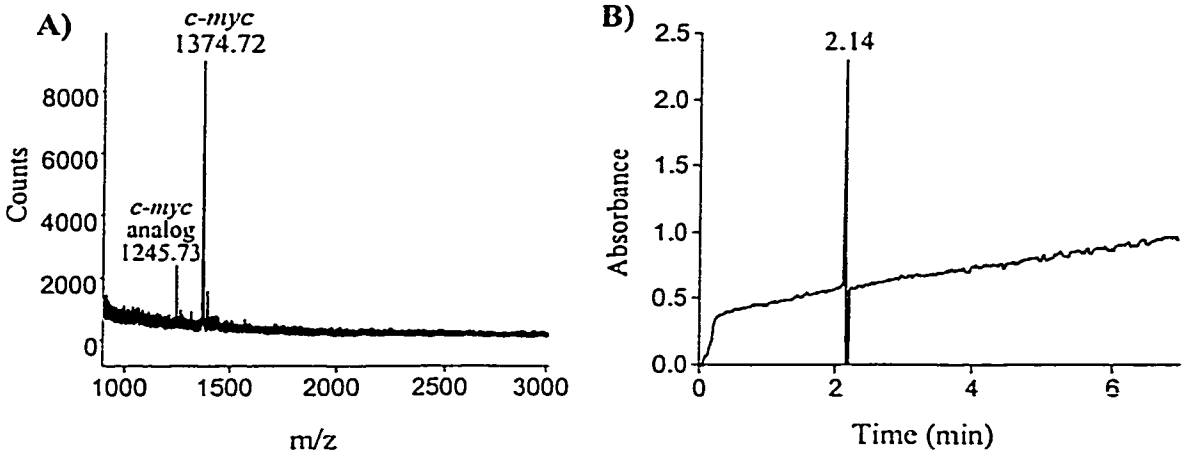

Figure 5.23 A) MALDI-MS and B) electropherogram of the *c-myc* peptide affinity-selected from human serum that had been precipitated with acetonitrile before spiking (1 μg/ml) with the peptide.

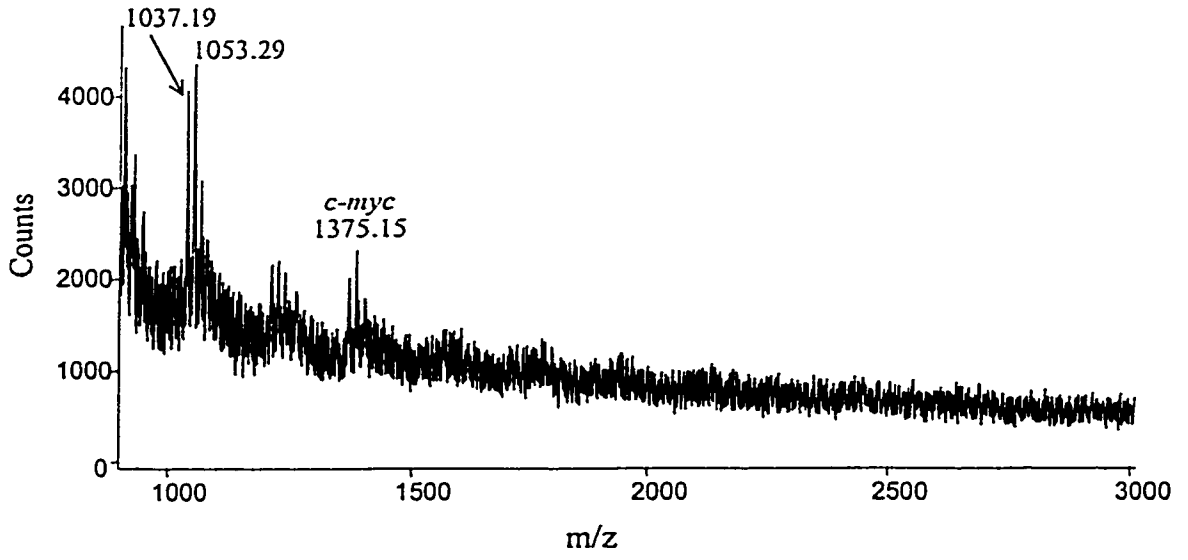

Figure 5.24 MALDI-MS of the *c-myc* peptide affinity-selected from human serum after protein precipitation of the 1 μg/ml spiked serum solution.

acetonitrile in 25 µl aliquots to 250 µl of a 1 µg/ml *c-myc* spiked serum solution. After centrifugation, the supernatant was freeze-dried and reconstituted in 250 µl of PBS buffer. Unfortunately this protein precipitation method yielded low recovery of the *c-myc* peptide due to the precipitation of the antigen from the serum (Figure 5.24).

5.7 Identification of the Extraneous Serum Proteins

As noted previously, a number of serum proteins were being selected by the immunomatrix. Consequently, the identification of these proteins was deemed necessary. A normal SDS-PAGE gel followed by in-gel digestion and database searching was carried out on the affinity-selected components from a 10 µg/ml *c-myc* spiked human serum sample as well as those obtained from the incubation of the serum with the protein G resin alone (Sections 2.8, 2.9.1, 2.10.1, and 2.19) (Figure 5.25). For both matrix selections investigated, the resin was rinsed with the β-alanine buffer prior to elution.

Band	# of Tryptic Peptides Identified	Protein identified
1	N/A	Insufficient number of tryptic peptides detected for database searching
2*	5	Human immunoglobulin heavy chain constant region
3	N/A	Insufficient number of tryptic peptides identified
4	N/A	Insufficient number of tryptic peptides identified
5	12	Human immunoglobulin heavy chain constant region
6	9	Human immunoglobulin heavy chain
7	7	Human immunoglobulin heavy chain
8*	2 (light chain) 4 (heavy chain)	Human IgG kappa light chain Human immunoglobulin fc heavy chain fragment
9	6	Human IgG kappa light chain

10	9	Human IgG1 fc heavy chain fragment
11	N/A	Insufficient tryptic peptides observed for database identification

Table 5.2 Identification (by in-gel digestion and peptide mass database searching) of serum proteins selected after incubation with the protein G resin (Figure 5.25). * indicates the bands that were identified by comparing the masses of the tryptic peptides detected with the predicted digests of the identified proteins.

Band	**# of Tryptic Peptides Identified**	**Protein Identified**
1	12	Human Immunoglobulin gamma-1 heavy chain constant region
2*	3	IgG kappa light chain

Table 5.3 Identification (by in-gel digestion and peptide mass database searching) of serum proteins selected after incubation with the anti-*c-myc* immunomatrix (Figure 5.25). * see Table 5.2 for description.

Thirteen bands in total were removed from the gel and digested by trypsin. MALDI-MS, followed by peptide mass database searching using the ProteinProspector searching program (Section 2.19), resulted in the identification of nine of these bands (Tables 5.2 and 5.3). In the above tables band numbers labeled with an asterisk (bands 2 and 8 of Table 5.2 and band 2 of Table 5.3) indicate those bands whose identity was not obtained directly from database searching due to an insufficient number of tryptic peptides detected for each by MALDI-MS. However, a comparison of the tryptic peptides that were detected for each band and the predicted digests for the band proteins that were identified provided the identification shown in the tables. Unfortunately, there were several weak bands that could not be identified since no tryptic peptides were detected (1, 3, 4 and 11 of Table 5.2). The weakly stained bands (#s 1, 2 (2), 3, 4, 8, and 11 in Figure 5.25) indicate that there was

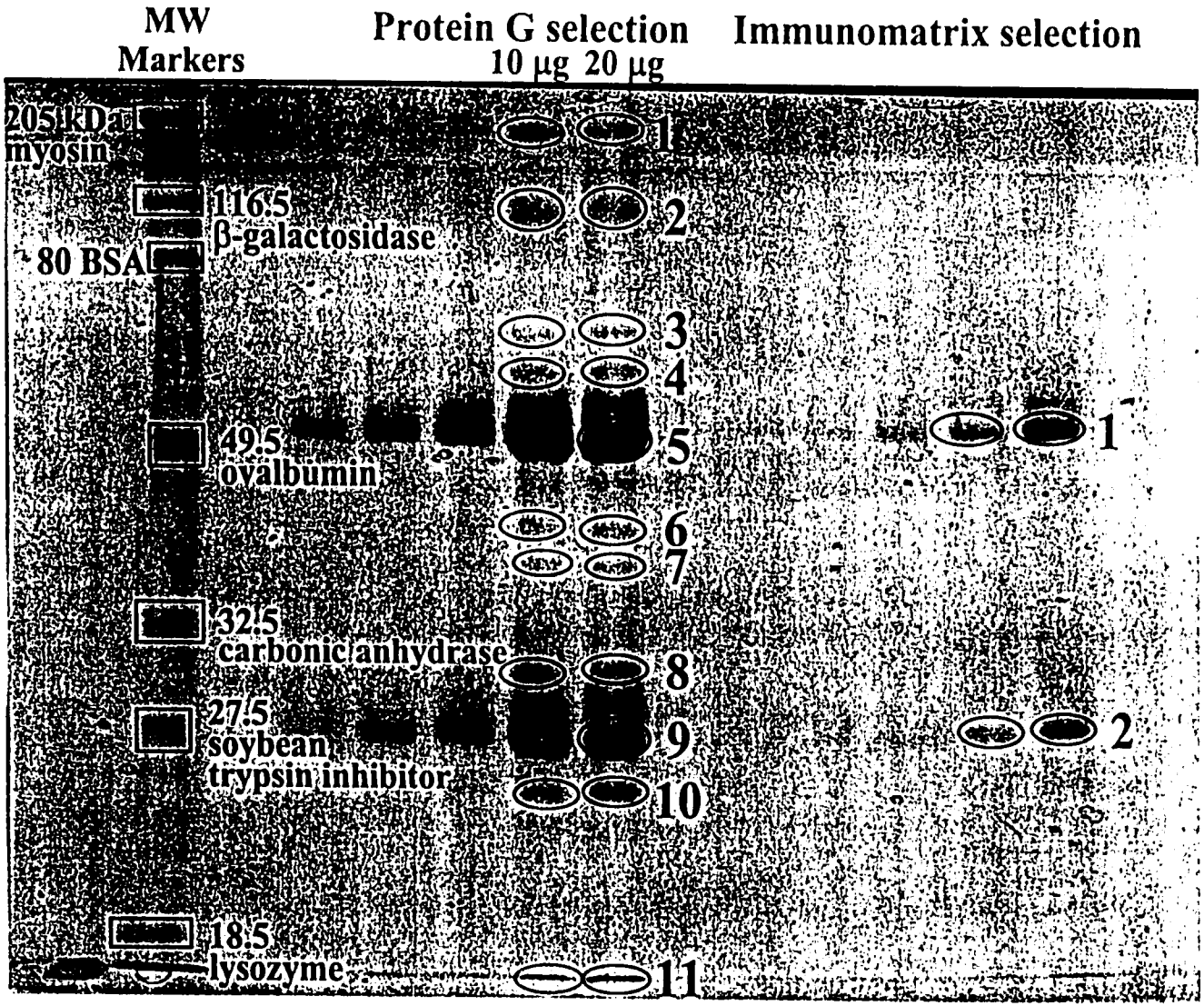

Figure 5.25 Regular SDS-PAGE of proteins selected by protein G and the anti-*c-myc* IgG immunomatrix.

probably an insufficient amount of protein in the extracted gel piece to allow proper identification.

Bands 2, 5, 6, 7, 8, and 10 of the protein G selection lanes were all related to similar proteins—human immunoglobulin heavy chain constant region. The presence of band 2 is probably due to tailing of band 5 since it appears that these lanes have been overloaded (an estimated 20 μg of total protein was applied to the first lane). The estimated mass of the band 5 protein (~ 50 kDa) is in agreement with that of the heavy chain constant fragment (51.5 kDa). The positions of bands 6, 7, 8, and 10 in the gel indicates that all these bands are fragments of the immunoglobulin heavy chain constant region that was observed in band 5. Interestingly, analysis of the sequence coverage from the tryptic peptides identified, shows peptides derived from the N-terminal of the immunoglobulin heavy chain constant region in the band 5 protein that are not observed in any of the other heavy chain bands. It is most likely that fragments of the heavy chain constant region are present in the serum and therefore appear in the gel as lower molecular weight bands.

Band 9 (~ 25 kDa) was found to be human immunoglobulin kappa light chain (23.5 kDa). Interestingly, this protein was also found along with the immunoglobulin heavy chain constant region in band 8. The presence of the light chain in this band is most likely a result of tailing of band 9 due to the overloading of this lane. The heavy chain in this band is probably, like bands 6, 7, and 10, a fragment of the whole region observed in band 5.

Only two bands were observed for the serum incubated with the immunomatrix. Band 1 was found to be the same as band 5 in the protein G selection—human

immunoglobulin heavy chain constant region—corresponding to their equivalent positions in the gel. Only three tryptic peptides were observed in the MALDI-MS of band 2; however, its comparable position with band 9 of the protein G selection suggests that they may be the same protein. The tryptic peptides of band 2 were found in the theoretical digest of the kappa light chain further supporting the proposal that this band is human immunoglobulin light chain.

All the bands in this gel were found to be of human immunoglobulin origin. Therefore, it is believed that the proteins observed in the affinity selection from human serum are antibodies or fragments of the antibodies that have been selected by the protein G of the immunomatrix. The observation of more bands for the protein G selection than for the crosslinked immunomatrix selection is expected since the immunomatrix has fewer available immunoglobulin binding sites than the protein G itself.

The poor selection of the *c-myc* peptide from the human serum (100 ng/ml) is believed to be associated with the co-selection of the human antibodies resulting in a congested, sterically confined immunomatrix. As a result, a means of removing these antibodies was explored.

5.8 Removal of Human Serum Immunoglobulins

Firstly, 10,000 and 100,000 nominal molecular weight limit (NMWL) filter units were used to remove any components above the molecular weight cutoff of the filter from the spiked serum prior to affinity selection (Section 2.7.2). CE-UV analysis showed that the 10 kDa filter units effectively removed the serum proteins such that

none were observed with the affinity-selected *c-myc* peptide (Figure 5.26A). In addition, a strong MALDI-MS signal was observed for the *c-myc* peptide selected from a 10 μg/ml serum solution (Figure 5.26B). The use of the 10 kDa filter units for the purification of complex matrices prior to selection would only be effective for proteins or peptides having a molecular weight less than 10 kDa. Proteins having a molecular weight higher than this would be retained on the filter membrane. As a result, these membranes would be ineffective for the purification of matrices containing a *c-myc*-tagged component with a mass greater than 10 kDa. Therefore, 100 kDa NMWL filter units were investigated.

Interestingly, the electropherograms of the affinity-selected *c-myc* peptide from 100 kDa purified spiked serum showed that serum proteins were still present (Figure 5.27). From the SDS-PAGE gel digestion (Figure 5.25), it was postulated that several of the bands (6, 7, 8, and 10) were fragments of the human immunoglobulin heavy chain constant region that were selected as such from the serum. The heavy chain and its fragments will pass through the 100 kDa filter unit and can be selected by the immunomatrix. As a result, these proteins may be observed in the elution of the selected *c-myc* peptide. However, any intact antibodies should be removed by the 100 kDa filter unit, thereby decreasing the amount of protein present in the filtered serum and in the elution from the immunomatrix. This is observed in Figure 5.27 in which the CE-UV preconcentration method was required to visualize the selected proteins.

As with the 10 kDa filter units, no *c-myc* peptide was observed for the affinity selection when a 1 μg/ml spiked serum was passed through a 100 kDa unit prior to

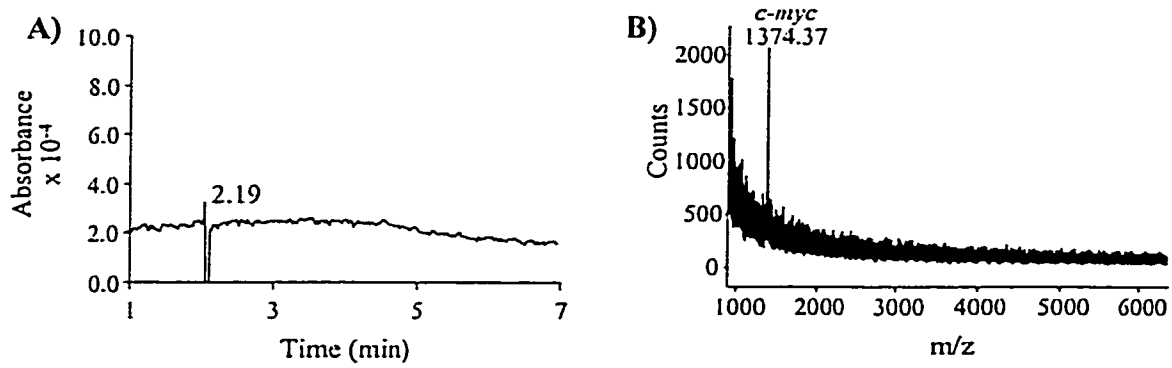

Figure 5.26 Removal of human serum proteins from a 10 μg/ml *c-myc* spiked serum solution using a 10 kDa NMWL filter unit. A) Electropherogram and B) MALDI-MS of the *c-myc* affinity-selected from the purified serum.

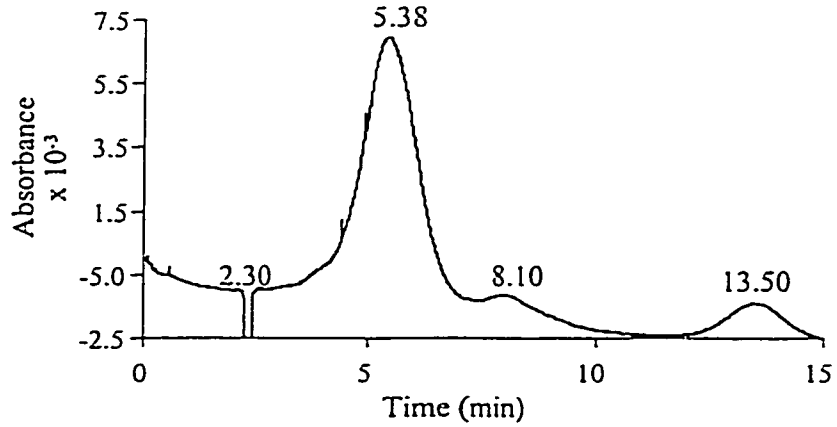

Figure 5.27 Electropherogram of the affinity-selected *c-myc* peptide from a 10 μg/ml spiked serum that had been purified using a 100 kDa NMWL filter unit prior to selection (preconcentration CE-UV method).

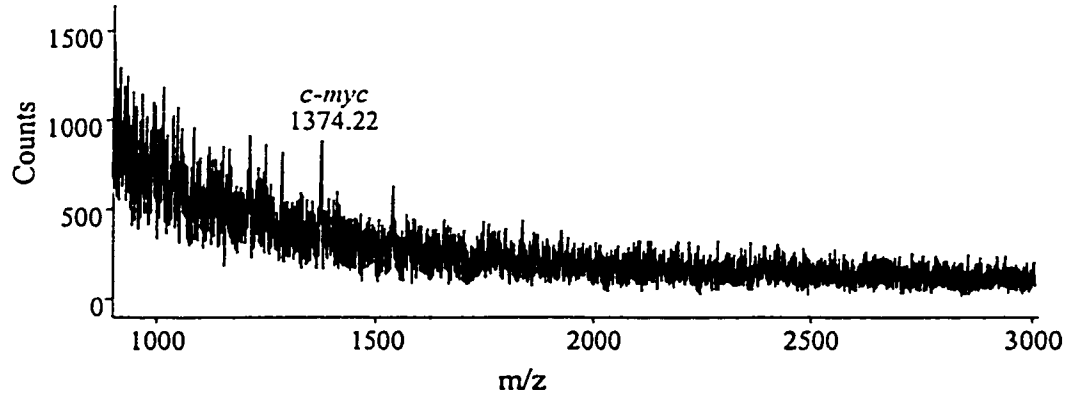

Figure 5.28 MALDI-MS of the *c-myc* peptide affinity-selected from a 0.1 μg/ml spiked serum solution where the serum was passed through a 100 kDa NMWL filter unit prior to being spiked with the peptide.

selection due to losses of the peptide during filtration. When the serum was filtered prior to being spiked with the *c-myc* peptide, selection was weakly observed by MALDI-MS from a 0.1 μg/ml spiked solution (Figure 5.28). It is expected that when these filtration units are used losses of the *c-myc* peptide will occur; however, these losses should be lower with the 100 kDa unit due to the large membrane mesh size.

To identify the proteins selected from the 100 kDa filtered serum, a second SDS-PAGE gel was carried out (Sections 2.8 and 2.9.2) (Figure 5.29).

Band	# of Tryptic Peptides Identified	Protein Identified
1	5	Human immunoglobulin gamma-1 heavy chain constant region
2	4	Human immunoglobulin gamma-1 heavy chain constant region
3	N/A	Insufficient number of tryptic peptides identified
4	19	Human serum albumin
5	6	Human immunoglobulin gamma-1 heavy chain constant region
6	8	Human immunoglobulin gamma-1 heavy chain constant region
7	9	Human immunoglobulin kappa light chain

Table 5.4 Identification (by in-gel digestion and peptide mass database searching) of proteins selected after incubation of the 0.1 μg/ml spiked human serum (serum was 100 kDa filtered prior to spiking) with the anti-*c-myc* immunomatrix (Figure 5.29).

Band	# of Tryptic Peptides Identified	Protein Identified
1	N/A	Insufficient number of tryptic peptides identified
2	16	Human serum albumin
3*	3	Human immunoglobulin gamma-1 heavy chain constant region

4*	4	Human immunoglobulin gamma-1 heavy chain constant region
5*	3	Human immunoglobulin kappa light chain

Table 5.5 Identification (by in-gel digestion and peptide mass database searching) of serum proteins from 100 kDa filtered human serum (Figure 5.29).
* indicates the bands that were identified by comparing the masses of the tryptic peptides detected with the predicted digests of the identified proteins.

A total of twelve bands were removed from the gel and digested by trypsin. MALDI-MS, followed by peptide mass database searching using the ProteinProspector searching program (Section 2.19), resulted in the identification of ten of these bands (Tables 5.4 and 5.5). As with the first gel, bands labeled with an asterisk (bands 3, 4, and 5 of Table 5.5) are those whose identity was not obtained directly from database searching due to an insufficient number of tryptic peptides detected by MALDI-MS. A comparison, however, of the tryptic peptides that were detected for each band and the predicted digests for the identified proteins provided the identification shown in the table. Unfortunately, there were several weak bands that could not be identified since no tryptic peptides were detected (band 3 in Table 5.4 and 1 in Table 5.5). The weakly stained bands (# 3 in Table 5.4 and #s 1, 3, 4, and 5 in Table 5.5) indicate that there was probably an insufficient amount of protein in the extracted gel pieces to enable any meaningful identification.

Bands 1, 2, 5, and 6 of Table 5.4 and 3 and 4 of Table 5.5 have all been identified through database searching as the constant region of the human immunoglobulin heavy chain. The intact heavy chain constant region has an average molecular weight of 52 kDa, which corresponds to the position of bands 3 and 4 of the filtered serum

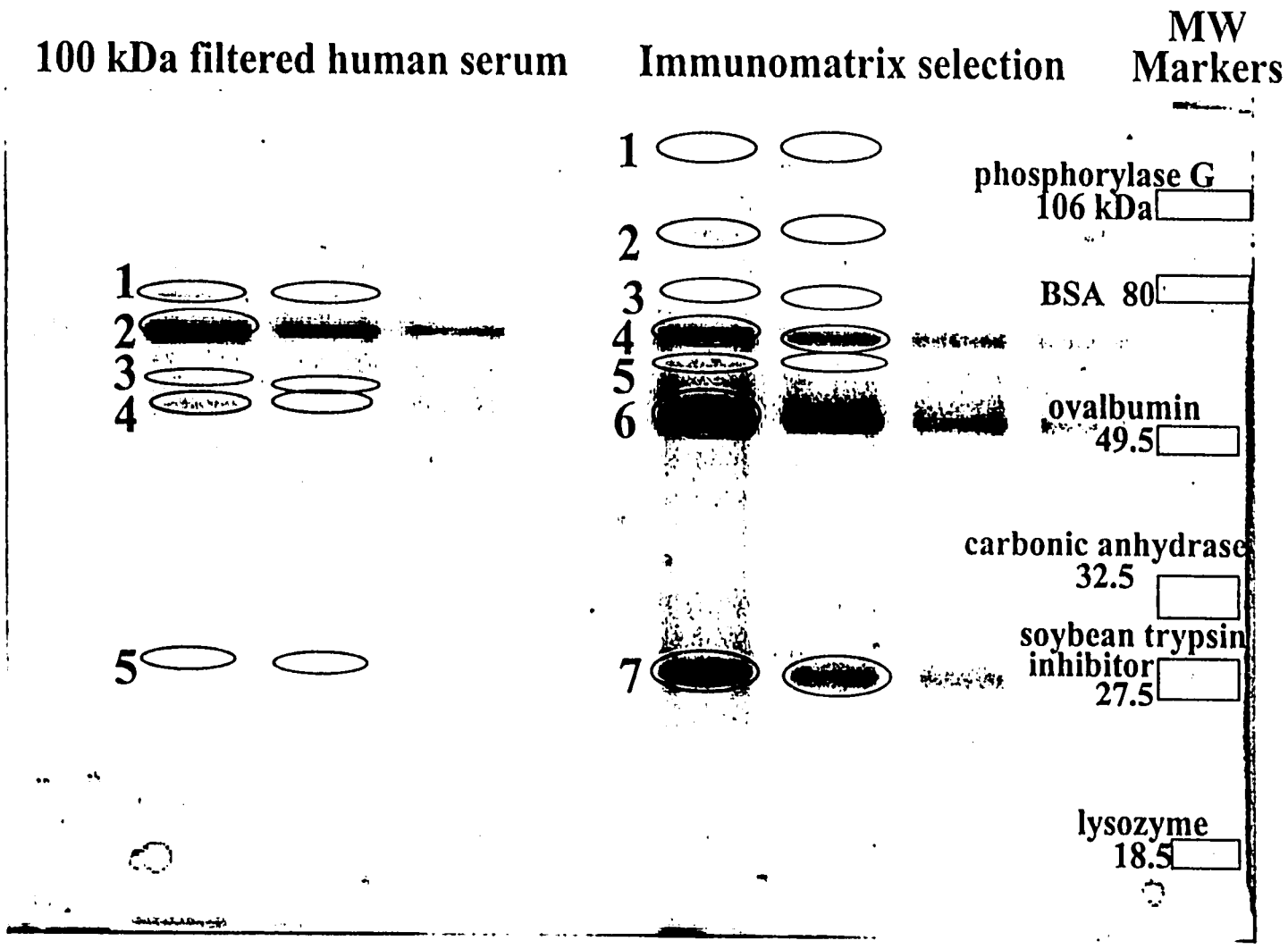

Figure 5.29 Mini SDS-PAGE of human serum purified through a 100 kDa filtration unit and of affinity-selected proteins from a 0.1 µg/ml *c-myc* spiked serum solution (serum passed through a 100 kDa filter prior to spiking).

lanes and 5 and 6 of the affinity-selected lanes in the gel. Bands 1 and 2 of the selected lanes are most likely a result of tailing due to sample overloading.

The human immunoglobulin kappa light chain was identified as band 7 of the affinity selection lanes and band 5 of the filtered serum lanes. The position of these bands (~ 25 kDa) is in agreement with the mass of the light chain (24 kDa). As previously observed, it is most likely that both the heavy and light chain fragments found in the serum are being selected by the protein G of the immunomatrix.

Interestingly, the immunomatrix also appears to be binding human serum albumin (band 4 of Table 5.4 and 2 of Table 5.5). The protein G used for the preparation of the immunomatrix is a recombinant protein with the albumin binding sites presumably removed. Therefore, selection of albumin by the protein G was not anticipated. An investigation of sequence similarity between the albumin and the *c-myc* peptide was carried out using Compugen's Smith and Waterman algorithm as well as the ProMac program as discussed in Section 4.3. No sequence similarity was identified between the *c-myc* peptide and the human serum albumin protein. From the discussion in Section 4.3, it is possible that the anti-*c-myc* antibody is cross-reacting with the albumin. It is also possible that the albumin binds non-specifically to the antibody fragments present in the serum and is carried through with the protein G-selected antibody chains.

A comparison of the bands observed for the filtered human serum and the affinity-selected sample indicates that the immunomatrix is binding all the components present in the filtered solution. However, filtration of the serum through the 100 kDa units does assist the affinity selection of the *c-myc* peptide by the

removal of the intact serum antibodies. As a result, selection of the *c-myc* peptide was observed at lower concentrations (20 ng/ml) of the peptide than observed for non-filtered sera (Figure 5.30).

In a final attempt to remove the extraneous proteins, the diluted serum was incubated with the protein G resin prior to affinity selection using the immunomatrix. Using 200 μl of the protein G beads and 250 μl of diluted serum, the same selection method was used as described in Section 2.5 for the immunomatrix. Figure 5.31 shows two broad peaks for the serum proteins that were selected by the protein G. Figure 5.32 shows the affinity selection after the protein G purification. It appears that the protein G alone effectively removes a lot of the protein present in the serum, however, two peaks remain. Perhaps the protein G binding sites were all occupied or hindered leaving the observed unselected proteins. Selection using half the volume of protein G beads showed a significant difference in the amount of protein present after affinity selection indicating that saturation of the protein G beads may be occurring (Figure 5.33).

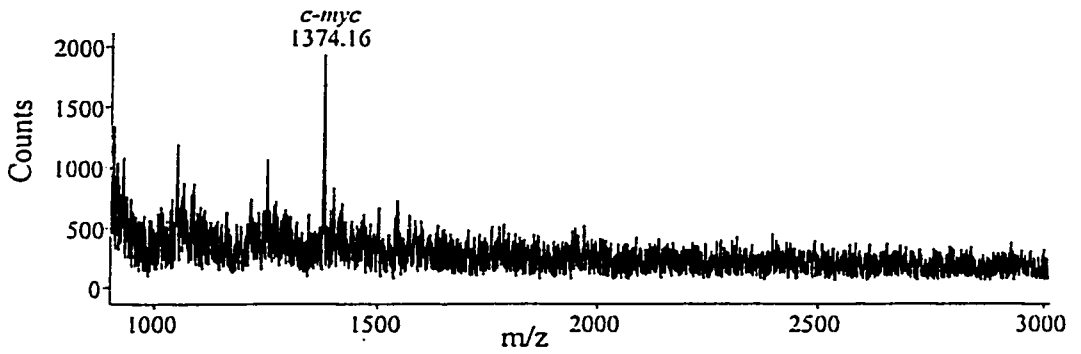

Figure 5.30 MALDI-MS of the *c-myc* peptide affinity-selected from a 20 ng/ml spiked human serum solution (peptide was added after purification of the serum using a 100 kDa NMWL filter unit). Sample volume for analysis was 5 µl.

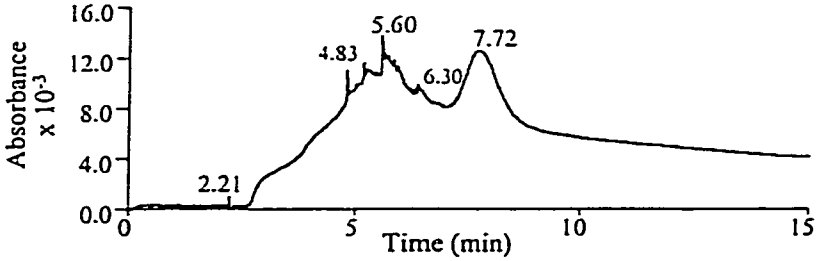

Figure 5.31 Electropherogram showing the human serum proteins selected by 200 µl of protein G resin.

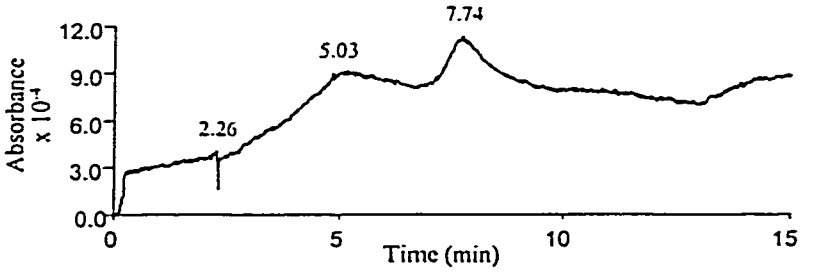

Figure 5.32 Electropherogram showing the human serum proteins selected by the immunomatrix after purification by the protein G resin (preconcentration CE-UV method).

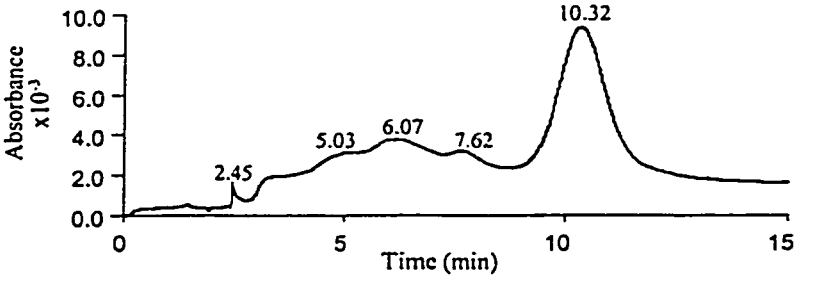

Figure 5.33 Electropherogram showing the human serum proteins selected by 100 µl of protein G resin.

Chapter 6 Conclusion

Affinity enrichment of the *c-myc* peptide and *c-myc*-tagged proteins from complex matrices was achieved using the anti-*c-myc* IgG1 mouse monoclonal antibody covalently immobilized on recombinant protein G resin through a chemical crosslinker—dimethyl pimelimidate. It was determined that 99 ± 1.3% of the applied antibody was immobilized on the resin resulting in a concentration of two mg of properly oriented antibody per ml of beads.

The crosslinked immunomatrix was used to selectively enrich both wild-type and mutant scFv antibodies specific for human blood group A antigens from the shock buffer periplasmic extract of *E. coli*. Selection of the antibodies was first confirmed by MALDI-MS; however, the characterization of the point mutations within the scFv mutant was accomplished by sequencing tryptic peptides derived from the purified protein using LC-MS/MS. A comparison of the MS/MS spectra of the T46-53 peptide from the mutant #1 and wild-type digests confirmed the L46N mutation. However the other two point mutations—N214Q and L215I—could not be identified by LC-MS/MS since the tryptic peptide containing these mutations was not detected. It is proposed that the size (6139.72 Da) and relative hydrophobicity of the peptide resulted in insufficient recovery due to poor solubility, adsorption on the eppendorf surface, poor ionization efficiency, or adsorption on the C18 PEPMAC column. Nevertheless, the peptide was weakly detected by MALDI-MS (6139.32) in the mutant #1 digest. The 14 Da mass difference from the wild-type tryptic 180-236 peptide (6125.29 Da) supports the proposed mutation.

Interestingly, the LC-MS of the scFv mutant #1 tryptic digest showed a number of unexpected peptides in addition to those from the digestion of the mutated protein. Partial sequence information obtained from the LC-MS/MS analysis was used to conduct database searching. A number of *E. coli* proteins were identified from the unexpected tryptic precursor ions. However, their presence in the affinity selection of the mutant from the periplasmic shock buffer could only be explained by cross-reactions between either the IgG antibody or the protein G. In spite of this, immunoaffinity selection was successfully used to enrich *c-myc* bearing proteins from *E. coli* periplasmic extracts thereby enabling further characterization using LC-MS/MS.

Immunoaffinity enrichment of the *c-myc* peptide from both non-complex (PBS buffer) and complex matrices (human serum) was also achieved using the crosslinked immunomatrix. A concentration study using LC-MS of the *c-myc* peptide affinity-selected from PBS buffer showed that an increase in the amount of peptide applied to the immunomatrix resulted in a linear increase in the total amount selected. The lowest detectable concentration of *c-myc* peptide selected from the PBS buffer using the present LC-MS procedure was 10 ng/ml. However, selection of the peptide from human serum was only observed for a 100 ng/ml *c-myc*-spiked serum solution. A decrease in the amount of peptide selected from the serum solution is expected since the complexity of the matrix would reduce the kinetics of binding. However, this apparent decrease in sensitivity when using serum sample may be related to the simultaneous selection of protein components by the immunomatrix. The identification of these proteins was achieved using gel electrophoresis followed by in-

gel digestion and database searching. Peptide mapping showed that the affinity-selected components from a 10 μg/ml *c-myc*-spiked human serum sample as well as those obtained from the incubation of the serum with the protein G resin alone were all related to human immunoglobulin G. Since selection of the antibody occurred with both the immunomatrix and the protein G resin alone, it was concluded that the human serum immunoglobulin G or its fragments (heavy or light chain) were selected by the protein G of the immunomatrix. The selection of the *c-myc* peptide (100 ng/ml) was therefore hampered by the co-selection of the human IgG resulting in a congested sterically-confined immunomatrix.

To enhance selection of the peptide, the serum was passed through 10,000 and 100,000 NMWL filter units prior to being spiked with the *c-myc* peptide. The 10 kDa filter units effectively removed the serum proteins such that none of the interferences were observed in the corresponding CE-UV analysis. However, selection from serum filtered through the 100 kDa units still showed proteins to be present with the selected peptide though to a significantly lower extent than that observed with the non-filtered sera. A second SDS-PAGE gel, followed by in-gel digestion and database searching, was carried out on the selected components from 100 kDa filtered sera. Again, the human IgG heavy and light chain fragments were identified in addition to human serum albumin. As previously observed, the protein G of the immunomatrix appears to be selecting human IgG light and heavy chain fragments present in the serum. The protein G used in the immunomatrix is a recombinant protein with the albumin-binding site presumably removed. However, selection of the albumin by the immunomatrix may be occurring due to the cross-reactivity of the anti-*c-myc* IgG.

Despite the presence of the human immunoglobulin G antibody and the serum albumin, detection of the selected *c-myc* peptide from a 100 ng/ml spiked human serum solution was achieved using LC-MS. In addition, LC-MS/MS sequencing was carried out to confirm the identity of the selected peptide. The removal of the intact antibody by passing the serum through a 100 kDa NMWL filtration unit prior to spiking allowed selection from a concentration as low as 20 ng/ml.

None of the extraneous proteins identified in either the *E. coli* or sera selections contained the *c-myc* epitope and therefore should not be immunoaffinity-selected. However, as discovered by Seigel and coworkers and Mai and Martensson cross-reactivity does occur with this antibody indicating that it is less specific than originally proposed by Evan and coworkers.

References

1. Janis, L. J.; Regnier, F. E. *J. Chromatogr.* **1988**, *444*, 1-11.

2. Van Emon, J. M.; Lopez-Avila, V. *Environmental Immunochemical Methods: Perspectives and Applications. 4th National Immunochemistry Summit*; American Chemical Society: Washington, 1996; pp 74-88.

3. Dallugc, J. J.; Sander, L. C. *Anal. Chem.* **1998**, *70*, 5339-5343.

4. Campbell, D. H.; Luescher, E.; Lerman, L. S. *Proc. Natl. Acad. Sci. USA* **1951**, *37*, 575.

5. Phillips, T. M.; Krum, J. M. *J. Chromatogr. B.* **1998**, *715*, 55-63.

6. Phillips, T. M.; Chmielinska, J. J. *Biomed. Chromatogr.* **1994**, *8*, 242-246.

7. Creaser, C. S.; Feely, S. J.; Houghton, E.; Seymour, M. *J. Chromatogr. A.* **1998**, *794*, 37-43.

8. Hage, D. S. *J. Chromatogr. B.* **1998**, *715*, 3-28.

9. Voet, D.; Voet, J. G. *Biochemistry*; John Wiley & Sons, Inc.: New York, 1995; p. 1211.

10. Harlow, E.; Lane, D. *Antibodies: A Laboratory Manual*; Cold Spring Harbor Laboratory: New York, 1988; pp 23-35, 513-552.

11. Little, M. C.; Siebert, C. J.; Matson, R. S. *BioChromatography* **1988**, *3*, 156-160.

12. Karas, M.; Hillenkamp, F. *Anal. Chem.* **1988**, *60*, 2299-2301.

13. Meng, C. K.; Mann, M.; Fenn, J. B. *Z. Phys. D-Atoms Mol. Clusters* **1988**, *10*, 361-368.

14. Fenn, J. B.; Mann, M.; Meng, C. K.; Wong, S. F.; Whitehouse, C. M. *Science* **1989**, *246*, 64-71.

15. Ehring, H.; Karas, M.; Hillenkamp, F. *Org. Mass Spectrom.* **1992**, *27*, 472-480.

16. Siuzdak, G. *Proc. Natl. Acad. Sci. USA* **1994**, *91*, 11290-11297.

17. Beavis, R. C.; Chait, B. T. *Methods Enzymol.* **1996**, *270*, 519-544.

18. Fenselau, C. *Anal. Chem.* **1997,** 1 Nov., 661A-665A.

19. Wong, S. T.; Meng, C. K.; Fenn, J. B. *J. Phys. Chem.* **1998,** *92*, 546-550.

20. Kebarle, P.; Tang, L. *Anal. Chem.* **1993,** *65*, 972A-986A.

21. Dole, M.; Hines, R. L.; Mack, R. C.; Mobley, R. C.; Ferguson, L. D.; Alice, M. B. *J. Chem. Phys.* **1968,** *49*, 2240-2249.

22. Iribarne, J. V.; Thompson, B. A. *J. Chem. Phys.* **1976,** *64*, 2287-2294.

23. Bruins, A. P.; Covey, T. R.; Henion, J. D. *Anal. Chem.* **1987,** *59*, 2642-2646.

24. Mann, M.; Wilm, M. *Trends Biochem. Sci.* **1995,** *20*, 219-224.

25. Wilm, M. S.; Mann, M. *Int. J. Mass Spectrom. Ion Proc.* **1994,** *136*, 167-180.

26. Wilm, M.; Mann, M. *Anal. Chem.* **1996,** *68*, 1-8.

27. Wilm, M.; Shevchenko, A.; Houthaeve, T.; Breit, S.; Schweigerer, L.; Fotsis, T.; Mann, M. *Nature* **1996,** *379*, 466-469.

28. Skoog, D. A.; Leary, J. J. *Principles of Instrumental Analysis*; Saunders College Publishing: New York, 1992; pp 429-432.

29. http://www.scimedia.com/chem-ed/ms/quadrupo.htm.

30. Morris, H. R.; Paxton, T.; Dell, A.; Langhorne, J.; Berg, M.; Bordoli, R. S.; Hoyes, J.; Bateman, R. H. *Rapid Commun. Mass Spectrom.* **1996,** *10*, 889-896.

31. Morris, H. R.; Paxton, T.; Panico, M.; McDowell, R.; Dell, A. *J. Protein Chem.* **1997,** *16*, 469-479.

32. Shevchenko, A.; Chernushevich, I.; Ens, W.; Standing, K. G.; Thomson, B.; Wilm, M.; Mann, M. *Rapid Commun. Mass Spectrom.* **1997,** *11*, 1015-1024.

33. Vinh, J.; Langridge, J. I.; Bré, M-H.; Levilliers, N.; Redeker, V.; Loyaux, D.; Rossier, J. *Biochemistry* **1999,** *38*, 3133-3139.

34. Yates, J. R. *Methods Enzymol.* **1996,** *271*, 351-377.

35. Dongré, A. R.; Eng, J. K.; Yates, J. R. *Trends Biochem. Sci.* **1997,** *15*, 418-425.

36. Hunt, D. F., Yates, J. R., Shabanowitz, J., Winston, S. Hauer, C. R. *Proc. Natl. Acad. Sci. USA* **1986,** *83*, 6233-6237.

37. Jorgenson, J. W.; Lukacs, K. D. *Anal. Chem.* **1981**, *53*, 1298-1302.

38. Heegaard, N. H. H.; Nilsson, S.; Guzman, N. A. *J. Chromatogr. B* **1998**, *715*, 29-54.

39. http://www.ceandcec.com/cethcory.htm.

40. Foret, F.; Sustacek, V.; Bocek, P. *J. Microcolumn Sep.* **1990**, *2*, 229-233.

41. Albin, M.; Grossman, P. D.; Moring, S. E. *Anal. Chem.* **1993**, *65*, 489-497.

42. Mazereeux, M.; Tjaden, U. R.; Reinhoud, N. J. *J. Chromatogr. Sci.* **1995**, *33*, 686-697.

43. Foret, F.; Szoko, E.; Karger, B. L *J. Chromatogr.* **1992**, *608*, 3-12.

44. Chien, R-L.; Burgi, D. S. *Anal. Chem.* **1992**, *64*, 489A-496A.

45. Silin, V.; Plant, A. *Trends Biochem. Sci.* **1997**, *15*, 353-359.

46. Homola, J.; Yee, S. S.; Gauglitz, G. *Sensor Actuator B* **1999**, *54*, 3-15.

47. http://www.biacore.com.

48. Stenberg, E.; Persson, B.; Roos, H.; Urbaniczky, C. *J. Colloid Interface Sci.* **1991**, *143*, 513-526.

49. Mackenzie, C. R.; Hirama, T.; Lee, K. K.; Altman, E.; Young, N. M. *J. Biol. Chem.* **1997**, *272*, 5533-5538.

50. Bateman, K. P.; White, R. L.; Thibault, P. *Rapid Commun. Mass Spectrom.* **1997**, *11*, 307-315.

51. Evan, G. I.; Hancock, D. C.; Littlewood, T.; Pauza, C. D. *CIBA Foundation Symposium* **1986**, *119*, 245-263.

52. Ryan, K. M.; Birnie, G. D. *Biochem. J.* **1996**, *314*, 713-721.

53. Salghetti, S. E.; Kim, S. Y.; Tansey, W. P. *EMBO J.* **1999**, *18*, 712-726.

54. Nanbru, C.; Lafon, I.; Audigier, S.; Gensac, M-C.; Vagner, S.; Huez, G.; Prats, A-C. *J. Biol. Chem.* **1997**, *272*, 32061-32066.

55. Schiweck, W.; Buxbaum, B.; Schätzlein, C.; Neiss, H. G.; Skerra, A. *FEBS Lett.* **1997**, *414*, 33-38.

56. Fuchs, P.; Breitling, F.; Little, M.; Dübel, S. *Hybridoma* **1997**, *16*, 227-233.

57. Pierce Reacti-Gel product information sheet.

58. Matson, R. S.; Little, M. C. *J. Chromatogr.* **1988**, *458*, 67-77.

59. Princeton Separations product information sheet.

60. Orthner, C. L.; Highsmith, F. A.; Tharakan, J.; Madurawe, R. D.; Morcol, T.; Velander, W. H. *J. Chromatogr.* **1991**, *558*, 55-70.

61. Hoffman, W. L.; O'Shannessy, D. J. *J. Immunol. Method.* **1988**, *112*, 113-120.

62. Prisyazhnoy, V. S.; Fusek, M.; Alakhov, Y. B. *J. Chromatogr.* **1988**, *424*, 243-253.

63. Pharmacia Biotech technical data sheet.

64. Colcher, D.; Bird, R.; Roselli, M.; Hardman, K. D.; Johnson, S.; Pope, S.; Dodd, S. W.; Pantoliano, M. W.; Milenic, D. E.; Schlom, J. *J. Nat. Cancer Inst.* **1990**, *82*, 1191-1197.

65. Mackenzie, C. R.; Sharma, V.; Brummell, D.; Bilous, D.; Dubuc, G.; Sadowska, J.; Young, N. M.; Bundle, D. R.; Narang, S. A. *Biotechnol.* **1994**, *12*, 390-395.

66. Ikegaki, N.; Xao, X. T.; Kay, B. K.; Kennett, R. H. *Immunotechnol.* **1996**, *2*, 37-46.

67. http://www2.ebi.ac.uk/bic_sw/

68. Evan, G. I.; Lewis, G. K.; Ramsay, G.; Bishop, J. M. *Mol. Cell. Biol.* **1985**, *5*, 3610-3616.

69. Siegel, J.; Brandner, G.; Hess, R. D. *Int. J. Oncol.* **1998**, *13*, 1259-1262.

70. Mai, S.; Martensson, I. *Nucl. Acid. Res.* **1995**, *23*, 1-9.

71. Schneider, C.; Newman, R. A.; Sutherland, D. R.; Asser, U.; Greaves, M. F. *J. Biol. Chem.* **1982**, *257*, 10766-10769.

72. Hornshaw, M. "Micro-Pipette Tip Affinity Columns for MS", 47th ASMS Conference, Dallas, TX, June 13-17, 1999.

Claims to Original Research

1. Development of an anti-*c-myc* mouse monoclonal IgG1 immunomatrix by the covalent immobilization of the antibody on protein G resin via the chemical crosslinker dimethyl pimelimidate.

2. Affinity enrichment of scFv antibodies from the periplasmic extract of *E. coli* and the subsequent identification of the site of mutation within the scFv mutant antibody #1 using LC-MS/MS sequencing of the corresponding tryptic digest.

3. Affinity enrichment of the *c-myc* peptide from spiked human serum at a concentration of 20 ng/ml. LC-MS/MS sequencing was used to confirm the identity of the selected peptide.

4. Development of immunoaffinity chromatography with on-line mass spectral detection using the anti-*c-myc* IgG immunomatrix.

5. Discovery and identification of extraneous *E. coli* and human serum proteins selected by the immunomatrix. The cross-reactivity of the anti-*c-myc* IgG antibody was proposed for the selection of most of these proteins.

Thesis Related Presentations

1) T. LeRiche, "Mass Spectrometry for the Characterization of Immunoaffinity Selected Components from Complex Matrices." 16th Ontario Gas Phase Ion Chemistry Meeting, Peterborough, ON, October, 1999.

2) J. Li, C. Skinner, C. Wang, J. Harrison, T. LeRiche, "Efficient Coupling of Microfabricated Devices to Nanoelectrospray Mass Spectrometry; Application to the Analysis of Trace Level Proteins." 26th Annual Conference of the Federation of Analytical Chemistry and Spectroscopy Societies, Vancouver, BC, October, 1999.

3) T. LeRiche, R. Wehbi, R. Mackenzie, P. Thibault, R. Roy, "Immunoaffinity Selection with Mass Spectrometry for the Characterization of Expressed Single Chain Antibodies and the *c-myc* Peptide from Complex Matrices." 47th American Society of Mass Spectrometry Conference, Dallas, TX, June, 1999.